

**ELECTROCHEMICAL TREATMENT OF TEXTILE DYE WASTE  
WATER BY ANODIC OXIDATION**

**BY**

**JUSTIN K. MAGHANGA**

**A THESIS SUBMITTED IN PARTIAL FULFILMENT OF THE  
REQUIREMENTS FOR THE DEGREE OF DOCTOR OF PHILOSOPHY IN  
ANALYTICAL CHEMISTRY OF UNIVERSITY OF ELDORET, KENYA.**

**2014**

## DECLARATION

### Declaration by the candidate

This thesis is my original work and has not been presented for a degree in any other University. No part of this thesis may be reproduced without the prior written permission of the author and/or University of Eldoret.

Maghanga Justin K.

.....

SC/D.Phil./024/08

Signature

Date

### Declaration by the Supervisors

This thesis has been submitted for examination with our approval as University Supervisors.

Prof. Fred K. Segor

University of Eldoret, Eldoret, Kenya.

.....

Signature

Date

Prof. Justin Irina

.....

Technical University of Mombasa, Mombasa, Kenya

Signature

Date

Prof. Mwakio Tole

Pwani University, Kilifi, Kenya

.....

Signature

Date

## **DEDICATION**

This thesis is dedicated to my dear wife Rose and our beloved children; Thomas, Delphin and Michael for their encouragement and support during the entire period of study.

## ABSTRACT

Textile factories such as Rift Valley Textile Limited (RIVATEX) in Eldoret Kenya produce large volumes of wastewater which is alkaline, highly coloured and has high chemical oxygen demand (COD) and can adversely affect human health and aquatic life. Two electrochemical oxidation methods using boron doped diamond (BDD) and stainless steel (SS) anode were investigated for the treatment of such wastewaters. Two dyes widely used at RIVATEX namely; C.I. Reactive Red 76 (RR) and C.I. Disperse Blue 79 (DB) were used as model dyes and the parameters studied were:- applied voltage, dye concentration, supporting electrolyte, current density, surface area to volume ratio, inter-electrode distance, pH and temperature. Treated water was then analyzed for pH, colour, electrical conductivity and chemical oxygen demand. Scanning electron microscopy-energy dispersive x-ray spectroscopy (SEM/EDX) was carried out to characterize SS electrode while UV-VIS was used to study the degradation of dye molecules. The optimum conditions obtained using SS were; potential difference of 10 V, S/V ratio of 16 m<sup>2</sup>/m<sup>3</sup> in RR and 20 m<sup>2</sup>/m<sup>3</sup> in DB, NaCl supporting electrolyte 4g/l and 6g/l in RR and DB respectively, electrode gap of 12 mm and a pH of 6.5. It was found that increasing current density led to a reduction in treatment time and a reduction in COD while increasing temperatures led to reduction in specific energy consumption as well as electrocoagulation time. It was found that DB had a lower specific energy consumption compared to RR. Electrocoagulation with SS anode produced Fe (III) hydroxide coagulant resulting from oxidation of Fe. Dye molecules were destabilized and formed “flocs” which were adsorbed on the surface of coagulant. The optimum conditions for BDD were; pH 8, temperatures below 40 °C, dye concentrations below 10 mg/L, electrode gap of 12 mm, current density of 300 Am<sup>-2</sup>, 4g/l NaCl (RR) and 2g/l Na<sub>2</sub>SO<sub>4</sub> (DB). Addition of NaCl reduced both degradation time and specific energy more than Na<sub>2</sub>SO<sub>4</sub>. Increasing current density enhanced degradation and reduced treatment time by 50 % while high temperatures reduced degradation efficiency. Increasing dye concentration led to increased specific energy consumption and treatment time. RR required lower specific energy and less time for complete mineralization than DB. SEM/EDX studies indicated that the SS electrode was chromic steel that underwent surface corrosion during electrocoagulation process. UV-VIS spectroscopy indicated that decolourization was achieved completely with SS and BDD electrodes. Hydroxyl radicals were developed on the BDD surface and degraded the dye molecule by oxidizing the organic molecule and shifting the absorption spectra from the VIS region. NaCl electrolyte was found to be superior to Na<sub>2</sub>SO<sub>4</sub> in degradation efficiency as high COD removal of 84 – 94 % was obtained at 30 – 60 Am<sup>-2</sup> current densities. Treatment of RIVATEX wastewaters required 180 min for 92 % COD reduction; however colour removal was achieved in 20 min. The key parameters in degradation were; pH, supporting electrolyte, current density and temperature. It was concluded that RIVATEX can adopt and use combined textile wastewater treatment technologies for colour removal followed by organic degradation.

**TABLE OF CONTENTS**

<b>DECLARATION .....</b>	<b>I</b>
<b>DEDICATION .....</b>	<b>II</b>
<b>ABSTRACT .....</b>	<b>III</b>
<b>TABLE OF CONTENTS .....</b>	<b>IV</b>
<b>LIST OF TABLES .....</b>	<b>XI</b>
<b>LIST OF FIGURES .....</b>	<b>XII</b>
<b>LIST OF PLATES .....</b>	<b>XVI</b>
<b>LIST OF ABBREVIATIONS .....</b>	<b>XVII</b>
<b>ACKNOWLEDGEMENT .....</b>	<b>XIX</b>
<b>CHAPTER ONE .....</b>	<b>1</b>
<b>INTRODUCTION .....</b>	<b>1</b>
<b>1.1 Background of the study .....</b>	<b>1</b>
<b>1.2 Problem statement .....</b>	<b>2</b>
<b>1.3 Objectives .....</b>	<b>3</b>

1.3.1 Overall Objective .....	3
1.3.2 Specific objectives.....	3
<b>1.4 Justification of the study .....</b>	<b>3</b>
<b>1.5 Hypotheses.....</b>	<b>4</b>
<b>CHAPTER TWO .....</b>	<b>5</b>
<b>LITERATURE REVIEW .....</b>	<b>5</b>
<b>2.1 Textile Dyes .....</b>	<b>5</b>
2.1.1 Disperse dyes .....	5
2.1.2 Reactive dyes .....	6
<b>2.2 Structures of dyes.....</b>	<b>6</b>
2.2.1 Reactive Dyes .....	6
2.2.2 Disperse Dyes .....	7
<b>2.3 Methods of wastewater treatment .....</b>	<b>8</b>
2.3.1 Electrochemical Mineralization of Organic Pollutants .....	8
2.3.4 Electrocoagulation methods.....	10
2.3.5 Chemical Coagulation and Flocculation.....	14
2.3.6 Advanced Oxidation Methods .....	15
2.3.7 Biological methods.....	16
2.3.8 Membrane filtration methods.....	16
2.3.9 Air flotation methods.....	16

2.3.10 Adsorption of industrial pollutants.....	17
<b>2.4 Water quality .....</b>	<b>18</b>
2.4.1 pH.....	18
2.4.2 Colour.....	19
2.4.3 Alkalinity .....	19
2.4.4 Chemical oxygen demand.....	20
2.4.5 Biochemical oxygen demand .....	20
<b>2.5 Scanning Electron microscopy.....</b>	<b>21</b>
<b>2.6 Energy Dispersive X-ray spectroscopy .....</b>	<b>22</b>
<b>CHAPTER THREE .....</b>	<b>23</b>
<b>MATERIALS AND METHODS .....</b>	<b>23</b>
<b>3.1 Experimental design.....</b>	<b>23</b>
<b>3.2 Chemicals, reagents and electrodes .....</b>	<b>23</b>
<b>3.3 Electrochemical cell .....</b>	<b>23</b>
3.3.1 Effect of voltage.....	25
3.3.2 Effect of dye concentration.....	25
3.3.3 Effect of supporting electrolytes .....	25
3.3.4 Effect of current density .....	25
3.3.5 Effect of surface area to volume ratio .....	26
3.3.6 Effect of Inter-electrode distance .....	26

3.3.7 Effect of contact time .....	26
3.3.8 Effect of pH.....	27
3.3.9 Effect of temperature.....	27
<b>3.4 Physico-chemical properties of effluent .....</b>	<b>27</b>
3.4.1 pH.....	27
3.4.2 Colour .....	28
3.4.3 Electrical conductivity.....	28
3.4.4 Chemical oxygen demand.....	28
<b>3.5 Microscopy and spectroscopic analysis .....</b>	<b>30</b>
3.5.1 UV-VIS studies .....	31
3.5.2 SEM and EDX Analysis .....	31
<b>3.6 Data analysis.....</b>	<b>32</b>
<b>CHAPTER FOUR.....</b>	<b>33</b>
<b>RESULTS AND DISCUSSION.....</b>	<b>33</b>
<b>4.1 Physicochemical characteristics of RIVATEX raw wastewater.....</b>	<b>33</b>
<b>4.2 The effects of electrochemical process parameters on specific energy in synthetic dye wastewater using steel anode. ....</b>	<b>34</b>
4.2.1 Effect of voltage.....	34
4.2.2 Effect of dye concentration.....	35
4.2.3 Effect of surface area to volume ratio .....	37



4.2.4	Effect of supporting electrolytes .....	39
4.2.5	Effect of pH.....	42
4.2.6	Effect of Inter-electrode distance .....	44
4.2.7	Effect of current density .....	46
4.2.8	Effect of temperature .....	48
4.2.9	Colour removal studies by UV-VIS .....	50
<b>4.3 Effects of electrocoagulation on physico-chemical parameters using optimized conditions .....</b>		<b>51</b>
4.3.1	Effect of dye concentration.....	51
4.3.2	Effect of colour removal on effluent pH.....	52
4.3.3	Effect of current density on chemical oxygen demand. ....	54
<b>4.4 Electrode mass losses .....</b>		<b>55</b>
<b>4.5 SEM and EDX images of Stainless Steel Electrode.....</b>		<b>57</b>
<b>4.6 Effects of electrochemical process parameters on the degradation of synthetic textile dye wastewater using BDD anode. ....</b>		<b>60</b>
4.6.1	Effect of current density .....	60
4.6.2	Effect of pH.....	62
4.6.3	Effect of temperature.....	64
4.6.4	Effect of dye concentration .....	66
4.6.5	Effect of electrode gap.....	67
4.6.6	Effect of supporting electrolytes .....	68

<b>4.7 UV-VIS studies .....</b>	<b>70</b>
<b>4.8 Effect of Stainless Steel electrocoagulation on chemical oxygen demand of synthetic dye wastewater .....</b>	<b>75</b>
<b>4.9 Electrochemical treatment of RIVATEX wastewater using Stainless Steel anode ...</b>	<b>76</b>
4.9.1 Effect of pH.....	76
4.9.2 Effect of inter-electrode distance .....	77
4.9.3 Effect of surface area to volume ratio .....	78
4.9.4 Effect of supporting electrolyte.....	78
4.9.5 Effect of temperature .....	80
4.9.6 Effect of Stainless Steel anode treatment on chemical oxygen demand .....	81
<b>4.10 Electrochemical mineralization of RIVATEX waste water using BDD anode ..</b>	<b>82</b>
4.10.1 Effect of pH on degradation .....	82
4.10.2 Effect of Electrode gap .....	83
4.10.3 Effect of supporting electrolytes .....	84
4.10.4 Effect of temperature .....	85
4.10.5 Effect of BDD treatment on Chemical oxygen demand .....	86
<b>4.11 Specific energy consumption.....</b>	<b>88</b>
<b>CHAPTER FIVE .....</b>	<b>90</b>
<b>CONCLUSION AND RECOMMENDATIONS.....</b>	<b>90</b>
<b>5.1 Conclusion .....</b>	<b>90</b>

<b>5.2 Recommendations .....</b>	<b>93</b>
<b>REFERENCES .....</b>	<b>94</b>
<b>APPENDICES.....</b>	<b>107</b>
<b>APPENDIX I: ELECTROCHEMICAL DATA USING STEEL ANODE .....</b>	<b>107</b>
<b>APPENDIX II: ELECTROCHEMICAL MINERALIZATION USING BORON DOPED DIAMOND ANODE.....</b>	<b>121</b>

**LIST OF TABLES**

Table 2.1: Oxidation power of the anode material in acid media.....	9
Table 4.1: Characteristics of RIVATEX wastewater.....	33
Table 4.2: Effect of S/V on current density for RR and DB dyes.....	38
Table 4.3: Effect of electrocoagulation on wastewater pH for DB and RR dyes.....	53
Table 4.4: Effect of current density (CD) on electrode mass for RR and DB dyes.....	55
Table 4.5: Conductivity of NaCl and Na <sub>2</sub> SO <sub>4</sub> as a function of concentration for RR and DB dyes (μS/cm).....	70
Table 4.6: Chemical oxygen demand using NaCl and Na <sub>2</sub> SO <sub>4</sub> supporting electrolytes, mg/L.....	75
Table 4.7: Effect of temperature on current density and current using NaCl and Na <sub>2</sub> SO <sub>4</sub> .....	81
Table 4.8: Effect of supporting electrolytes on Chemical Oxygen Demand levels.....	82
Table 4.9: Oxidizing potential for conventional oxidizing agents.....	88
Table 4.10: Specific energy consumption, kWh/m <sup>3</sup> for RIVATEX wastewater, RR and DB model dyes in presence of electrolyte using SS and BDD electrodes.....	89

## LIST OF FIGURES

Figure 2.1: General Structure of reactive dyes.....	7
Figure 2.2: Structure of Disperse Blue 79.....	7
Figure 4.1: Effect of voltage on specific energy consumption with 1g/L NaCl and 10 mm inter electrode spacing.....	34
Figure 4.2: Effect of dye concentration at 10 and 12 V on a) DB, b) RR .....	35
Figure 4.3: Effect of surface area/ volume ratio at 10 V, 10 mm inter-electrode spacing and 1% NaCl supporting electrolyte.....	38
Figure 4.4: Effect of supporting electrolytes on specific energy consumption using 10 mg/L dyes a) NaCl b) Na <sub>2</sub> SO <sub>4</sub> on RR and DB dyes.....	39
Figure 4.5: Effect of supporting electrolytes and concentration on decolourization of a) RR and b) DB dyes.....	40
Figure 4.6: Effect of wastewater pH on specific energy consumption at 10 mm electrode spacing, 1% NaCl and 10 V for RR and DB dyes.....	42
Figure 4.7: Crystal field stabilization energy of a) Fe <sup>2+</sup> b) Fe <sup>3+</sup> system.....	43
Figure 4.8: Effect of inter-electrode spacing on specific energy consumption using 10 V, 1% NaCl and 250 mL wastewater for RR and DB dyes.....	43
Figure 4.9: Effect of current density on a) specific energy consumption at 10 mg/L and 50mg/L b) decolourization at 10 and 50 mg/L dye concentrations.....	47
Figure 4.10: Effect of temperature on a) specific energy consumption and b) colour removal	

time in RR and DB dyes.....	49
Figure 4.11: Effect of current density on colour removal time using 10 mg/L of a) DB dye and b) RR dye.....	50
Figure 4.12: Effect of concentration on specific energy consumption of RR and DB dyes...	52
Figure 4.13: Effect of current density on COD removal for RR and DB dyes.....	54
Figure 4.14: Effect of current density on a) Electrode mass loss b) Faradaic mass differences for RR and DB dyes.....	56
Figure 4.15: Effect of current density on specific energy consumption using 10 mg/L dye concentration for both RR and DB dyes.....	61
Figure 4.16: Effect of current density on dye degradation time at 10 mg/L dye concentration for RR and DB dyes.....	62
Figure 4.17: Effect of dye pH on a) specific energy consumption and b) degradation time; using 10 mg/L dye concentration for RR and DB dyes.....	63
Figure 4.18: Effect of temperature on a) specific energy consumption and b) degradation time; at 10 mg/L dye concentration of RR and DB dyes.....	65
Figure 4.19: Effect of dye concentration on a) specific energy consumption and b) degradation time using 10 mg/L dye concentration for RR and DB dyes.....	66
Figure 4.20: Effect of electrode gap on a) specific energy consumption and b) degradation time using 10mg/L dye concentration for RR and DB dyes.....	67
Figure 4.21: Effect of supporting electrolytes and concentration on a) specific energy and b) degradation time of RR and DB at 10mg/L.....	69

Figure 4.22a: UV-VIS absorption spectrum of DB.....	71
Figure 4.22b: UV-VIS absorption spectrum of RR.....	72
Figure 4.22c: UV-VIS absorption spectrum of raw DB sample (green) with SE and clarified wastewater (blue and pink).....	73
Figure 4.22d: UV-VIS absorption spectrum of Clarified water at DB 30 mg/L (blue), RR 30 mg/L (red) and DB 10 mg/L (black).....	74
Figure 4.23: Effect of pH on specific energy consumption (kWh/m <sup>3</sup> ) and colour removal time.....	76
Figure 4.24: Effect of electrode gap on specific energy consumption and colour removal time.....	77
Figure 4.25: Effect of surface area to volume ratio on specific energy consumption and colour removal time.....	78
Figure 4.26: Effect of supporting electrolytes on decolourization and specific energy of RIVATEX waste water.....	79
Figure 4.27: Effect of temperature of on a) specific energy consumption and b) coagulation time of RIVATEX wastewater using NaCl and Na <sub>2</sub> SO <sub>4</sub> .....	80
Figure 4.28: Effect of pH on decolourization of RIVATEX wastewater using NaCl electrolyte.....	82
Figure 4.29: Effect of electrode gap on decolourization of RIVATEX wastewater.....	83
Figure 4.30: Effect of supporting electrolytes on decolourization and specific energy consumption of RIVATEX wastewater.....	85
Figure 4.31: Effect of temperature on a) specific energy consumption demand and b)	

degradation time of RIVATEX wastewaters.....	86
Figure 4.32a: Effect of time on COD levels of RIVATEX wastewater using BDD.....	87
Figure 4.32b: Effect of time on % COD reduction in RIVATEX wastewater using BDD.....	87



**LIST OF PLATES**

Plate 1: SEM image of SS electrode before electrocoagulation.....	57
Plate 2a: SEM image of SS electrode after electrocoagulation with NaCl adsorbed on surface .....	58
Plate 2b: SEM image of SS electrode after cleaning the electrode in distilled water .....	58
Plate 3: EDX spectrum of SS electrode .....	59
Plate 4: EDX spectrum of SS electrode after electrocoagulation using NaCl as the SE.....	60

**LIST OF ABBREVIATIONS**

AC	Alternating current
AOP	Advanced oxidation processes
BDD	Boron doped diamond electrode
BOD	Biochemical oxygen demand
CD	Current density
COD	Chemical oxygen demand
CRD	Complete randomized design
DB	Disperse Blue
DC	Direct current
DO	Dissolved oxygen
EDX	Energy dispersive x-ray spectroscopy
EOP	Electro oxidation potential
FAS	Ferrous ammonium sulphate
MB	Methylene blue dye
MCL	Maximum contaminant level
NEMA	National environmental Management Authority
pH	power of hydrogen
RIVATEX	Rift Valley Textile Factory
RR	Reactive red dye
SEM	Scanning electron microscopy
SS	Stainless steel
S/V	Surface area to volume ratio

TEM	Transmission electron microscopy
UV-VIS	Ultraviolet –Visible spectroscopy

## ACKNOWLEDGEMENT

I would like to extend my sincere gratitude to the people who contributed directly or indirectly to this work. First, I thank my supervisors, Prof. F.K. Segor, Prof. J. Irina and Prof. M. P. Tole for the mentorship, guidance and encouragement they afforded me in the entire process of research and preparation of thesis. I also wish to thank the entire staff of Chemistry and Biochemistry Departments of the University of Eldoret and Pwani University for the assistance they accorded me during my studies.

Secondly, my sincere thanks also go to the Director, Rivatex East Africa Limited (RIVATEX) for providing me with the dye materials and wastewater from the Factory. I also extend my gratitude to Dr. P. Guyo of Pwani University for assisting in the design of treatments, Dr. G. Otieno for SEM/EDX analysis at Oxford University, Mr. Habel Mwarabu and Mr. Erastus Kailo of Pwani University for laboratory experiments. I would also like to acknowledge National Commission for Science, Technology and Innovation, Kenya (NACOSTI) for awarding me a PhD STI research grant No. NCST/5/003/3<sup>rd</sup> CALL PhD /072, to carry out this research. I sincerely wish to thank my wife Mrs. Rose Kambale for encouraging me during the research period and editing my work.

To God is glory forever!

## CHAPTER ONE

### INTRODUCTION

#### 1.1 Background of the study

There are more than 100,000 types of commercially available dyes with over  $7 \times 10^5$  tons of dyes produced yearly. Direct, reactive, acid, disperse, pre-metalized, vat and basic dyes account for about 85% of the total dyes used in the industry. The total dye consumption of the textile industries alone is in excess of  $10^7$  kg/year and an estimated 90% of this total end-up on fabric (Hameed *et al.*, 2007), with the balance 10% ending up in waste streams. Consequently, approximately  $10^6$  kg/year of dyes are discharged into the waste streams by textile industries. Dyeing industry effluents constitute one of the most problematic wastewaters to be treated not only for their high chemical and biological oxygen demands, total suspended solids and content of toxic compounds but also for colour. The human eye can detect concentration of 0.005 mg/L of dye in water and therefore, the presence of dye exceeding this limit would not be permitted on aesthetic grounds and may also be toxic to the aquatic environment (Pearce *et al.*, 2003).

Typical textile dye wastewater composition is quite complex. These waste streams contain dyeing process auxiliaries that may include xylenes, phenols, buffers, bleaches and scouring agents, water softeners, surfactants, enzymes, caustic compounds and acids (Martinez & Brillas, 2009). Considering both volumes discharged and effluent composition, the wastewater generated by the textile industry is rated as the most polluting among all the industrial sectors (Reid and Green, 1996). Dyes usually have synthetic origins and complex aromatic molecular structures which make them stable and difficult to biodegrade. Textile dyes are also designed to be fast. They must also be

resilient to both high temperatures and enzyme degradation resulting from the detergent washing. For these reasons, biodegradation of dyes is typically a very slow process and due to dye characteristics, wastewater containing dyes must be properly treated before being discharged to the environment. Dyes have also been found to be potentially health hazardous to human beings and have other adverse impacts such as toxicity to aquatic life (Zawani *et al.*, 2009).

## **1.2 Problem statement**

Water quality regulations have been set by National Environmental management Authority (NEMA) in Kenya. The NEMA Water Quality Regulations of 2006 gives guidelines for domestic water quality and also monitoring guide for discharge into the environment. According to schedule 4, the parameters most critical to monitor for textile discharge are; pH, biochemical oxygen demand (BOD), total suspended solids (TSS) chemical oxygen demand (COD), colour, phenols, sulphide, total chromium, temperature, fecal coliforms, oil and grease (Water Quality Regulations of 2006). Disposal of textile wastewater in RIVATEX is a major concern as large volumes of waste water are released daily during factory processing procedures. The discharged effluent has high pH, chemical oxygen demand (COD) and colour hence not safe for discharge to water courses. Conventional methods for waste water treatment cannot remove the dyes from the wastewater hence if released to natural water bodies will affect aquatic environment and man. The constitution of Kenya grants everyone in Kenya the right to a clean and healthy environment.

This study is geared towards developing a low cost and environmentally friendly method

that is reliable and efficient, capable of treating textile wastewater in RIVATEX to meet National standards for re-use or discharge to a water course with no pollution.

### **1.3 Objectives**

#### **1.3.1 Overall Objective**

The overall objective of this study was to determine the most effective parameters for the electrochemical treatment of textile dye wastewaters using stainless steel and Boron Doped Diamond anodes to meet NEMA environmental discharge standards.

#### **1.3.2 Specific objectives**

- i). To determine the effects of voltage, dye concentration, surface area to volume ratio, supporting electrolyte, pH, inter-electrode distance, current density and temperature on specific energy consumption (a) using SS anode and (b) using BDD anode.
- ii). To determine the effects of pH, supporting electrolyte, inter-electrode distance and temperature on specific energy consumption of RIVATEX wastewater using SS and BDD anode.
- iii). To determine the effect of electrochemical treatments on the chemical oxygen demand of synthetic and RIVATEX treated wastewater using BDD and SS anodes.

### **1.4 Justification of the study**

The RIVATEX wastewater is discharged into river Sosiani which is a tributary of river

Nzoia that drains into Lake Victoria. Colour, inorganic and organic pollutant loads affect the quality of water hence should be removed before discharge to water bodies. Electrochemical methods have proved to be effective in colour removal and wastewater treatment in tea wastewater (Maghanga *et al.*, 2009 a, b) and paper and pulp wastewaters (Etiégni *et al.*, 2007) and hence are useful in industrial wastewater management.

Electrochemical method for the mineralization of organic pollutants is a new technology that has attracted great attention recently and is in competition with the process of chemical oxidation (Khataee and Habibi, 2010). However, the method is only useful for the treatment of dilute wastewater (Ayten *et al.*, 2011). Because the process gradually breaks down the contaminant molecules, no residue of the original material remains, hence no sludge requiring disposal to landfill is produced (Comninellis and Chen, 2010).

In this study electrochemical treatment using boron doped diamond (BDD) electrodes and stainless steel (SS) as anode materials were investigated for degradation of textile wastewater.

### **1.5 Hypotheses**

- i). Current density, pH and supporting electrolyte are the main parameters that affect the removal of pollutants in dye wastewaters.
- ii). BDD electrodes have higher specific energy consumption than sacrificial steel electrodes in the removal of pollutants from dye wastewater.
- iii). BDD electrodes have better efficiency in removal of COD than steel electrodes.



## CHAPTER TWO

### LITERATURE REVIEW

#### 2.1 Textile Dyes

Dyes are generally classified as anionic (direct, acid, and reactive dyes), cationic (basic dyes), and nonionic (disperse dyes). The chromophores found in ionic and nonionic dyes mostly consist of azo groups or anthraquinone types (Srinivasan and Viraragharan, 2010). Azo dye compounds constitute almost a half of the dyes that are used in the textile industry (Baiocchi *et al.*, 2002). This group of compounds is characterized by the presence of the azo group ( $-N=N-$ ) chromophore, which is associated with aromatic systems and other groups, such as hydroxyls ( $-OH$ ) and sulphonic groups ( $-SO_3H$ ) (Augugliaro *et al.*, 2002). The azo group can be present once or many times in the molecular structure of a compound. An environmental problem associated with the use of azo dyes in the textile industry is the high consumption of potable water and where it is scarce; wastewater recycling has been recommended (Santos *et al.*, 2008).

##### 2.1.1 Disperse dyes

The use of disperse dyes has increased in the textile industry ever since the discovery of synthetic fibers. Most of them contain amino or substituted amino groups and dyes in this class are almost totally insoluble in water. Disperse dyes exist as dispersion of microscopic particles with only a tiny amount of solution at any time in the dye bath. These are the only dyes effective for polyester while some types are used for nylon and acetate (Azban, 2004).

### **2.1.2 Reactive dyes**

Reactive dyes are characterized by their ready water solubility as well as their high stability and persistence due to their complex structure. They are designed to have high resistance against degradation by any means (Brown and Hamburger, 1987). Reactive dyes in nature are non toxic. However, under anaerobic conditions, they may break down into aromatic amines which are potentially carcinogenic and toxic (Pinheiro *et al.*, 2004). Reactive dyes contain one or more groups capable of forming covalent bonds with the hydroxyl groups of cellulosic fibers with the amino, hydroxyl, and mercapto groups of protein fibres; and with the amino groups of polyamides (Zollinger, 1991).

## **2.2 Structures of dyes**

### **2.2.1 Reactive Dyes**

These dyes contain reactive groups and in the colour index (CI) is the second largest dye class. The reactive dyes form covalent bonds with -OH, -NH-, or -SH groups of fibers. The general structure of reactive dyes is shown in Figure 2.1. The reactive group is often a heterocyclic aromatic ring substituted with chloride or fluoride or vinyl sulphone. The hydrolysis of a reactive group during dyeing lowers the degree of fixation of reactive dyes which create the problem of coloured effluent.

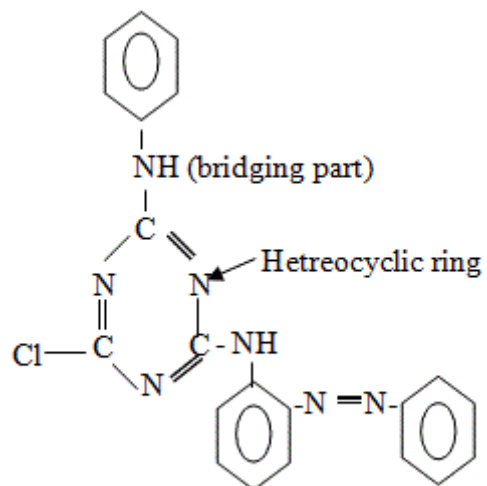


**Figure 2.1: General Structure of a reactive dye**

### 2.2.2 Disperse Dyes

Disperse dyes are highly water insoluble and are used for dyeing polyester and acetate fibers. Disperse dye molecule is the smallest dye molecule among all dyes. It is based on an azo benzene or anthraquinone molecule with nitro, amine, hydroxyl, etc. groups attached to it. The structure of C.I Disperse Blue 79 is shown in Figure 2.2

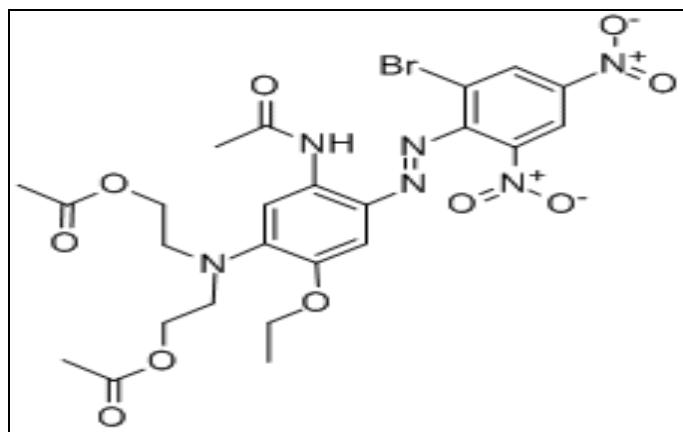


**Figure 2.2: Structure of C.I. Disperse Blue 79**

## **2.3 Methods of wastewater treatment**

### **2.3.1 Electrochemical Mineralization of Organic Pollutants**

Biological treatment of polluted water is the most economical process and it is used for the elimination of readily degradable organic pollutants present in wastewater. However, the situation changes when the wastewater contains toxic and refractory organic pollutants which are resistant to biological treatment. Complete mineralization of the organic pollutants is preferred and can be achieved by complete oxidation using oxygen at high temperature or strong oxidants combined with UV radiation (Boye *et al.*, 2004).

The electrochemical method for the mineralization of organic pollutants is a new technology which is useful for the treatment of dilute wastewater with COD < 5 g/L. This method is in competition with the process of chemical oxidation using strong oxidants. The main advantage of this technology is that chemicals are not used. In fact, only electrical energy is consumed for the mineralization of organic pollutants (Chen *et al.*, 2005; Boye *et al.*, 2006).

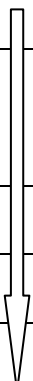
### **2.3.2 Influence of anode material on the reactivity of electrolytic hydroxyl radicals**

The reaction of organics with electro-generated electrolytic hydroxyl radicals is in competition with the side reaction of the anodic discharge of these radicals to oxygen. The activity of these electrolytic hydroxyl radicals are strongly linked to their interaction with the electrode surface. As a general rule, the weaker the interaction, the lower is the electrochemical activity toward oxygen evolution (high O<sub>2</sub> overvoltage anodes) and the higher is the chemical reactivity toward organics oxidation (Comninellis and Chen,

2010). Different anode materials can hence be classified according to their oxidation power in acid media (Table 2.1).

**Table 2.1: Oxidation power of the anode material in acid media**

Electrode	Oxidation potential (V)	Overpotential of O <sub>2</sub> evolution (V)	Oxidation power of the anode
RuO <sub>2</sub> -TiO <sub>2</sub> (DSA-Cl <sub>2</sub> )	1.4-1.7	0.18	low oxidation power
IrO <sub>2</sub> -Ta <sub>2</sub> O <sub>5</sub> (DSA-O <sub>2</sub> )	1.5-1.8	0.25	
Ti/Pt	1.7-1.9	0.3	
Ti/PbO <sub>2</sub>	1.8-2.0	0.5	
Ti/SnO <sub>2</sub> -Sb <sub>2</sub> O <sub>5</sub>	1.9-2.2	0.7	
p-Si/BDD	2.2-2.6	1.3	High oxidation power



**Source: (Comninellis and Chen, 2010)**

The oxidation potential of the anode (which corresponds to the onset potential of oxygen evolution) is directly related to the overpotential for oxygen evolution and to the adsorption enthalpy of hydroxyl radicals on the anode surface. This implies that for a particular anode material, the higher the O<sub>2</sub> overvoltage the higher is its oxidation specific energy (Comninellis and Chen, 2010).

A low oxidation specific energy anode is characterized by a strong electrode-hydroxyl radical interaction resulting to a high electrochemical activity for the oxygen evolution reaction (low overvoltage anode) and to a low chemical reactivity for organics oxidation

(low current efficiency for organics oxidation). A typical low oxidation specific energy anode is the IrO<sub>2</sub>-based electrode. This anode has a strong interaction between IrO<sub>2</sub> and hydroxyl radical such that a higher oxidation state of oxide IrO<sub>3</sub> can be formed. This higher oxide can act as mediator for both organics oxidation and oxygen evolution. However, a high oxidation specific energy consumption anode is characterized by a weak electrode–hydroxyl radical interaction resulting to a low electrochemical activity for the oxygen evolution reaction (high overvoltage anode) and to a high chemical reactivity for organics oxidation (high current efficiency for organic oxidation) (Chen and Chen, 2006).

### **2.3.3 Electrode materials in organic degradation of wastewater**

Although organic wastes in general can be oxidized at numerous electrode materials, the electrochemical effects depend on the kinds and structure of anode materials (Stucki *et al.*, 1991; Feng and Li, 2003). The current efficiency is usually found to be poor with the electrode graphite or Ni (James *et al.*, 1999). Some organics can be degraded quickly at Pt anode, but it is reported that phenols can cause the inactivation of Pt anode by the deposition of oligomers (Comninellis and Pulgarin, 1991). A great success in development has been obtained since the discovery of dimensionally stable anodes (Jose *et al.*, 2008).

### **2.3.4 Electrocoagulation methods**

In the Industrial applications using sacrificial electrodes, electrochemical process has been known to be highly dependent on the chemistry of the wastewater, especially its

conductivity. In addition, other characteristics such as pH, particle size, and chemical constituent influence the process (Kashefialasl, et al., 2006). This method has been applied in the treatment of tea wastewater (Maghanga et al., 2009a), dye wastewaters (Kashefialasl et al., 2006), textile dye wastewater (Baryamoglu et al., 2007), restaurant wastewater (Chen et al., 2003), semiconductor wastewater (Lai and Lin, 2003), distillery alcohol wastewater (Yavuz, 2007), tannery wastewater (Mugurananthan et al., 2004), dairy wastewater (Sengal and Oscar, 2006), pulp and paper mill effluent (Orori et al., 2005) among others. Catalysts have also been introduced to make electrocoagulation more efficient in the treatment of dye wastewater (Yangming et al., 2006). Electrochemical treatment combined with wood ash leachate was effective in Kraft and paper mill colour reduction in Kenya. However, over electrical polarization within electrodes, which causes excess voltage remains the biggest impediment in this method (Orori et al., 2005; Eteigni et al., 2007).

There has been a range of laboratory, pilot and industrial scale electrocoagulation units produced with the designs ranging from fully integrated units to unit reactors. The design of the electrocoagulation process influences its operation and efficiency and should consider geometry, scale up issues and current density (Holt et al., 2006). Geometry of the reactor affects operational parameters including bubble path, flotation effectiveness, floc formation, fluid flow regime and mixing/settling characteristics. The most common approach involves plate electrodes (aluminium or iron). Water is dosed with dissolved metal ions as it passes through the electrocoagulation cell.

The surface area to volume ratio (S/V) was anticipated as being a significant scale-up parameter. Electrode area influences current density, position and rate of cation dosage,

as well as bubble production and bubble path length. As the S/V ratio increases the optimal current density decreases (Mameri and Yeddou, 1998).

Current density is the current delivered to the electrode divided by the active area of the electrode and is expressed as A/m<sup>2</sup>. It is measured by varying the current using a supporting electrolyte such as a salt and maintaining the surface area of the electrode in contact with the solution. It determines both the rate of electrochemical metal dosing to the water and the electrolytic bubble density production. Current densities ranging from 10 to 2000 A/m<sup>2</sup> have been used; however current density in the range 10 to 150 A/m<sup>2</sup> has proved efficient (Cheng, 2004). Different current densities are desirable in different situations; high current densities are desirable for separation processes involving flotation cells or large settling tanks, while small current densities are appropriate for electro-coagulators that are integrated with conventional sand and coal filters. A systematic analysis is required to define and refine the relationship between current density and desired separation effects (Cheng, 2004).

The electrode material used affects the performance of the electrocoagulation reactor. The anode material used determines the cation introduced into solution. Several researchers have studied the choice of electrode material. The most common electrodes were aluminium or iron plates (Vik et. al. 1984). The size of the cation produced was suggested to contribute to the higher efficiency of iron electrodes as compared to aluminium electrodes in removal of organic waste (Baklan and Kolesnikova, 1996).

One of the greatest operational issues with electrocoagulation is electrode passivation. The passivation of electrode is concerned with the longevity of the process. Various methods of preventing and / or controlling electrode passivation have been investigated.



These include; changing polarity of the electrode; hydro mechanical cleaning; introducing inhibiting agents and mechanical cleaning of the electrodes. The most efficient and reliable method of electrode maintenance is to periodically clean the electrodes mechanically (Nikolaev et al., 1982).

In the electrocoagulation process, the destabilization mechanism of the contaminants, particulate suspension, and breaking of emulsions may be summarized as :- (1) Compression of the diffuse double layer around the charged species by the interactions of ions generated by oxidation of the sacrificial anode. (2) Charge neutralization of the ionic species present in wastewater by counter ions produced by the electrochemical dissolution of the sacrificial anode. These counter ions reduce the electrostatic interparticle repulsion to the extent that the van der Waals attraction predominates, thus causing coagulation as a zero net charge results in the process. (3) Floc formation: the floc formed as a result of coagulation creates a sludge blanket that entraps and bridges colloidal particles that are still remaining in the aqueous medium (Comninellis and Chen 2010). Water is also electrolyzed in a parallel reaction, producing small bubbles of oxygen at the anode and hydrogen at the cathode. These bubbles attract the flocculated particles and float the flocculated pollutants to the surface through natural buoyancy. In addition, other physiochemical reactions may also take place in the EC cell (Paul, 1996) such as :- (1) cathodic reduction of impurities present in wastewater; (2) discharge and coagulation of colloidal particles; (3) electrophoretic migration of the ions in solution; (4) electroflotation of the coagulated particles by O<sub>2</sub> and H<sub>2</sub> bubbles produced at the electrodes; (5) reduction of metal ions at the cathode; and (6) other electrochemical and chemical processes (Modirshahla et al., 2007).

The disadvantages of EC are:- the “sacrificial electrodes” are dissolved into wastewater as a result of oxidation, and need to be regularly replaced; the passivation of the electrodes over time has limited its implementation; the use of electricity may be expensive in many places and high conductivity of the wastewater suspension is required (Yildiz et al., 2007).

### **2.3.5 Chemical Coagulation and Flocculation**

Coagulation is a process in which destabilization of a given solution is effected and flocculation is the process whereby destabilized particles or the particles formed as a result of destabilization in the coagulation process, are induced to clump together, make contact and thereby form large agglomerates (Benefield *et al.*, 1982).

Flocculation is the addition of certain chemicals to water containing soluble and finely suspended impurities to form an insoluble gelatinous substance. The “floc” formed is denser than water and sinks to the bottom of the container absorbing colloidal matter. First, a coagulating chemical is applied to the water and for the chemical to react uniformly it must be distributed uniformly throughout the body of water by rapid agitation. Second, a complex chemical and physicochemical reactions and changes occur, leading to coagulation and the formation of the microscopic particles. Third, much more gentle agitation of the water causes the agglomeration of the particles; in other words, the fine particles are flocculated into settleable flocs (Benefield *et al.*, 1982; Skoog *et al.*, 1997). The main parameters affecting the destabilization reactions are initial humus concentration in the wastewater, coagulation pH, and coagulant dose.

Metal coagulants can be grouped into two categories; those based on aluminum, e.g.

aluminum sulphate, aluminum chloride and sodium aluminates and those based on iron, e.g. ferrous sulphate, ferric sulphate and ferric chloride. Mostly the choice of coagulants is made in laboratory by conducting a jar-test (Schulz and Okun, 1992). The most widely used coagulants for water treatment are aluminum and iron salts. The common metal salt is aluminum sulphate, which is a good coagulant for water containing organic matter. Iron coagulants are effective over a wide pH range and are generally more effective in removing colour from water, but they usually cost more than aluminum salts. For some waters, cationic polymers are effective as primary coagulant, but polymers are more commonly applied to aid coagulation. The final choice of coagulants and “chemical aids” is based on being able to achieve the contaminant removals and low turbidity desired in the filtered water at a lower cost (Song *et al.*, 2004; Prasad, 2008).

### **2.3.6 Advanced Oxidation Methods**

Advanced oxidation processes (AOPs) using  $O_3$ ,  $H_2O_2/UV$ ,  $Fe^{2+}/H_2O_2$  have been applied to remove colour and reduce COD from a polyester and acetate fiber dyeing effluent. Chemical treatment methods using alum,  $Al_2(SO_4)_3 \cdot 18H_2O$ ,  $FeCl_3$  and  $FeSO_4$  were compared with the AOPs. AOPs showed superior performance compared to conventional chemical treatment and achieved colour and COD removal of 50% and 60%, respectively. A combination of  $O_3 / H_2O_2$  among other AOPs methods gave the best results with 99% COD removal and 96% colour removal (Comminellis and Chen, 2010).

However, use of  $Fe^{2+}/H_2O_2$  showed a satisfactory COD and colour removal performance and was an economically viable choice for acetate and polyester fiber dyeing effluent on the basis of 90% colour removal (Azban *et al.*, 2004).

### **2.3.7 Biological methods**

Typical biological processes accomplish very low colour removal. In tea industry, constructed wetlands are introduced and the effluent passes through a series of ponds containing waterweeds. These waterweeds are selected on the basis of feeding on some nutrients especially nitrates and phosphates and also the ability to oxygenate the effluent through their roots. Reduction of COD and BOD are normally achieved, however colour removal remains a big problem for the tea industry (Zhen-Gang, 2008).

### **2.3.8 Membrane filtration methods**

Reverse osmosis and ultra filtration have been tested since 1970 and have proved to be effective in the removal of undesirable components from wastewater streams (DePinho *et al.*, 1996). High membrane cost and fouling occurrence has made this method economically impossible for a pulp and paper mill wastewater treatment (Manjunath and Mehrotra, 1981).

### **2.3.9 Air flotation methods**

Air flotation is a new method of colour removal as well as reduction of suspended solids. The principle behind this process is the de-linking operation using air flotation. The pre-treatment of the effluent by air flotation by membrane reduced drastically the bottleneck of employing membranes in the effluent wastewater of Kraft pulp and paper industry (Pinho *et al.*, 2000).

The process combines flotation of dissolved gases to remove suspended solids particularly colloidal matter responsible for membrane fouling, followed by ultra filtration to remove the chromophores in the effluent. Dissolved air flotation is optimized both in terms of carrier gases, air and carbon dioxide, and operating conditions, pressure and recirculation rate. Air flotation and ultra filtration reduced colour by 30% and over 90%, respectively (Pinho *et al.*, 2000).

### **2.3.10 Adsorption of industrial pollutants**

Fly ash has been utilized as a potential low-cost adsorbent for the removal of methylene blue, malachite green and rhodamine B from artificial textile wastewater. Adsorption of these dyestuffs has been studied in terms of various process factors such as initial concentration, pH, and temperature and contact time (Singer and Reckhow, 1999).

A study investigating the ability of rice husk to adsorb methylene blue (MB) from aqueous solution was carried out in a fixed-bed column. The effects of important parameters, such as the value of initial pH, type of salt and its concentration, the flow rate, the influent concentration of MB and bed depth, were studied. The Thomas model was applied to adsorption of MB at different flow rate, effluent concentration and bed depth to predict the breakthrough curves and to determine the characteristic parameters of the column useful for process design using non-linear regression (Holt *et al.*, 2006). In a study by Qaiser *et al* (2007), the powder of the leaves of *Ficus religiosa* was found to be a very good adsorbent for hexavalent chromium and lead.

## **2.4 Water quality**

The NEMA Water Quality Regulations of 2006 gives guidelines for domestic water quality and also monitoring guide for discharge into the environment. According to schedule 4, the parameters most critical to monitor for textile discharge are; pH, biochemical oxygen demand (BOD), total suspended solids (TSS) chemical oxygen demand (COD), colour, phenols, sulphide, total chromium, temperature, fecal coliforms, oil and grease (GOK, 1999).

### **2.4.1 pH**

Water pH is one of the most common water quality measurements made because it influences many chemical, physical, and biological processes. The pH dramatically influences the bioavailability of some nutrients, metals, and pesticides to plants and animals. It may also influence the bioavailability and fate of several other environmental contaminants (Bobe *et al.*, 1998).

The pH of soil and water within the environment can significantly influence many different chemical bioavailability and fate processes and for most natural waters it ranges from 6 - 9 due to bicarbonate buffering. A pH from 6.5 to 9.0 is tolerated by most fish (Burton and Pitt, 2002) while 6.0 to 6.5 is not likely to be harmful to fish unless the CO<sub>2</sub> concentration is greater than 100 mg/L (Burton and Pitt, 2002). Water and soil pH can dramatically impact the fate of some organic pesticides in the environment. Some pesticides degrade more quickly within certain pH ranges and are more stable within others. Several pesticides belonging to the carbamate and organophosphorus chemical

families degrade more quickly by hydrolysis at alkaline pH relative to neutral or acidic conditions (Gunasekara *et al.*, 2007). The pH of water and the soil solution can have profound impacts on the bioavailability of nutrients. In order for nutrients in the soil to be useful for plant growth and maintenance, they must be dissolved within the soil solution so they can enter and move through the plant. Soil pH is especially important for nutrients such as phosphorus and for micronutrients such as copper, iron, zinc, and aluminum (Schachtman *et al.*, 1998).

#### **2.4.2 Colour**

Water clarity refers to the transparency or clearness of water. Turbidity is caused by presence of suspended and colloidal materials such as clay, silt, finely divided organic and inorganic matter, and plankton or other microscopic organisms. The causes of colour are; turbidity, natural metallic ions (iron and manganese), humus and peat materials, plankton, weeds, and industrial wastes. Metallic ions such as iron and manganese typically impart a reddish-brown colour to water. Tannins and dissolved organic carbon, a by-product of the degradation of plants and other organisms, usually impart a brown to black colour to water. Some living plants such as Parrot feather (*Myriophyllum aquaticum*) also release coloured organic compounds into the water column (Holt *et al.*, 2006).

#### **2.4.3 Alkalinity**

Alkalinity is a measure of the acid-neutralizing capacity of water. It is an aggregate

measure of the sum of all titratable bases in the sample. Alkalinity in most natural waters is due to the presence of carbonate ( $\text{CO}_3^{2-}$ ), bicarbonate ( $\text{HCO}_3^-$ ), and hydroxyl ( $\text{OH}^-$ ) anions. However, borates, phosphates, silicates, and other bases also contribute to alkalinity if present. This property is important when determining the suitability of water for irrigation and / or mixing some pesticides and when interpreting and controlling wastewater treatment processes. Alkalinity is usually reported as equivalents of calcium carbonate (APHA, 2002).

#### **2.4.4 Chemical oxygen demand**

Generally, COD represents the reduction of dissolved oxygen (DO) caused by chemical reactions. It is widely used to represent the overall level of organic contamination in wastewater; the larger the COD value, the more oxygen the wastewater discharge demands from the receiving water body. However, in some water quality models COD is used to represent the oxygen demand from reduced substances, such as sulphide in saline water or methane in freshwater (Cerco and Cole, 1994; Park *et al.*, 1995). Both sulphide and methane are quantified in units of oxygen demand and are treated with the same kinetic formulation (Zhen-Gang, 2008).

#### **2.4.5 Biochemical oxygen demand**

Biochemical oxygen demand (BOD) is a measure of the total amount of oxygen removed from water biologically or chemically in a specified time and at a specific temperature. It indicates the total concentration of DO that is required during the degradation of organic



matter and the oxidation of some inorganic matter. Microorganisms require oxygen to decompose organic matter. Oxygen depletion can also result from oxygen - demanding chemical reactions, such as the nitrification process. BOD is therefore an indicator rather than a true physical or chemical substance. BOD is widely used to measure water quality pollution and has traditionally been the most important parameter for organic pollutions. However, BOD remains a key measurement of wastewater treatment plant discharges (Zhen-Gang, 2008).

### **2.5 Scanning Electron microscopy**

The scanning electron microscope (SEM) uses a focused beam of high-energy electrons to generate a variety of signals at the surface of solid specimens. The signals that derive from electron-sample interactions reveal information about the sample including external morphology (texture), chemical composition, and crystalline structure and orientation of materials making up the sample. In most applications, data are collected over a selected area of the surface of the sample, and a 2-dimensional image is generated that displays spatial variations in these properties. Areas ranging from approximately 1 cm to 5 microns in width can be imaged in a scanning mode using conventional SEM techniques with magnification ranging from 20X to about 30,000X, spatial resolution of 50 to 100 nm. The SEM is also capable of performing analyses of selected point locations on the sample and this approach is useful in qualitatively or semi-quantitatively determining chemical compositions (using energy dispersive x-ray spectroscopy), crystalline structure, and crystal orientations (Goldstein, 2003)

## **2.6 Energy Dispersive X-ray spectroscopy**

Energy Dispersive X-Ray spectroscopy (EDX), is an x-ray technique used to identify the elemental composition of materials. Applications include materials and product research among others. EDX systems are attachments to SEM where the imaging capability of the microscope identifies the specimen of interest. The data generated by EDX analysis consist of spectra showing peaks corresponding to the elements making up the true composition of the sample being analyzed. The EDX technique is non-destructive and specimens of interest can be examined in situ with little or no sample preparation (Tertian and Claisse, 1982).

## **CHAPTER THREE**

### **MATERIALS AND METHODS**

#### **3.1 Experimental design**

Data was collected according to complete randomized design (CRD) with a factorial arrangement. The variables were: potential difference, supporting electrolyte, inter-electrode spacing, surface area into effluent volume ratio, effluent pH, current density and effluent temperature. The two factors at each level were: current passed and the time taken to form flocs.

#### **3.2 Chemicals, reagents and electrodes**

All the chemicals and reagents that were used were of analytical grade. All solutions were prepared in the laboratory using distilled deionized water. Stainless steel electrodes were obtained from commercial steel plates. BDD electrodes with a surface area of 12.5 cm<sup>2</sup> were purchased from CD Technology Company, a commercial manufacturer in Switzerland. The thin film was deposited on Silicon substrate to produce p-Si/BDD material. The model azo dye samples (C.I Reactive Red 76® (RR) and C.I Disperse Blue 79 (DB)) were obtained from RIVATEX in Eldoret, Kenya.

#### **3.3 Electrochemical cell**

A sample of 250 mL wastewater was put in a 300 mL glass beaker. Stainless steel and BDD electrodes were used as anode electrodes while SS was used as cathode electrodes in all experiments. The electrodes were suspended into the solution and kept apart using

an insulator and were connected in series with an ammeter. The reaction was carried out to complete colour removal while recording current flow and the time taken. Absorbance measurements were taken at some interval during the process to monitor colour removal. Specific energy consumption, was calculated using equation 3.1.

$$P = \frac{VIt}{v} * 1000 \dots \dots \dots \text{Equation 3.1}$$

Where;

V= cell potential in Volts

P=specific energy consumption in kWh/m<sup>3</sup>

I= current in Amperes

t= time taken to form flocs in hours

v = sample volume (cm<sup>3</sup>) used in the reaction

Fouling on SS electrodes was removed by rinsing in 8% sulphuric acid.

In dye degradation studies using boron doped diamond anode, 100 mL of wastewater were used in all experiments. The anode material was a p-BDD/Si electrode with a surface area of 12.5 cm<sup>2</sup> while the cathode was made of stainless steel of the same area. The surface area in contact with the dye solution was maintained at 8.8 m<sup>2</sup> / m<sup>3</sup> and the potential difference applied was 10V in all the experiments. The variations studied were: current density, pH of dye wastewater, temperature, inter-electrode distance and initial dye concentration.

### **3.3.1 Effect of voltage**

Direct current was obtained using an AC – DC converter and varied at two levels of 10 and 12 volts. Electrochemical reaction was carried out using a 10 mg/L model dye concentration while keeping other factors constant.

### **3.3.2 Effect of dye concentration**

A 100 mg/L stock solution for each dye was made by weighing 100 mg of dye and dissolving it in 1000 mL of distilled water. The stock solution was diluted to give concentrations of 10, 20, 30, 40 and 50 mg/L using distilled water. Electrochemical reaction was then carried out to complete decolourization.

### **3.3.3 Effect of supporting electrolytes**

NaCl and Na<sub>2</sub>SO<sub>4</sub> supporting electrolyte was each added separately to 10 mg/L dye solution at different concentrations of 0, 1, 2, 4, 6, 8 and 10 g/l. A 5-mL of each concentration was added to 250 mL dye solution and electrochemical reaction carried out until complete colour removal while maintaining the other parameters constant.

### **3.3.4 Effect of current density**

Current density (CD) was adjusted to give 10, 20, 30, 40, 50 and 60 A/m<sup>2</sup>. This was achieved using a stabilized variable rheostat connected in series and addition of different amounts of NaCl supporting electrolyte while maintaining the other parameters constant. A specific current was required to achieve a specific CD hence NaCl was added gradually

from a burette drop-wise and current measured using a digital multimeter.

### **3.3.5 Effect of surface area to volume ratio**

The surface area of the electrode to volume ratio of the effluent (S/V) was varied at four levels to achieve 15, 17, 19 and 21 m<sup>2</sup> / m<sup>3</sup>. This was obtained by varying the depth of the anode plate and holding other parameters constant. Electrochemical reaction was then carried out to complete colour removal

### **3.3.6 Effect of Inter-electrode distance**

The electrode distance between cathode and anode was varied at five levels; 9, 10, 12, 14 and 16 mm. This was achieved by separating the electrodes using insulated material. The electrodes were immersed in the electrochemical cell and the reaction carried out to complete colour removal

### **3.3.7 Effect of contact time**

Colour removal of dye wastewater was studied using UV-VIS spectrometry at different current densities of 10, 20, 30 A/m<sup>2</sup> with 10 mg/L of the dye concentrations. The absorption spectrum for each dye was obtained in a scanning UV-VIS spectrophotometer and the maximum wavelength for absorption,  $\lambda_{\max}$  for each dye was established, which was then used in determining absorbance values. Samples were taken at intervals of 2 minute, for ten minutes period while reading their absorbance in a UV-VIS spectrophotometer.

### **3.3.8 Effect of pH**

The initial pH of 250 mL wastewater was determined. The pH was then adjusted to 3, 5, 7, 9 and 10. A 0.1 M NaOH solution was used to increase the pH while a 0.1M HCl was used to reduce the pH to the required level.

### **3.3.9 Effect of temperature**

The initial temperature of the waste water was determined. The temperature was then adjusted to 30, 40, 45 and 50 °C using a thermostated water bath. At each temperature, electrochemical reaction was carried out to complete colour removal.

## **3.4 Physico-chemical properties of effluent**

To determine the effects of electrochemical treatment of wastewater, raw and clarified wastewater was analyzed for pH, colour, alkalinity, electrical conductivity and COD using standard method procedures (APHA, 2002).

### **3.4.1 pH**

A sample of 100 mL of effluent was put into a 300 mL-glass beaker and the pH meter was calibrated with pH buffer 4.0 and 7.0. The buffers were made by dissolving separately potassium dihydrogen phosphate tablet weighing 10 g and sodium tetra borate tablet weighing 10 g respectively in 100 mL volumetric flasks and making to the mark using distilled water. A combined glass membrane electrode was inserted into the solution. The temperature and pH measurements of the sample were taken.

### 3.4.2 Colour

Colour of the samples was measured using the APHA platinum-cobalt standard method (APHA, 2002). The HACH DR 2000 spectrophotometer was used to measure colour concentration in the samples. Colour standard solution of 500 platinum – cobalt colour units was used to test the accuracy of the spectrophotometer. A sample of wastewater was filtered through a 0.45 µm glass membrane filter. Blank comprising de – ionized water was also filtered. The store program for true colour was entered and the wavelength was displayed as 455 nm. A 25 mL of the blank in the sample cell was used to zero the spectrophotometer while the filtered wastewater sample was placed in the cell holder and the light shield closed. The result of true colour in platinum-cobalt units was displayed in Co-Pt colour units.

### 3.4.3 Electrical conductivity

Wastewater conductivity depends on the presence of ions, their total concentration, mobility, valence and temperature of the effluent. The probe of the electrical conductivity meter was dipped into a 100 mL sample in a glass beaker maintained at 25 °C and the measurement recorded.

### 3.4.4 Chemical oxygen demand

Preparation of reagents

*1. Standard potassium dichromate digestion solution 0.0167M.*

A 4.913 g  $K_2Cr_2O_7$  – previously dried for 2 hrs at 103 °C was weighed and added to a



mixture of 167 mL conc.  $\text{H}_2\text{SO}_4$ , and 33.3 g  $\text{HgSO}_4$ . The mixture was then dissolved in a little distilled water, cooled to room temperature and diluted to 1000 mL.

*2. Sulphuric acid/Silver sulphate reagent solution.*

$\text{Ag}_2\text{SO}_4$  was added to conc.  $\text{H}_2\text{SO}_4$  at the ratio of 5.5 g  $\text{Ag}_2\text{SO}_4$  against 1 kg  $\text{H}_2\text{SO}_4$ . This was then allowed to stand for 1-2 days to dissolve  $\text{Ag}_2\text{SO}_4$ .

*3. Ferroin indicator solution.*

1.4885g of 1, 10-phenanthroline monohydrate and 695 mg  $\text{FeSO}_4 \cdot 7\text{H}_2\text{O}$  was dissolved in distilled water and diluted to 100 mL.

*4. Standard ferrous ammonium sulphate (FAS) titrant, 0.10 M*

This was prepared by dissolving 39.2 g  $\text{Fe}(\text{NH}_4)_2(\text{SO}_4) \cdot 6\text{H}_2\text{O}$  in 100 mL distilled water. 20 mL of conc.  $\text{H}_2\text{SO}_4$  was added, cooled and diluted to 1000 mL. For each experiment, the solution was standardized against standard potassium dichromate as follows: 5 mL distilled water, 3-mL standard potassium dichromate digestion solution and 7 mL of sulphuric acid reagent was mixed, cooled to room temperature, then 1-2 drops of ferroin indicator added. This was followed by titration with FAS.

*Procedure*

A 2.5mL wastewater sample was measured and transferred into a digestion tube and 1.5 mL of digestion solution was then added. 3.7 mL sulphuric acid reagent was carefully run down inside the vessel so that an acid layer was formed under the sample digestion solution layer. Contents were mixed thoroughly before applying heat. The tubes were then placed in a block digester and refluxed for 2 hrs, cooled to room temperature and the tubes placed in tube rack. The contents were then transferred into an Erlenmeyer flask

and placed on a magnetic stirrer.

1-2 drops of ferroin indicator was added and stirred while titrating with 0.1M FAS. The end point was marked by a sharp colour change from blue-green to reddish brown. Distilled water blank was made and treated in the same manner. COD was determined using Equation 3.2.

$$\text{COD as mg O}_2\text{/l} = \frac{(A-B)*M*8000}{\text{mL of sample}} \dots\dots\dots \text{Equation 3.2}$$

Where:

A= mL FAS used for blank

B= mL FAS used for sample

M= molarity of FAS.

### 3.5 Microscopy and spectroscopic analysis

Spectroscopic analysis was carried out on Stainless Steel (SS) electrode. Scanning electron microscopy (SEM) was carried out on SS surface while Energy Dispersive X-ray Spectroscopy (EDX) was used to quantify the elemental composition of the electrode before use and after electrochemical treatment. UV-VIS analysis was carried out to follow the rate of colour removal and degradation. The absorption spectrum of each dye solution was obtained by scanning within the 200-800 nm wavelengths. The absorbance of electrochemically treated wastewater was determined in the predetermined  $\lambda_{\text{max}}$ .

### 3.5.1 UV-VIS studies

A 10 mg/L solution was prepared by dissolving 0.01g/L of each dye in distilled water to make 1000 mL in a volumetric flask. The sample was shaken to homogenize the mixture. A 2mL sample was put in a 1 cm cuvette and then scanned between 200 nm – 800 nm and the absorbance was then determined at the obtained  $\lambda_{max}$  for each dye. Electrochemical treatment was carried out using different conditions and after colour removal, the samples were again scanned through 200 nm-800 nm to determine any new band or removal of other bands in the spectra. This process was carried out in SS and BDD treated wastewater and the amount of dye degraded or removed was calculated using equation 3.3. The experiments were carried out at Environmental research laboratory of Pwani University in Kenya,

$$R\% = [(A_0 - A_e) / A_0] * 100 \dots \dots \dots \text{Equation 3.3}$$

Where, R% is the amount removed,  $A_0$  is the initial dye absorbance,  $A_e$  is the final absorbance (mg/L).

### 3.5.2 SEM and EDX Analysis

The SS plate of size 25 mm X 50 mm was cleaned, dried, and fitted into the SEM chamber. Care was taken to prevent charge build-up on electrically insulating samples. This being a conducting material was most effective for high resolution electron imaging. EDX was used for qualitative analysis of elements present on the SS surface. The

analysis was done by a Hitachi S-4300 scanning electron microscope system connected to an EDX detector at Material Science Laboratory, Oxford University in Britain. The instrument uses an electron beam accelerated at 500V to 30kV and operates at a variety of different currents.

### **3.6 Data analysis**

Statistical analysis was carried out using general statistical package version 12 (GenStat Ver. 12). Levels of significance were tested at 95% confidence limits ( $P < 0.05$ ) in all treatments.

## CHAPTER FOUR

### RESULTS AND DISCUSSION

#### 4.1 Physicochemical characteristics of RIVATEX raw wastewater.

The results of analysis of RIVATEX wastewater samples obtained in 2011 are shown in Table 4.1. The textile wastewater is alkaline, has high colour level, high BOD and COD above the maximum contaminant level (MCL) outlined in the National Environmental Management Authority (NEMA) of Kenya water guidelines of 2006 (GOK, 1999). The quality of this wastewater is poor and it clearly requires treatment before discharge into the environment.

**Table 4.1: Characteristics of RIVATEX wastewater**

Parameter	Units	Value	NEMA Standards (GOK, 2006)
pH	pH units	10.7	6.5-9.0
Colour	Pt-Co units	1585	< 5
COD	mg O <sub>2</sub> /L	1174	50
BOD <sub>5</sub>	mg O <sub>2</sub> /L	468	30

Colour absorbs the sunlight responsible in the photosynthesis of aquatic plants, preventing it from penetrating into the water hence causes serious threat to the ecosystem (Etiégni *et al.*, 2007). The high levels are toxic to the aquatic life as well as man hence need to be lowered below the MCL values by advanced wastewater treatment methods. It was in this light that model dyes were used since the wastewater chemical composition changes each day.

## 4.2 The effects of electrochemical process parameters on specific energy in synthetic dye wastewater using steel anode.

### 4.2.1 Effect of voltage

The effect of variation of voltage applied and specific energy consumption is shown in Figure 4.1. A potential difference of 10 volts (V) direct current (dc) led to lower specific energy consumption as compared to 12 V during colour removal and the difference was significantly different ( $P \leq 0.005$ ).

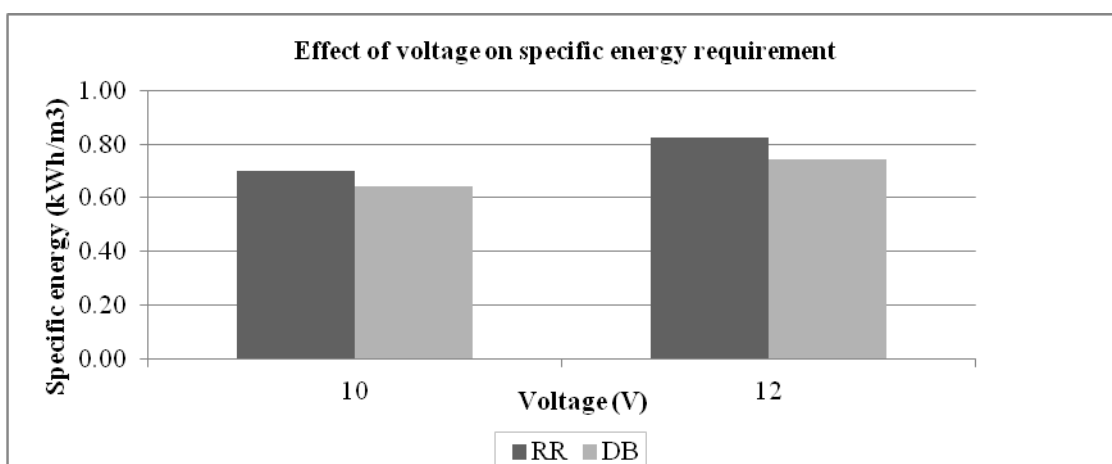


**Figure 4.1: Effect of voltage on specific energy requirement with 1g/l NaCl and 10 mm inter electrode spacing on RR and DB dyes.**

Increasing voltage from 10V to 12V, led to an increase of 18.0 % and 15.7 % specific energy consumption by C.I reactive red 76 (RR) and C.I. disperse blue 79 (DB) respectively. The mean specific energy consumption at 10V was 0.694 kWh/m<sup>3</sup> for DB and 0.763 kWh/m<sup>3</sup> for RR. Therefore DB required less specific energy consumption than RR by 9.9 %.

#### 4.2.2 Effect of dye concentration

The effect of dye concentration on specific energy consumption is shown in Figure 4.2. The effect of five dye concentrations of 10, 20, 30, 40 and 50 mg/L were studied on specific energy consumption. There was a general reduction in specific energy requirement as the dye concentrations increased from 10 mg/L to 50 mg/L.

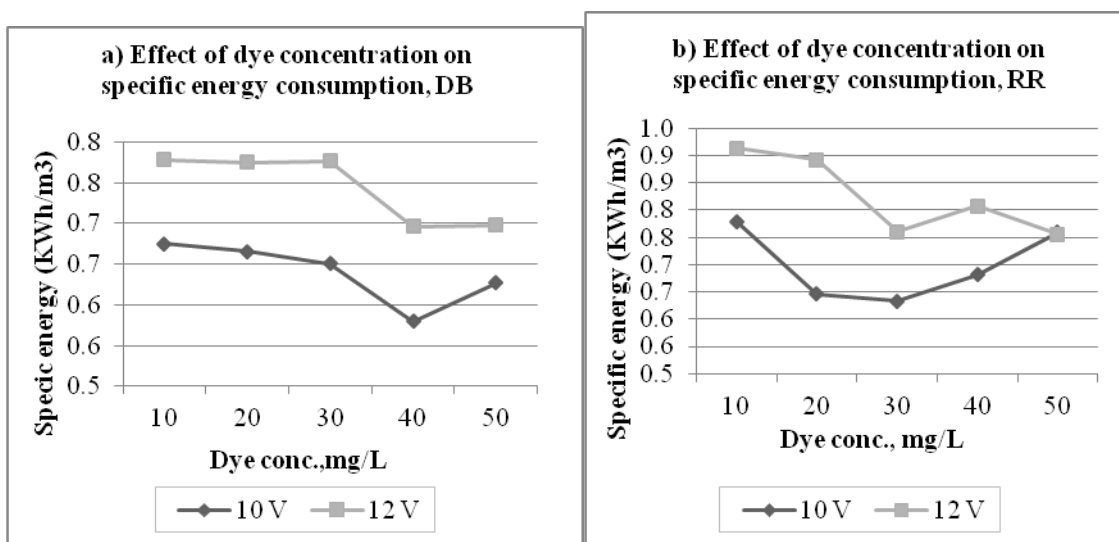
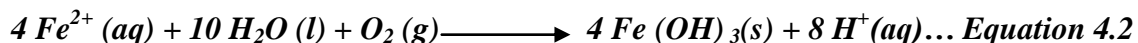
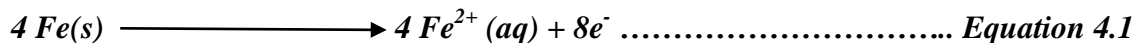


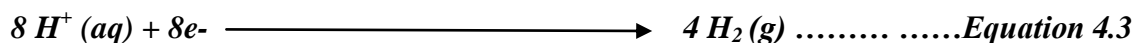
**Figure 4.2: Effect of dye concentration on power consumption at 10 and 12 V on a) DB, b) RR**

Specific energy for DB reduced gradually from 10 mg/L to 40 mg/L then rose again at 50 mg/L, however in RR, the specific energy reduced from 10 mg/L to 30 mg/L then rose again at 40- 50 mg/L at 10 V and 12 V. The reduction could be attributed to an increase in conductivity as the dye concentrations increased leading to more current flow in the cell which enhanced Fe (III) ions production at the anode. Upon oxidation in an electrolytic system, Fe produces iron hydroxide, Fe (OH)<sub>n</sub> where n = 2 or 3 (Mollah, *et al.*, (2001). The mechanisms for the production of Fe (OH)<sub>n</sub> are presented in Eqns. 4.1 – 4.4.

At Anode:



At Cathode:



Overall reaction:



The insoluble iron hydroxides can remove pollutants by surface complexation or electrostatic attraction. Furthermore, the prehydrolysis of  $\text{Fe}^{3+}$  cations also leads to the formation of reactive clusters for wastewater treatment (Mollah, *et al.*, 2001).

The 40 mg/L DB and 30 mg/L RR concentration recorded the lowest specific energy consumption with current densities of 59  $\text{A}/\text{m}^2$  and 72  $\text{A}/\text{m}^2$ , respectively. The high current densities could be responsible for fast decolourization taking less than 5 minutes in each case. As current densities increase, current flow increases and the production of Fe (III) increase.

The initial concentration of a dye determines the specific energy requirement for decolourization. One of the most important pathways of dye removal by electrocoagulation is adsorption of dye molecules on the metallic hydroxide flocs. According to Faraday's law (Faraday, 1832), a constant amount of Fe (III) is released to the solution at same current, voltage and time for all concentration hence the same



amount of flocs will be produced in the solution. However, increasing dye concentration led to increased current which in turn increased Fe (III) production. Therefore as the Fe (III) production increases, the adsorption capacity increases leading to reduced time since the adsorption capacity is limited and a specific amount of floc is able to adsorb specific amount of dye molecules (Dalvand *et al.*, 2011). It is evident that, the higher the concentration of the dye wastewater (the dirtier the wastewater) the better will be the colour removal.

#### **4.2.3 Effect of surface area to volume ratio**

The results of surface area to volume ratio (S/V) in  $\text{m}^2/\text{m}^3$  are illustrated in Figure 4.3. From the results, there was a reduction in specific energy consumption as the S/V ratio decreased from  $28.0 \text{ m}^2/\text{m}^3$  to  $16.6 \text{ m}^2/\text{m}^3$  and an increase in requirement when the S/V decreased from  $16.0 \text{ m}^2/\text{m}^3$  to  $8.0 \text{ m}^2/\text{m}^3$ . The lowest specific energy consumption was recorded at S/V ratio of  $16 \text{ m}^2/\text{m}^3$  in RR dye and  $20 \text{ A}/\text{m}^3$  in DB dye. The current in RR and DB was constant at 0.10 A (Appendix 1.3 & 1.4) which translated to current densities of  $25.0 \text{ A}/\text{m}^2$  and  $20 \text{ A}/\text{m}^2$  respectively. These current densities are in agreement with the recommended range of between  $20 \text{ A}/\text{m}^2$  and  $25 \text{ A}/\text{m}^2$  for long life of electrodes (Comninellis and Chen, 2010).

The S/V ratios have been found to vary depending on the nature of wastewater such as tea wastewater with the optimum of  $18.1 \text{ m}^2/\text{m}^3$  (Maghanga *et al.*, 2009a).

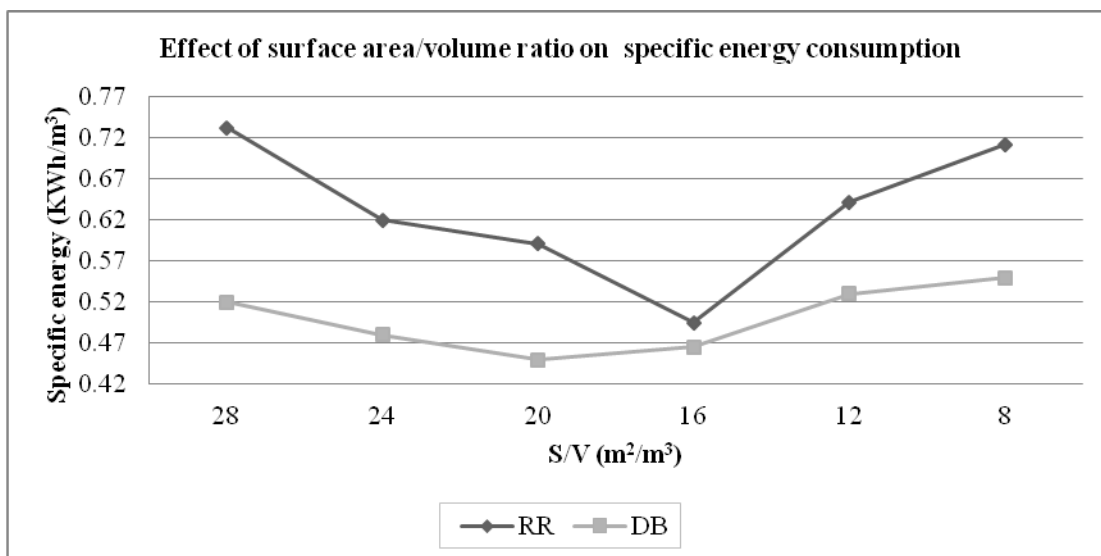


**Figure 4.3: Effect of surface area/ volume ratio on specific energy at 10 V, 10 mm inter-electrode spacing and 1% NaCl supporting electrolyte for RR and DB dyes**

It was found that electrode surface area influences; current density, position and rate of cation dosing and bubble production.

**Table 4.2: Effect of S/V on current density for RR and DB dyes**

S/V , m <sup>2</sup> /m <sup>3</sup>	Current density, A/m <sup>2</sup>	
	DB	RR
28.0	15.7	15.7
24.0	16.7	18.3
20.0	20.0	22.0
16.0	22.5	25.0
12.0	33.0	26.7
8.0	40.0	35.0

As the S/V ratio increased, current density decreased (Table 4.2) and this trend was also experienced by Holt and Mitchel (2006). As the surface area increases, the current

reduces since it is distributed on a larger surface and this reduces the ratio of current/surface area thus lowering the rate of release of Fe (III) hence reduced electrocoagulation.

#### 4.2.4 Effect of supporting electrolytes

The effect of the type of supporting electrolyte and concentration was investigated on specific energy consumption and time for total decolourization of the dye wastewater.

The results are shown in Figure 4.4 and 4.5

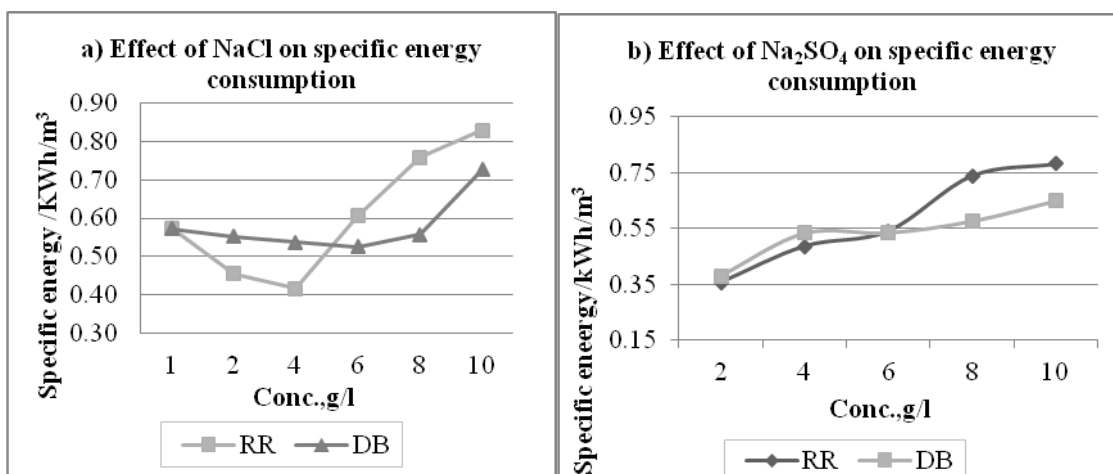


**Figure 4.4: Effect of supporting electrolytes on specific energy consumption using 10 mg/L dyes a) NaCl b) Na<sub>2</sub>SO<sub>4</sub> on RR and DB dyes.**

From the results, there was a decrease in specific energy consumption as the NaCl supporting electrolyte concentration was increased from 1g/l to 4g/l (RR) and 1 g/l to 6g/l (DB). For RR, the optimum concentration was found to be 4 g/l with a current of 0.08A and current density of 23 A/m<sup>2</sup>. However for DB, the lowest specific energy consumption was recorded at 6 g/l with a corresponding current density of 37 A/m<sup>2</sup> with a current of 0.13 A.

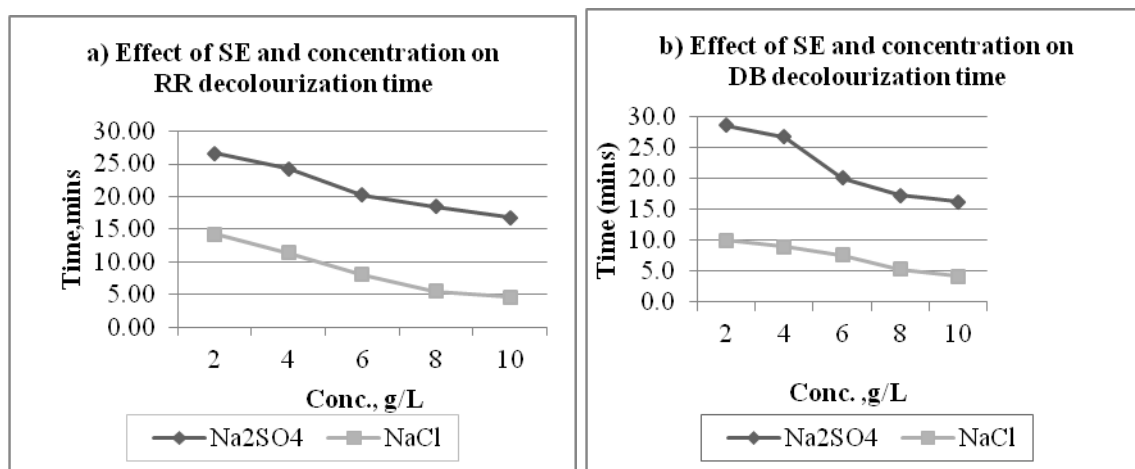


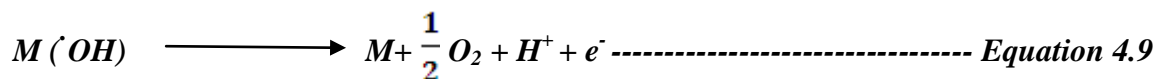
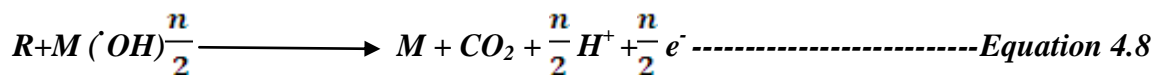
**Figure 4.5: Effect of supporting electrolytes and concentration on decolourization of a) RR and b) DB dyes**

The optimum NaCl concentrations differs in different dyes and concentration since C.I. acid yellow 36 gave an optimum of 8 g/l with a dye concentration of 50 mg/L (Kashefialasl *et al.*, 2006). Sodium sulphate had a higher specific energy consumption demand than sodium chloride; however the coagulation time reduced with increasing concentration in both electrolytes. The presence of sodium chloride in solution causes formation of hypochlorite ion at the anode (Equations 4.5 – 4.7).



The hypochlorite ion leads to increased dye removal by oxidation of the dye molecules (Comminellis and Chen, 2010) as shown in equations 4.8 and 4.9. The electrochemical oxygen transfer reaction between an organic compound R (supposing none adsorbed on the anode) and the hydroxyl radicals (loosely adsorbed on the anode) takes place close to

the anode's surface:

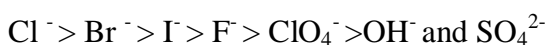


Sulphates have also been found to produce peroxodisulphates during oxidation using BDD electrodes (equation 4.10) which are very specific powerful oxidants that oxidize organic matter hence increasing COD and colour removal rate (Panizza and Cerisola, 2008).



The coagulation time for DB and RR was almost the same with sodium sulphate electrolyte at different concentrations (Fig. 4.4a).

Sodium chloride was more efficient in the reduction of coagulation time than sodium sulphate when used in both dyes (Fig. 4.4c and 4.4d). Comminellis and Chen, (2010) reported that addition of anions will also slow down the electrode passivation with apposite effect following the order:



Therefore addition of a certain amount of  $Cl^-$  into the aqueous solution will inhibit the electrode passivation process largely as well as reduce the specific energy for electrocoagulation giving another advantage over the  $SO_4^{2-}$  which has a lesser effect.

#### 4.2.5 Effect of pH

The effect of pH on colour removal was investigated by adjusting the pH of the wastewater to 4.0, 6.0, 6.5, 7.0 and 8.0 using either NaOH to increase the pH or HCl to reduce the pH. The results obtained are shown in Figure 4.6.

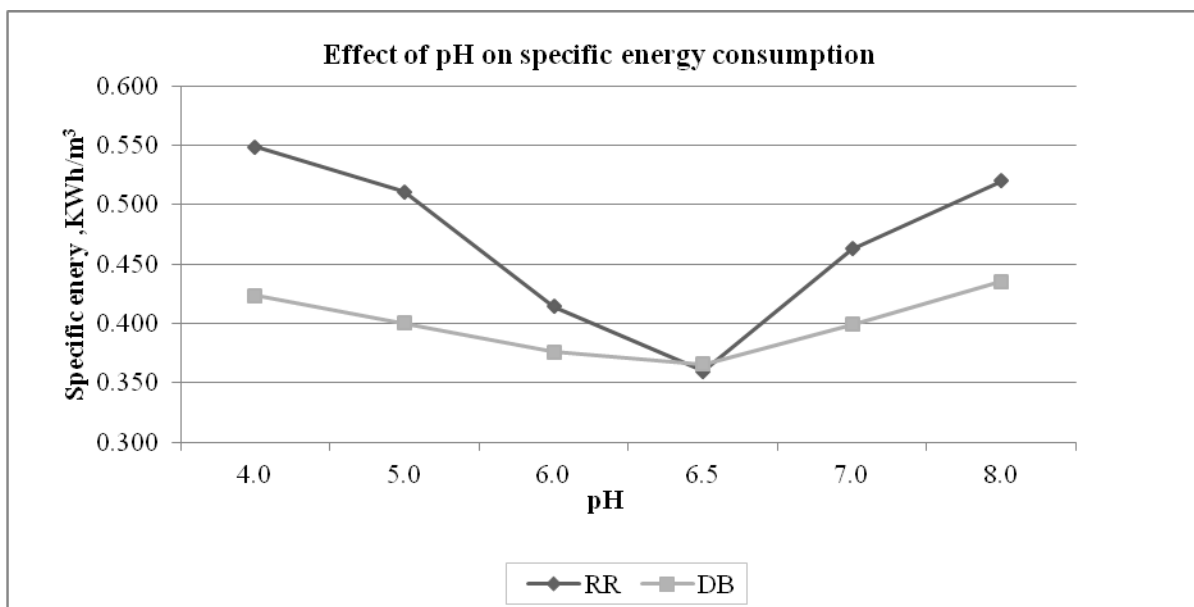


**Figure 4.6: Effect of wastewater pH on specific energy consumption at 10 mm electrode spacing, 1% NaCl and 10 V for RR and DB dyes**

Solution pH determines the speciation of metal ions and also influences the state of other species in solution and the solubility of products formed. Therefore solution pH influences the overall efficiency and effectiveness of electrocoagulation (Holt *et al.*, 2006). Specific energy consumption for complete colour removal was high at pH 4 and reduced gradually until pH 6.5 then increased as the pH increased. In both RR and DB, the lowest specific energy consumption for total decolourization was at a pH of 6.5 which is in agreement with the optimal pH range of 6.5 – 7.5 suggested to be optimal for a given pollutant in electrocoagulation with iron electrodes (Holt *et al.*, 2006). At low

pH, speciation of iron is mainly  $\text{Fe}^{2+}$  which is very stable in acidic media; however, at pH 6.0 – 6.5,  $\text{Fe}(\text{OH})_3$  complex is the most stable hydroxide of iron (Dalvand, 2011). The most stable complex must have a lower crystal field stabilization energy (CFSE) hence the stability of Fe (II) is due to it having lower CFSE as opposed to Fe (III) with higher energy. This arises because Fe (II) is a  $d^6$  system while Fe (III) is a  $d^5$  system as shown in Figure 4.7.

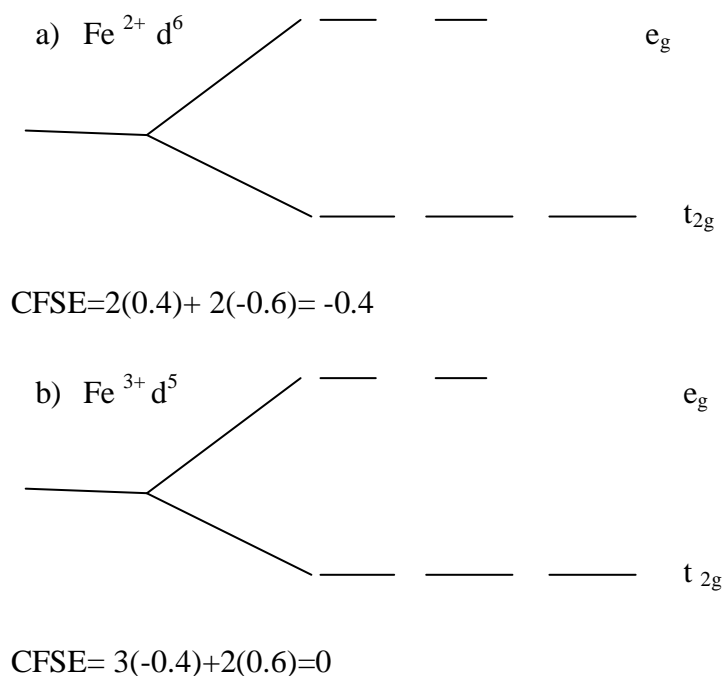


**Figure 4.7: Crystal Field Stabilization energy of a)  $\text{Fe}^{2+}$  and b)  $\text{Fe}^{3+}$  systems**

Fe (III) was hence the most stable complex that occurred at pH 6.5. Since Fe (III) is a coagulant and at this pH, there was a high number of Fe (III) ions that led to a reduction in coagulation time.

#### 4.2.6 Effect of Inter-electrode distance

The effect of inter-electrode distance between the anode and cathode was investigated by varying the electrode gap at 5, 7, 9, 10, 12, 14 and 16 mm using an insulator. The results are shown in Figure 4.8. Specific energy was high at a small inter-electrode distance of 7 and 10 mm and a larger separation of 14 mm and 16 mm. However, the lowest specific energy consumption was obtained at 12 mm inter-electrode spacing which had a corresponding current density of 25 A/m<sup>2</sup> in RR and 30 A/m<sup>2</sup> in DB respectively.

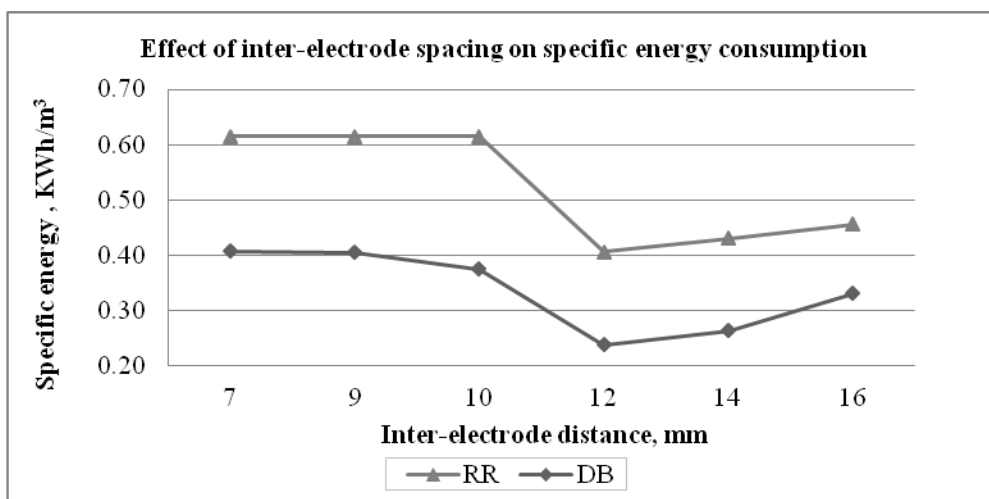


**Figure 4.8: Effect of inter-electrode spacing on specific energy consumption using 10 V, 1% NaCl and 250 mL waste water for RR and DB dyes**

At 7 and 10 mm electrode gap, the current density was 30 and 40 A/m<sup>2</sup>, respectively and could have led to high overpotential hence slowed the activity of the production of Fe (III). This could be attributed to a high rate of release of Fe (II) ions initially which were not all immediately oxidized to Fe (III) coagulant but remained in the Fe (II) state thus taking more time to form flocs.



When the electrode gap was increased from 12 to 16 mm, specific energy consumption increased. This could be attributed to less interaction of the dye with the metal hydroxyl decreasing electrostatic attraction thus reduces dye removal efficiency. The results are in agreement with those of Dalvand *et al* (2011), who found that dye removal efficiency reduced from 98.6% to 90.4% when the inter-electrode distance was varied from 1 to 3 cm using sacrificial electrodes.

The increase of inter- electrode distance leads to increase in cell potential (V) which also increases the resistance and adversely affect the wastewater treatment. According to Ohm's law, the amount of electric current through a metal conductor in a circuit is directly proportional to the voltage impressed across it, for any given temperature. This relationship is expressed as:

$$= \dots\dots\dots \text{Equation 4.11}$$

Ohmic potential drop (IR drop) is potential drop due to solution resistance and hence the difference in potential required to move ions through the solution. IR drop has a significant influence on electrochemical parameters. The variation in IR drop is governed by Equation 4.12

$$IR = I \cdot \frac{d}{A \cdot \kappa} \dots\dots\dots \text{Equation 4.12}$$

Where:

I = current (A)

d = distance between cathode and anode (m)

A = active anode surface area (m<sup>2</sup>)

κ = specific conductivity (10<sup>3</sup> mS/m)

Equation 4.12 implies that, IR drop will increase by increasing the distance between electrodes. During the reaction, the current suddenly drops after some time; hence applied voltage must be increased in order to maintain the constant current. This situation occurs due to the rising of Ohmic loss (IR drop) which lead to reduction in the rate of anodic oxidation. Therefore, increasing the distance between anode and cathode leads to increase of IR drop reducing the efficiency of electrocoagulation process (Nasrullah *et al*, 2012).

The IR drop is related to the distance ( $d$  in cm) between the electrodes, surface area ( $A$  in  $m^2$ ) of the cathode, specific conductivity of the solution ( $\kappa$  in  $mSm^{-1}$ ), and the current ( $I$  in A). The IR drop can be easily minimized by decreasing the distance between the electrodes and increasing the area of cross section of the electrodes and the specific conductivity of the solution (Yildiz *et al.*, 2007).

#### **4.2.7 Effect of current density**

The effect was tested using 10 mg/L and 50 mg/L dye concentrations and the results obtained are presented in Figure 4.9. The increase in current density led to an increase in colour removal in both RR and DB dye wastewater and a reduction in the time taken for separation (Figure 4.9b). This observation agrees with Ponnusamy *et al* (2010) who found out that increase of current density to  $50 A/m^2$  increased electrochemical colour removal from reactive red 120. A concentration of 10 mg/L DB showed lower specific energy than that of 50 mg/L. Removing colour from 10 mg/L DB required lower specific energy than RR; however, at 50 mg/L, DB required more specific

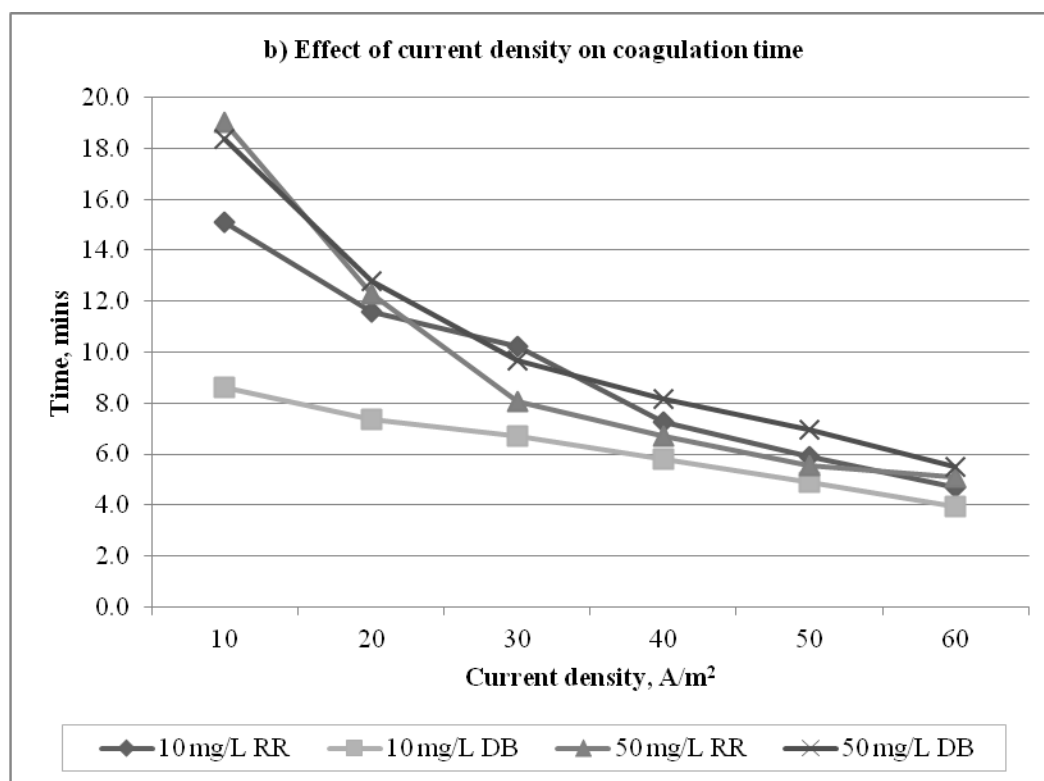
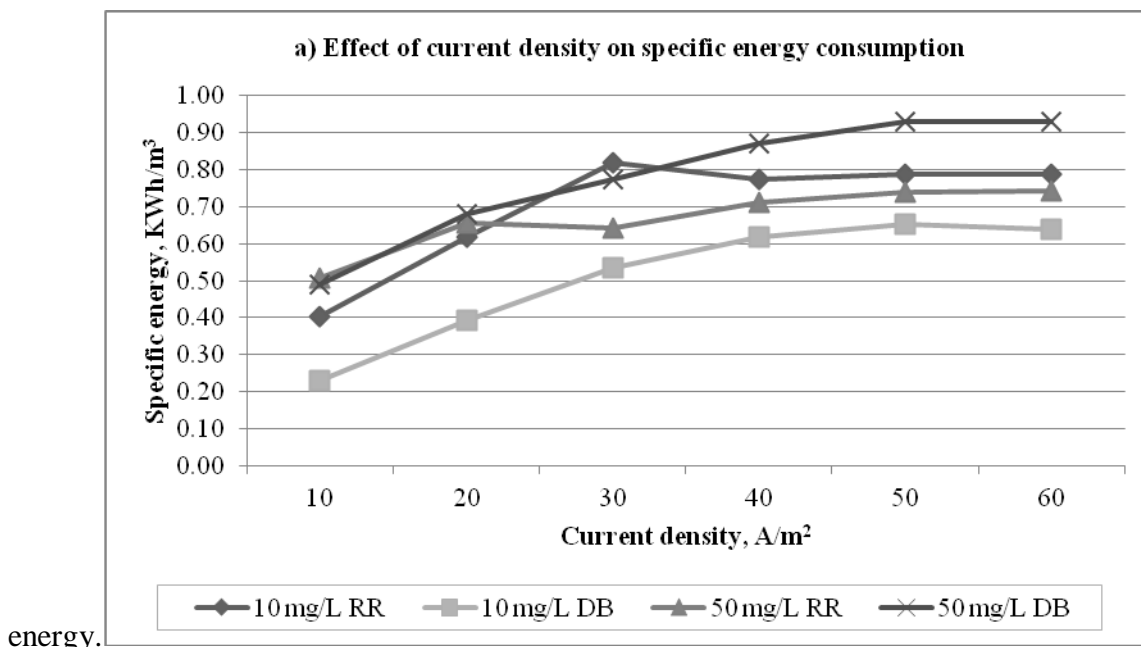


**Figure 4.9: Effect of current density on a) specific energy consumption at 10 mg/L and 50 mg/L b) decolourization at 10 and 50 mg/L dye concentrations.**

Specific energy consumption became constant at and beyond a current density of 30 A/m<sup>2</sup> in RR and at and beyond 50A/m<sup>2</sup> in DB (Fig. 4.9a) when using 10 mg/L concentrations of both dyes (Fig. 4.8a).This implies that the optimum current densities are 30 A/m<sup>2</sup> and 50 A/m<sup>2</sup> for RR and DB dyes.

Operating current density is very important in electrocoagulation because it is the only operational parameter that can be controlled directly (Nasrullah et al., 2012). In such a system, electrode spacing is fixed and current is continuously supplied. Current density directly determines both coagulant dosage and bubble generation rates which strongly influences both solution mixing and mass transfer at the electrodes (Koby *et al.*, 2007). The amount of metal dissolved is dependent on the quantity of electricity passed through the electrolytic solution. The relationship between current density (Acm<sup>-2</sup>) and the mass of substances (W) dissolved (g of Wcm<sup>-2</sup>) can be derived from Faraday's law:

$$W = it \frac{M}{Nf} \dots\dots\dots \text{Equation 4.13}$$

where W is the quantity of electrode material dissolved (g of Mcm<sup>-2</sup>), *i* the current density Acm<sup>-2</sup>, *t* the time in s; M the relative molar mass of the electrode material concerned, *n* the number of electrons in redox reaction, and *f* is the Faraday's constant, 96,500 Cmol/L

#### 4.2.8 Effect of temperature

The effect of temperature on specific energy consumption and time taken was investigated at 30, 40, 45 and 50 °C and the results are shown in Figure 4.10. Increasing

temperatures lowered the specific energy consumption and treatment time for both dyes. However, DB shows lower specific energy consumption than RR.

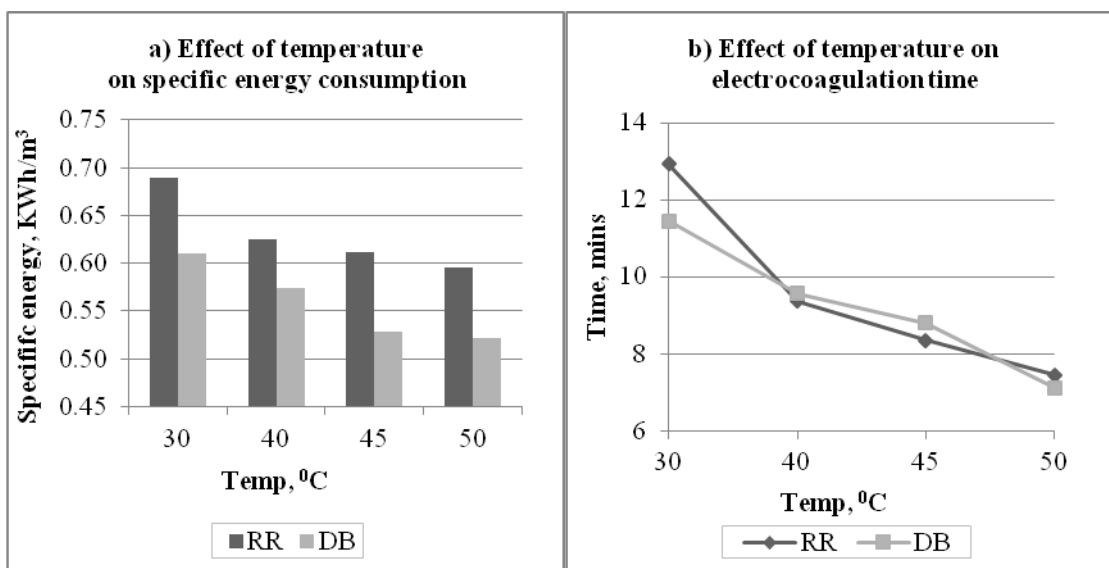


**Figure 4.10: Effect of temperature on a) specific energy consumption and b) colour removal time in RR and DB dyes**

At high temperatures, the production of Fe (II) and its subsequent oxidation to Fe (III) was favoured thus lowering the time taken for electrocoagulation. Increasing temperatures from 30 to 50 °C led to a significant reduction in the time of electrocoagulation in both dyes from 12 to 7 minutes (Fig. 4.10b). Springer *et al.*, (1995) found that high temperatures favour colour removal and this results to low specific energy. This can be explained by the molecules having lower kinetic energy hence the rates of reactions are increased. Increasing the temperatures by 10 °C doubles the rates of reaction (Atkins, 2006). However, the electrocoagulation time for both dyes at same current densities was not significantly different ( $\leq 0.05$ ) which implies that increasing current density affected colour removal at any dye concentration.

#### 4.2.9 Colour removal studies by UV-VIS

A graph of absorbance versus time was plotted to show colour removal changes with time as shown in Figure 4.11. The initial absorbance of DB was lower than that of RR at 10 mg/L concentration as shown in Figure 4.11a. DB dye was degraded faster than RR and colour removal was achieved within 5 min at a current density of 30 A/m<sup>2</sup> while the time taken for colour removal in the RR dye was about 12 min at the same current density.

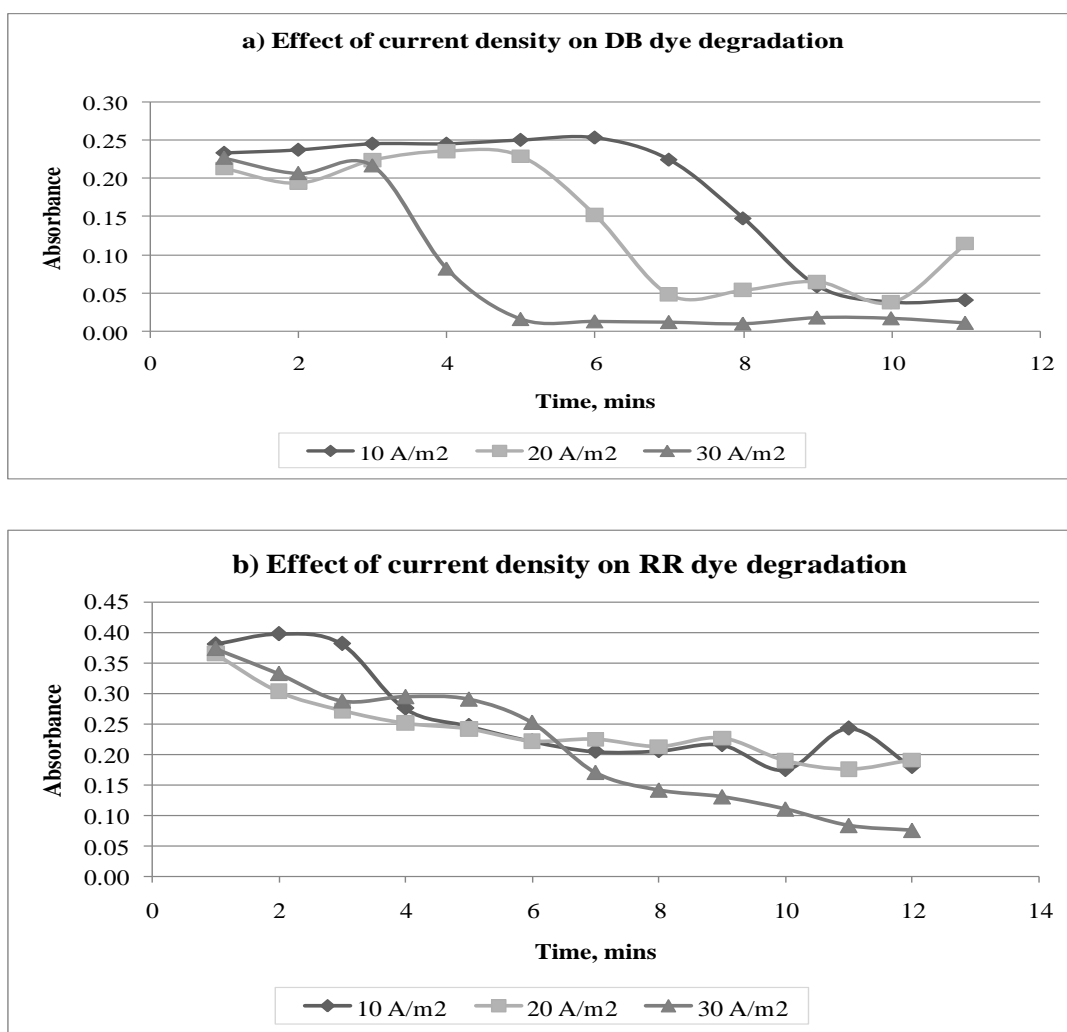


**Figure 4.11: Effect of current density on colour removal time using 10 mg/L of a) DB dye and b) RR dye**

Lower current densities of  $10 \text{ A/m}^2$  and  $20 \text{ A/m}^2$  were also effective but their removal efficiency was lower than that of  $30 \text{ A/m}^2$  in both dyes. The degradation of DB dye was much more rapid than that of RR as shown by the steep decline in absorbance between 3 – 5 min achieving 98% colour removal while in RR the decline was gradual until 11 min that gave 85% colour removal.

From the results obtained, colour removal from DB required lower specific energy than RR and this could be attributed to differences in their chemical structures and electrical properties. The faster removal of DB dye from the wastewater could imply that the dye has a lower zeta potential value than RR hence the compression of the electrical double layer (EDL) was easily achieved compared to RR.

### **4.3 Effects of electrocoagulation on physico-chemical parameters using optimized conditions**

#### **4.3.1 Effect of dye concentration**

There was a reduction in specific energy consumption as DB dye concentration increased from 10 mg/L to 50 mg/L as shown in Figure 4.12. However, RR did not show a particular trend with increasing dye concentration although lowest specific energy was achieved at 50 mg/L. Results indicate that a higher dye concentration require less specific energy for decolourization. DB had a lower specific energy consumption compared to RR dye at all concentrations used. The lowest variation in specific energy consumption was 4.8 % at 50 mg/L while the highest was 12.1% at 40 mg/L .At 10, 20 and 30 mg/L, DB

dye had lower specific energy consumption by 7.3%, 8.5%, 10.8% and 12.1% respectively. The variation in specific energy consumption could be attributed to their differences in electrical conductivities at respective concentrations with DB having higher conductivities than RR at respective concentrations. The high conductivities coupled with the chemistry of the dye molecule could have led to a faster flocculation.

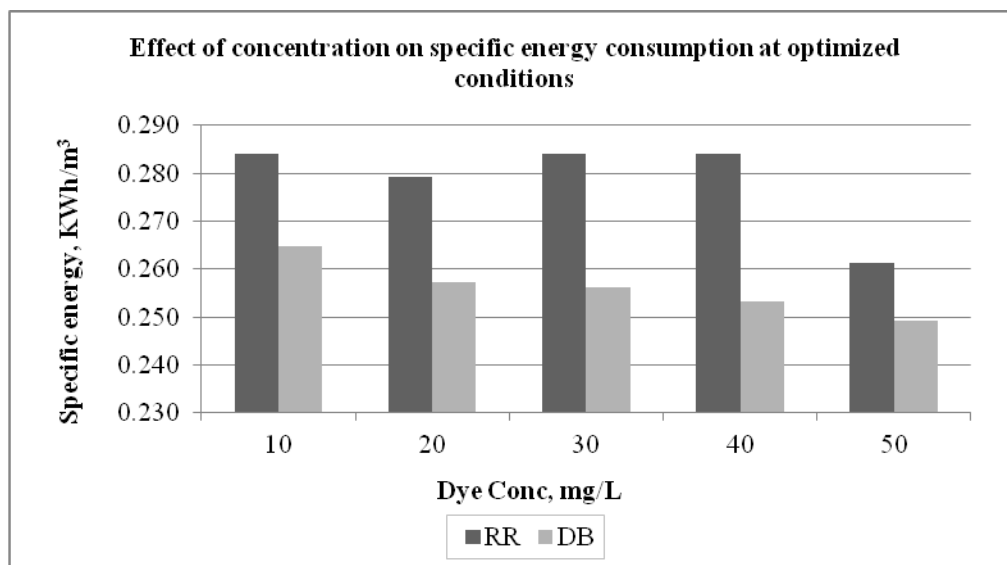


**Figure 4.12: Effect of concentration on specific energy consumption of RR and DB dyes**

#### 4.3.2 Effect of colour removal on effluent pH

The effect of colour removal on the effluent pH at different dye concentration is shown in Table 4.3. The initial pH of both RR and DB dyes was the same but varied with increasing concentration. At 10 mg/L and 20 mg/L DB dye had a higher pH increase than RR dye; however there was no trend with increasing concentrations. There was marginal increase in pH of the final treated wastewater for both dyes. The final pH for both raw and treated samples lay within the control value of 6.5- 9.5 under the NEMA water quality regulations of 2006 (GOK, 1999).



The increase in pH of the wastewater after electrochemical treatment was due to the reduction of water to H<sub>2</sub> gas at the cathode (Eqns. 4.14 and 4.15).



**Table 4.3: Effect of electrocoagulation on wastewater pH for DB and RR dyes**

Dye type	Conc., mg/L	pH before electrocoagulation	pH after electrocoagulation	% change
DB	10	8.06	8.20	1.74
	20	8.12	8.24	1.44
	30	8.18	8.22	0.45
	40	8.18	8.20	0.24
	50	8.20	8.28	1.02
RR	10	8.06	8.16	1.28
	20	8.10	8.19	1.11
	30	8.18	8.24	0.73
	40	8.08	8.18	1.24
	50	8.12	8.18	0.74

The generation of hydrogen gas can be used to produce energy using a hydrogen fuel cell. With the reduction in H<sup>+</sup> ions, there were relatively high OH<sup>-</sup> ions in the clarified effluent than the initial influent with colour, leading to a higher pH. This observation is in agreement with Kobya *et al.* (2003), who found that electrocoagulation with steel electrodes led to an increase in pH.

### 4.3.3 Effect of current density on chemical oxygen demand.

After process optimization, COD was used as the reference factor to obtain the final optimized condition for RR and DB dyes. Current densities were varied to 10, 20, 30, 40, 50 and 60 A/m<sup>2</sup> and the electrochemically treated samples were analyzed for their COD content. The results of COD for DB and RR dyes are presented in Figure 4.13. The initial COD observed for DB dye was higher than for RR dye. Increasing current density from 10 to 60 A/m<sup>2</sup> led to an increase in COD removal in both dyes. At higher current density, the amount of metal oxidized increased, leading to a higher amount of hydroxide flocs for the removal of dyes (Eqns. 4.4). This also increases cell current resulting in a faster removal of pollutants (Feng *et al.*, 2007). The applied current density has been found to directly affect operation costs and process performance (Kobya *et al.*, 2010), hence a very important factor in optimization.

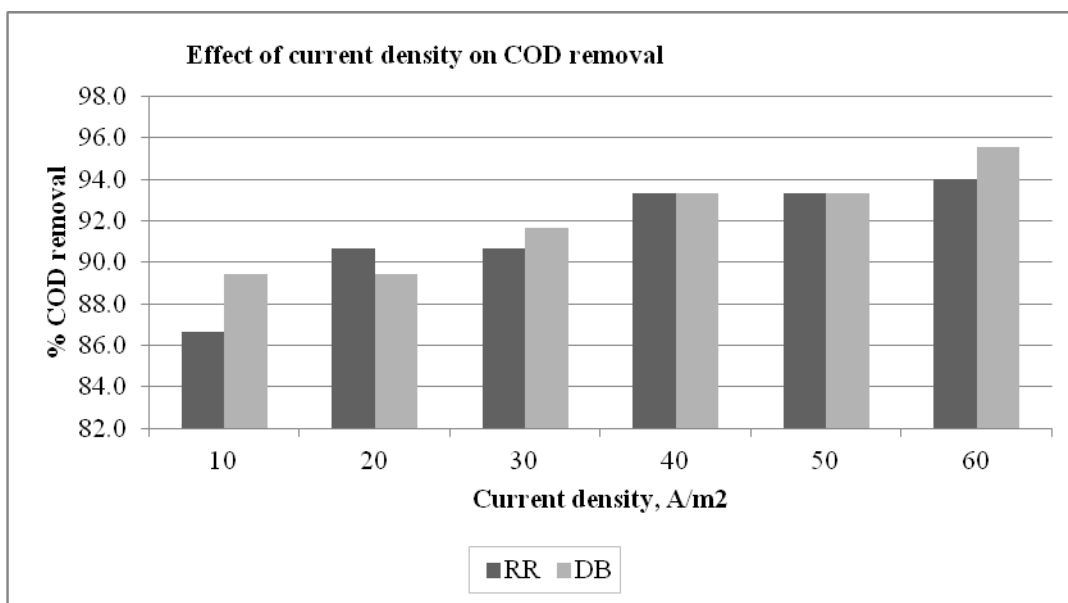


Figure 4.13: Effect of current density on COD removal for RR and DB dyes

The removal percentages ranged between 86.7% to 94.0% in RR and 89.4% to 95.6% in DB. However, DB generally showed a relatively higher COD removal than RR dye at the same current density except at 10 mg/L which had a lower removal value. This implies that DB had a high refractory effect of being less oxidizable than RR with a lower effect. The final COD values in both RR and DB dye wastewaters after treatment were below the MCL value of 50 mg/L recommended by NEMA (GOK, 1999)

#### 4.4 Electrode mass losses

The mass of SS anode electrode was determined before the treatment and after the treatment and the results are shown in Table 4.4.

**Table 4.4: Effect of current density (CD) on electrode mass for RR and DB dyes.**

Dye	CD (A/m <sup>2</sup> )	Initial mass, g	Final mass, g	Actual mass loss of Fe, g	Theoret. Faradaic mass loss, g	Difference (Act. - Theoret.), g	% difference
RR	10	81.87	81.79	0.08	0.04	0.04	100.0
	20	81.79	81.72	0.07	0.05	0.02	40.0
	30	81.72	81.62	0.10	0.07	0.03	42.9
DB	10	82.99	82.72	0.27	0.08	0.19	237.5
	20	82.72	82.33	0.39	0.17	0.22	129.4
	30	82.33	81.87	0.46	0.20	0.26	130.0

The difference in mass was compared to the expected Faradaic mass loss using Faraday's Law of electrolysis. Electrode (SS) mass losses were higher in DB than RR at different current densities of 10, 20 and 30 A/m<sup>2</sup>. (Fig 4.14). As the current density increased, electrode mass losses increased and most of which was not oxidized to Fe (III) hence not

used to form the coagulant that eventually neutralize and coagulate the colour pigments. There was hence a lot of Fe (II) species present than stoichiometrically required for Faradaic mass, leading to high waste of the electrode. This phenomenon is also seen in the differences in Faradaic losses where DB showed a higher difference than RR as the current density was increased from 10 -30 A/m<sup>2</sup>. Increasing current density leads to a higher oxidation rate of the SS electrode to release Fe (II). From the results, increasing current density enhances degradation; however specific energy is increased and higher electrode mass loss is observed.

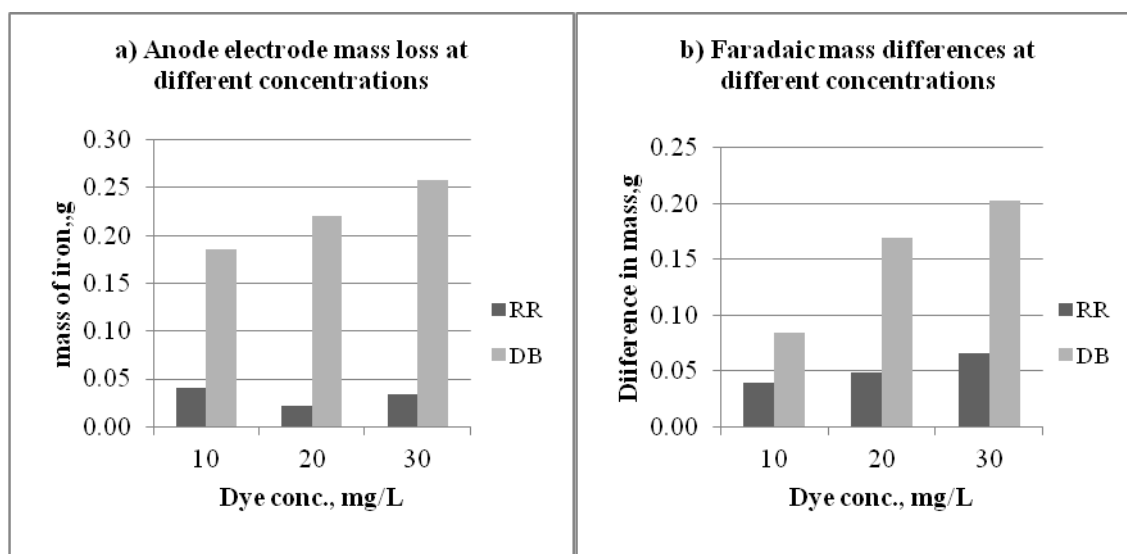


**Figure 4.14: Effect of current density on a) Electrode mass loss b) Faradaic mass differences for RR and DB dyes**

DB requires more electrode material than RR wastewater. Actual electrode material losses were more than the Faradaic losses in both dyes (Figure 4.14); however DB dye had lower difference than RR, which could be attributed to overpotential that resulted from formation of oxide on the SS electrode among other factors such as inter-electrode distance. From the results, it can be concluded that RR dye wastewater could be treated with greater ease than DB wastewater.

#### 4.5 SEM and EDX images of Stainless Steel Electrode

The SEM images of SS electrodes are shown in plates 1 and 2. The images show that the surface of the SS electrode had almost regularly packed atomic structures with a few irregularly arranged atomic patterns (Plate 1). However during the electrolysis process, most iron was oxidized to Fe (III) causing the surface to wear out (Plate 2b). It is evident that electrode dissolution took place and some salt electrolyte (NaCl) adsorbed on the surface of the SS electrode seen as white patches (Plate 2a).

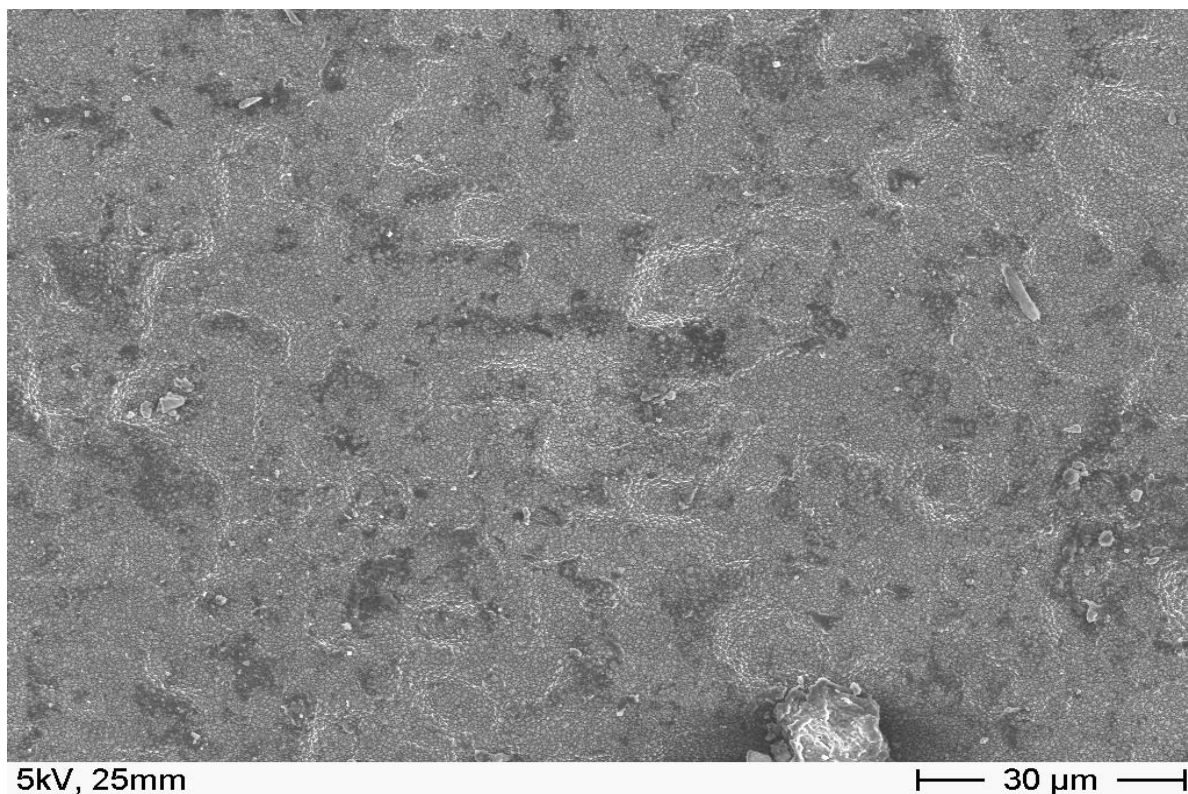


**Plate 1:SEM image of SS electrode before electrocoagulation  
(Source: Author, 2013)**

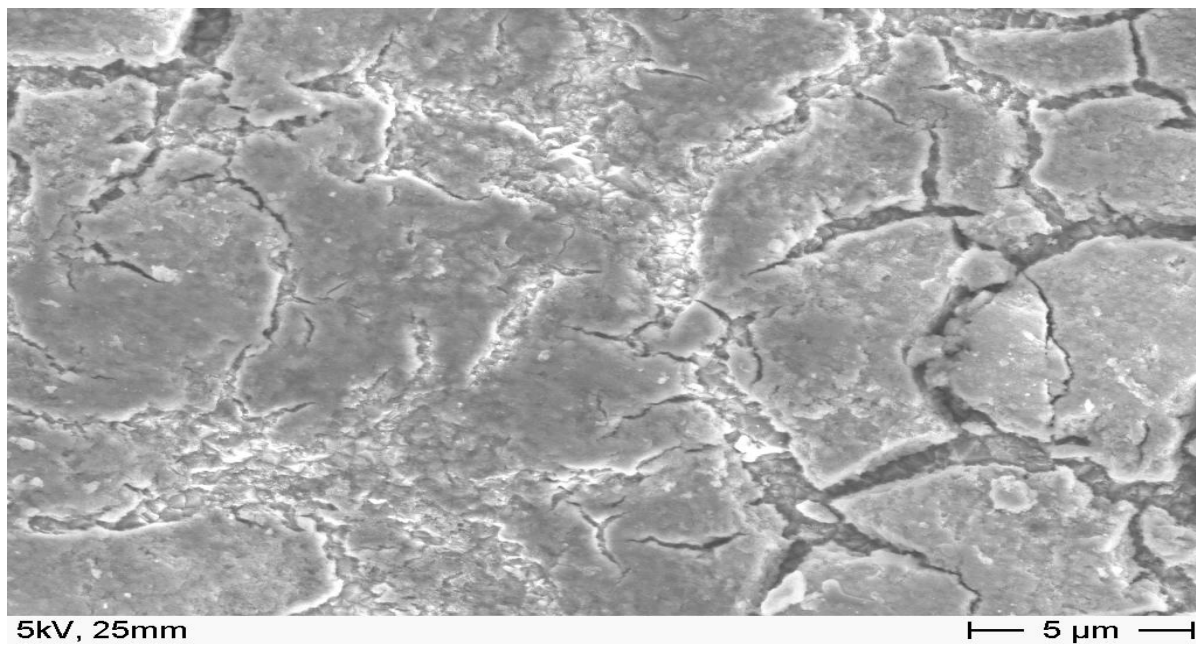


**Plate 2a: SEM image of SS electrode after electrocoagulation with NaCl adsorbed on surface (Source: Author, 2013).**

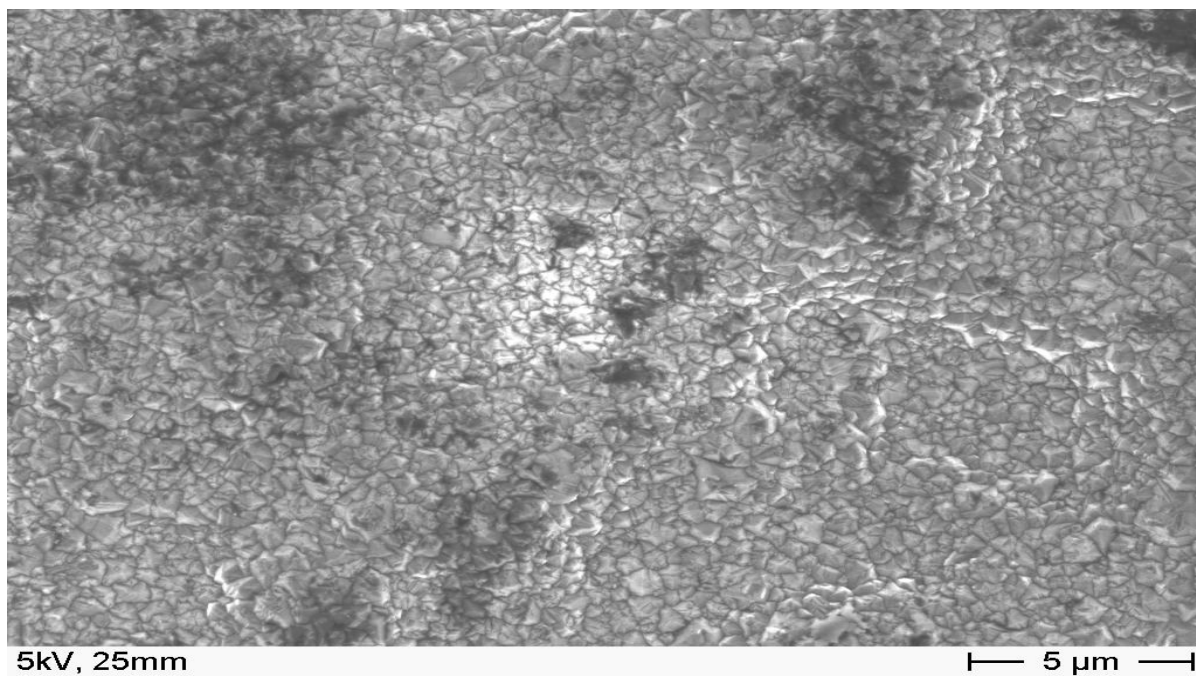


**Plate 2b: SEM image of SS electrode after de-fouling (Source: Author, 2013)**

After de – fouling the surface with dilute HCl followed by distilled water, the adsorbed salt was removed and a clear deformed atomic arrangement was observed (Plate 2b) which was attributed to the dissolution of the electrode. EDX spectrum confirmed that SS electrode material used was chromic steel as Cr was detected at 0.5 and between 5.5 - 5.7 keV (Plate 3). Dissolution phenomenon was supported by the EDX image that shows some sites initially occupied by iron were left vacant and some that were containing chromium were occupied by chlorine (Plate 4).

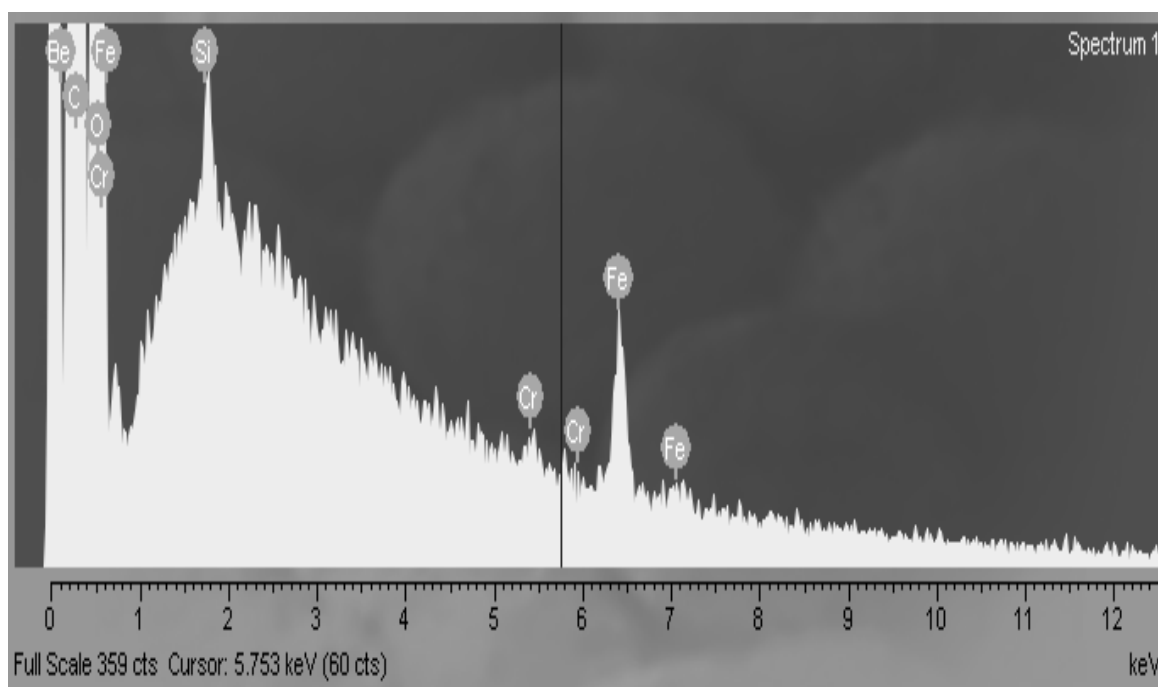


**Plate 3: EDX spectrum of SS electrode (Source: Author, 2013)**

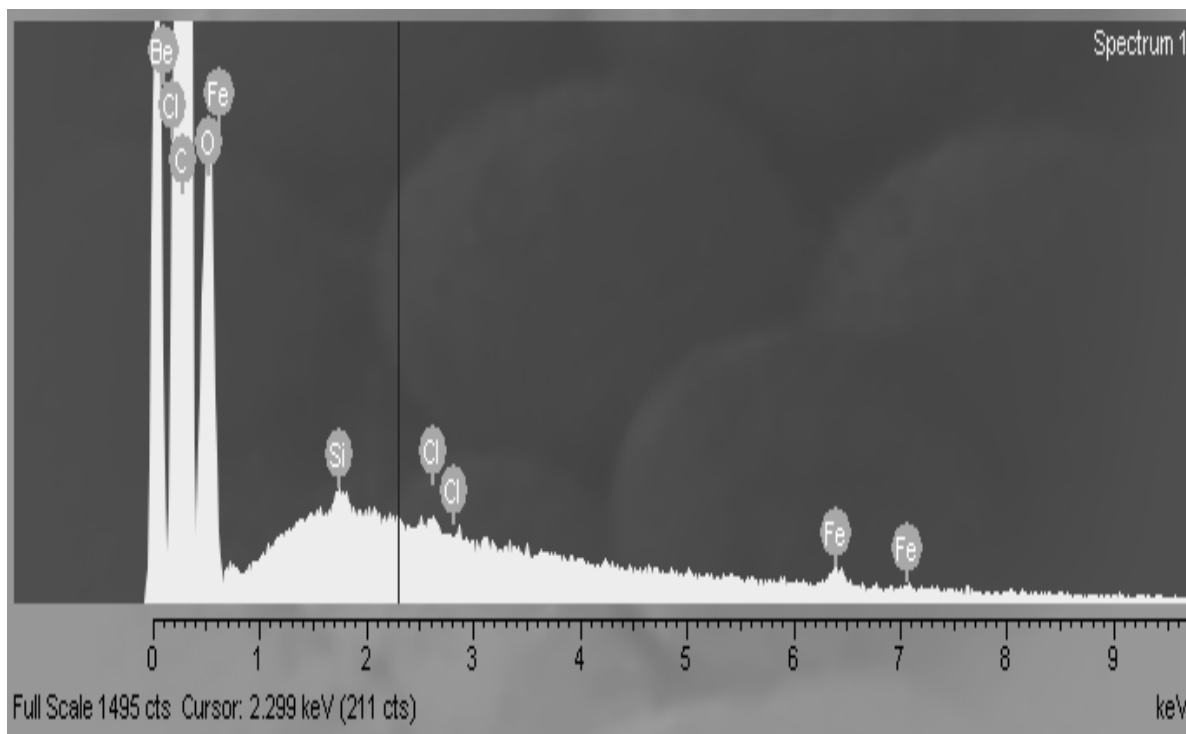


**Plate 4: EDX spectrum of SS electrode after electrocoagulation using NaCl as the SE (Source: Author, 2013)**

#### **4.6 Effects of electrochemical process parameters on the degradation of synthetic textile dye wastewater using BDD anode.**

##### **4.6.1 Effect of current density**

The effect of current density (CD) on degradation was studied by varying applied current density between 50-350 A/m<sup>2</sup> and maintaining constant dye concentration at 10 mg/L. Variation of CD was achieved by adding different amounts of a 3% NaCl electrolyte solution. Specific energy consumption and the time taken for complete decolourization are shown in figures 4.15 and 4.16 respectively.



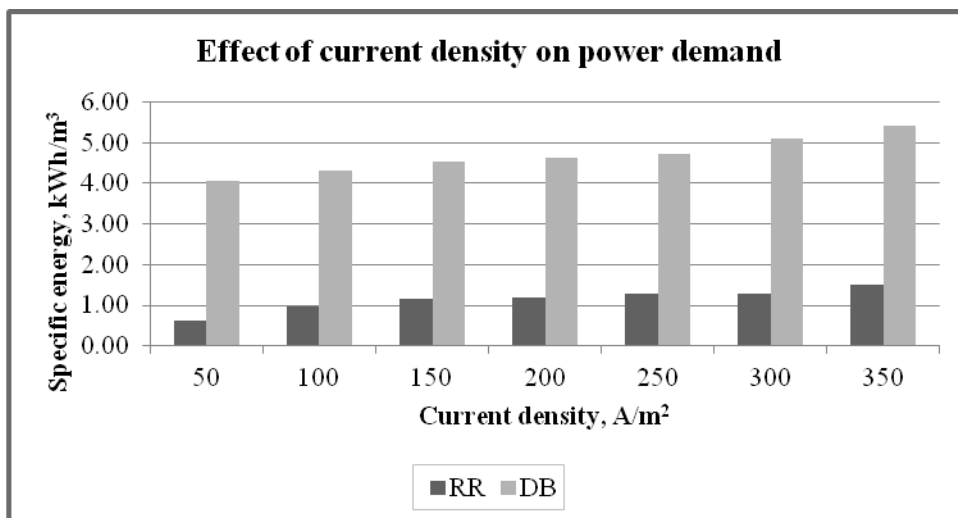


**Figure 4.15: Effect of current density on specific energy consumption using 10 mg/L dye concentration for both RR and DB dyes**

Decolourization of dyes required different current densities; RR required lower specific energy consumption than DB at the same current densities and this could be attributed to the structures of the dyes. Both RR and DB are azo dyes with a characteristic  $-N=N-$  functional group between aromatic rings and in general possess  $-SO_3H$  groups that increase dye solubility and auxochrome groups (like  $-COOH$ ,  $-OH$ ,  $-NH_2$ ,  $-NHR$ ,  $-NR_2$ ) that intensify the colour and increase dye ability to bind to fibers, making them resistant to complete biodegradation. However the colour forming chromophores have different functional groups that require different amounts of energy to degrade (Santos *et al.*, 2008). This phenomenon is also seen in the time taken for complete decolourization (Figure 4.15). At 150 A/m<sup>2</sup>, RR required almost double the time (5.3 min) while DB required 50% of the RR time (2.6 min) to degrade (Fig 14.15). However, as the current density increased, the time taken to degrade the dyes reduced. Panizza *et al.*, (2007) found that an increase in current density results into a decrease in current efficiency due

to increased side reactions in oxygen evolution (Eqn. 4.16).



From the results, RR required less time to degrade as compared to DB, and this could be attributed to differences in their molecular masses and chemical structures.

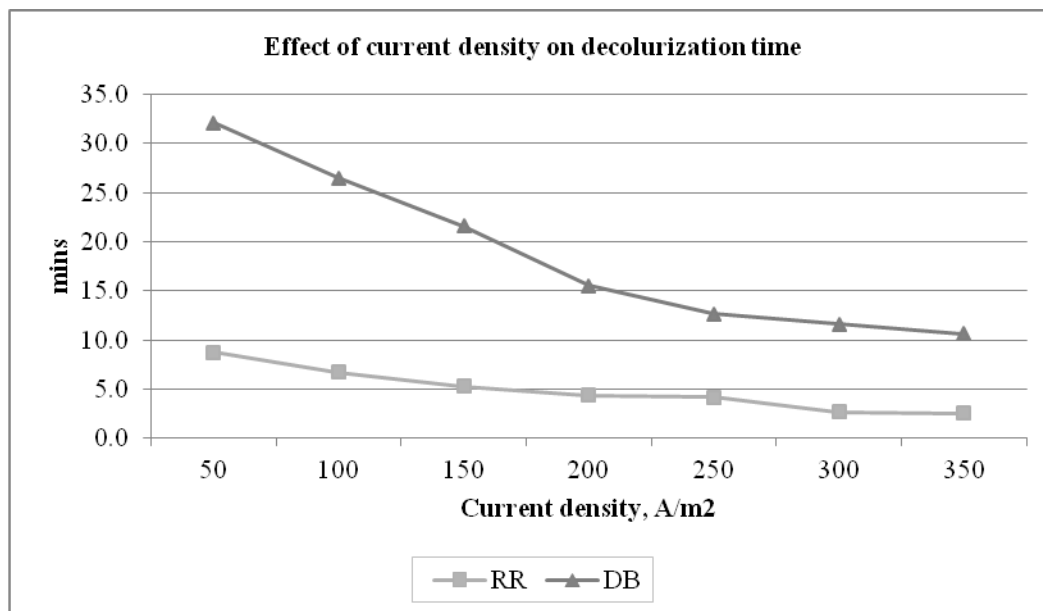


**Figure 4.16: Effect of current density on dye degradation time at 10 mg/L dye concentration for RR and DB dyes**

The concentration of NaCl used at 3% is comparable to the salinity of sea water implying that for plants lying within coastal Kenya, sea water can be used as a supporting electrolyte as it contains NaCl.

#### 4.6.2 Effect of pH

The pH of the initial dye solution was adjusted to 4.0, 5.0, 6.0, 6.5, 7.0, 8.0, and 9.0.

Degradation was carried out at constant voltage using BDD anode; electrode spacing and current density of  $150 \text{ Am}^{-2}$ . The results on specific energy consumption and degradation time are presented in Figure 4.17

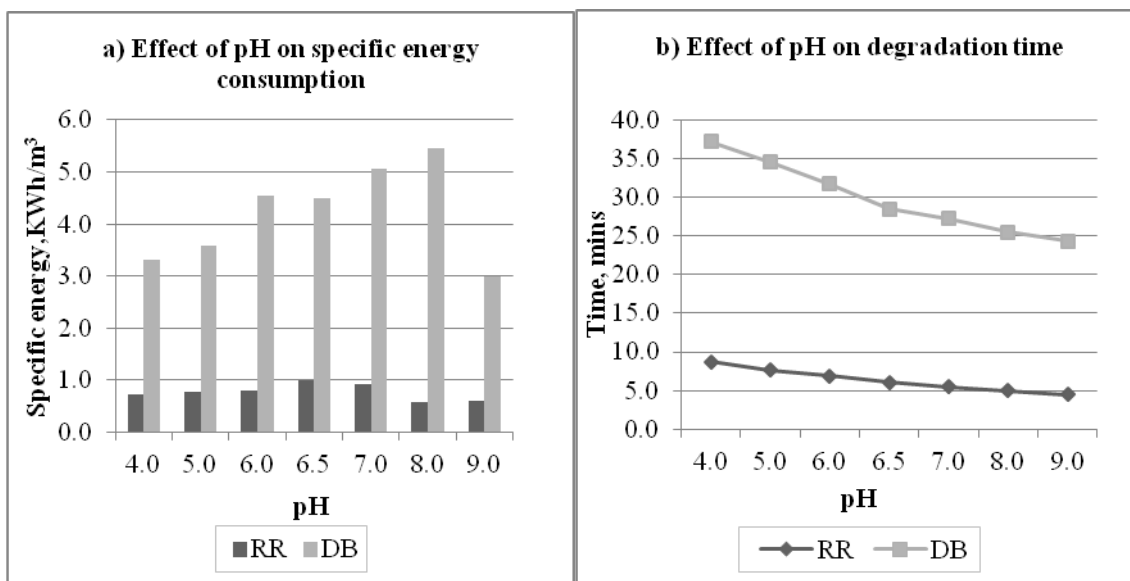


**Figure 4.17: Effect of dye pH on a) specific energy consumption and b) degradation time; using 10 mg/L dye concentration for RR and DB dyes.**

DB required a higher specific energy than RR by a factor of five and also took three times more the time required to degrade RR; implying that it is relatively stable to anodic oxidation. Specific energy consumption for DB increased between pH 4 – 8, then dropped at pH 9 while in RR specific energy consumption was almost uniform between pH 6 and 7 then dropped to the lowest at pH 8 and 9. It took a shorter time to remove colour at pH 8 and 9, than at other pH values (Fig.4.16b) which is advantageous in treating textile wastewaters such as that of RIVATEX which produce alkaline effluents (Table 4.1).

Among process variables, pH has been found to be very important when

electro - oxidation is carried out in the presence of chloride ions, due to the generation of chloro - oxidant species which are pH dependent. Cheng and Kelsall, (2007) reported the best pH for organic degradation occurred under acidic conditions at  $\text{pH} < 4$  and  $[\text{NaCl}] > 1.5 \text{ g/l}$ , due to the generation of the  $\text{HClO}$  species. Under basic conditions ( $\text{pH} > 7.5$ ), generation of the  $\text{OCl}^-$  species was favoured, which is a weaker oxidant than  $\text{HClO}$ . Cañizares *et al.* (2006a) found that chloro oxidants in higher oxidation states (like  $\text{ClO}_3^-$  and  $\text{ClO}_4^-$ ) can be generated at basic conditions though they are inefficient to oxidize organic molecules due to their very low oxidation potential (Gheraout *et al.*, 2011) and can result in decreased availability of  $\bullet\text{OH}$  radical for organic oxidation on the BDD film surface, as observed by Polcaro *et al.* (2009).

While studying variable effects, Chen and Chen (2006) found that high pH was beneficial in the anodic oxidation of orange II dye on Ti/BDD electrode while Muruganathan *et al.* (2007) observed that electrolyte pH has a vital role on dye degradation on Si/BDD thin film electrode. However BDD electrode has the advantage of having a wide pH window and can operate efficiently from acidic to basic conditions (Comninellis and Chen, 2010).

#### **4.6.3 Effect of temperature**

The results of the effect of temperature are presented in Figure 4.18. The degradation time increased with increase in temperature from  $30^\circ\text{C}$  to  $55^\circ\text{C}$ . Increasing temperatures from  $30^\circ\text{C}$  to  $45^\circ\text{C}$  led to increase in specific energy consumption by the dyes

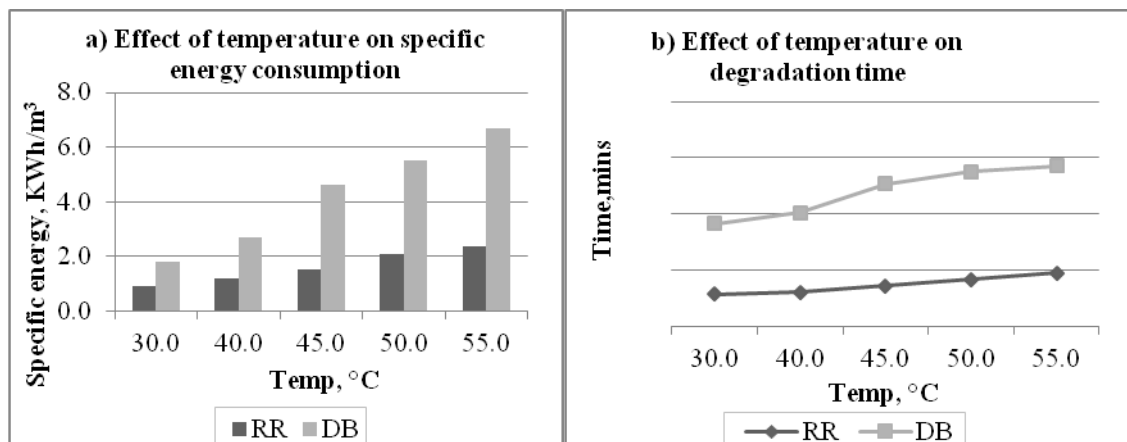
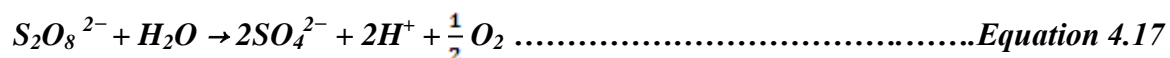


**Figure 4.18: Effect of temperature on a) specific energy consumption and b) degradation time; at 10 mg/L dye concentration of RR and DB dyes.**

This could be as a result of destroying the oxidizing agents of the orthochloride and sulphate based intermediates from the supporting electrolytes. Temperature has little impact on electrochemical oxidation when only  $\cdot\text{OH}$  radicals are in solution but on mediated electro-reagents such as peroxodisulphates. Generally an increase in temperature leads to increases in mediated oxidation rates due to their chemical nature. However, at high temperature, peroxodisulphates are also chemically decomposed into oxygen (Panizza *et al.*, 2007) as shown in Equation 4.17.



Thus, an increase in temperature accelerated both the oxidation rate of organics with peroxodisulphate, and peroxodisulphate decomposition. The processes that prevail depend on organic pollutant temperature and nature of dye (Panizza and Cerisola, 2008). The impact of temperature on oxidation rate is related to the nature of organic pollutants. Canizares *et al.* (2004) reported that COD removal increased with temperature while others reported that COD removal decreased with temperature (Canizares *et al.* 2003).

#### 4.6.4 Effect of dye concentration

The effect of dye concentration on specific energy consumption and degradation time is shown in Figure 4.19. Specific energy consumption and degradation time increased with increase in dye concentration.

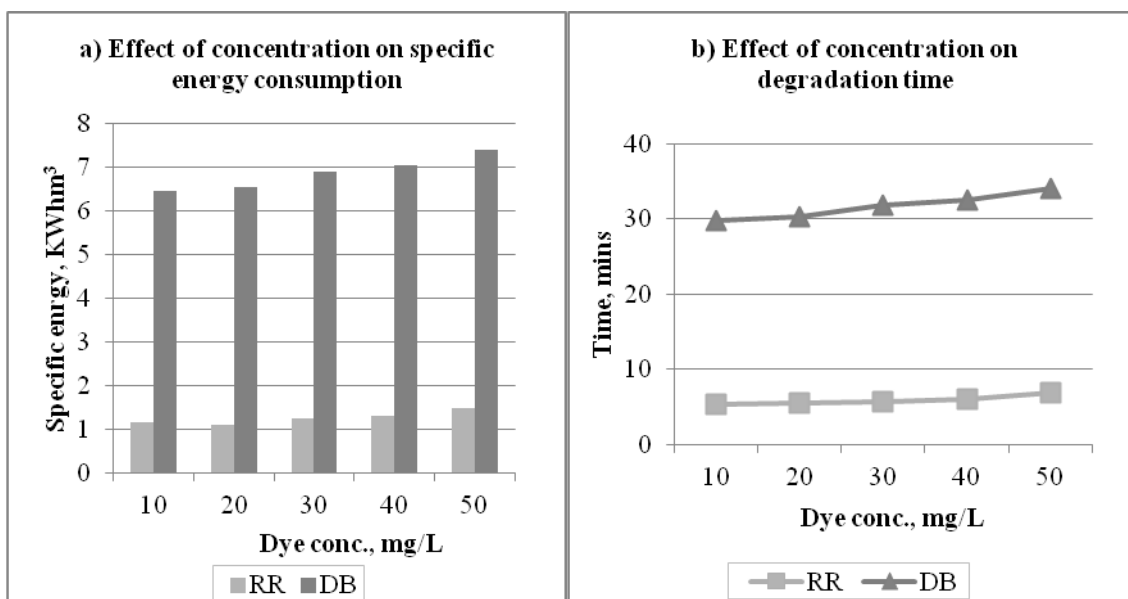


**Figure 4.19:** Effect of dye concentration on a) specific energy consumption and b) degradation time using 10 mg/L dye concentration for RR and DB dyes.

This observation is opposite to when SS electrodes were used as the lower the concentration, the better is the degradation. This could be attributed to the fact that as more dye molecules are increased, more radicals are required for mineralization resulting to a higher specific energy and increased time for degradation. Xueming and Guohua (2006) found that low concentrations favoured orange 11 dye degradation since they reduce formation of polymeric materials that affect efficiency of BDD electrodes. At all concentrations studied, degradation of DB required higher specific energy consumption than RR and the same trend is observed in the time taken for degradation.

#### 4.6.5 Effect of electrode gap

The effect of increasing the electrode gap on specific energy consumption and degradation time is shown in Figure 4.20.

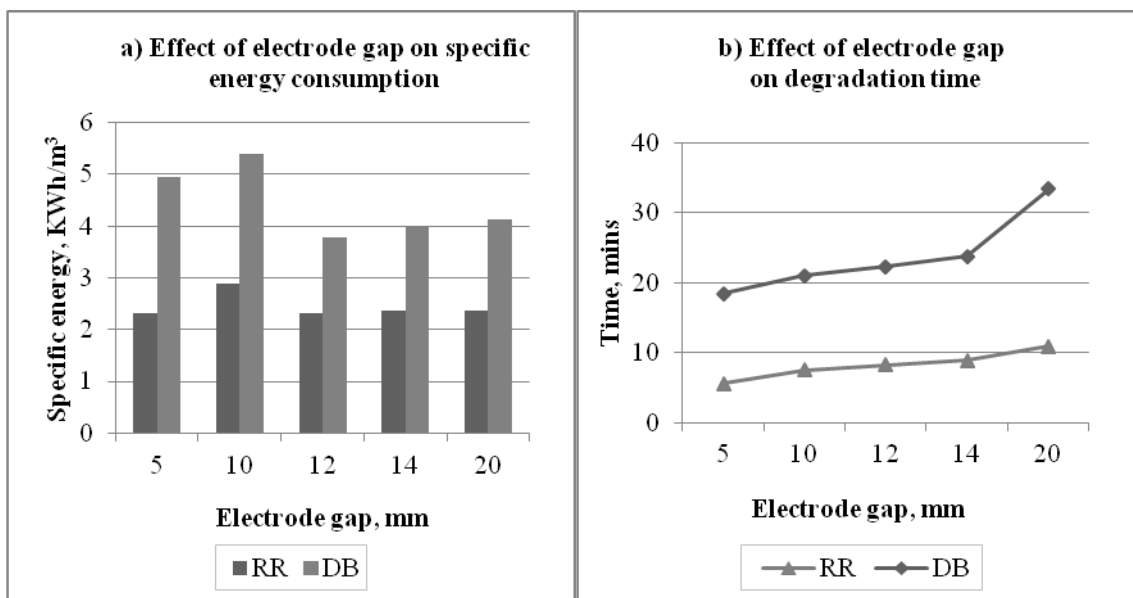


**Figure 4.20: Effect of electrode gap on a) specific energy consumption and b) degradation time using 10mg/L dye concentration for RR and DB dyes.**

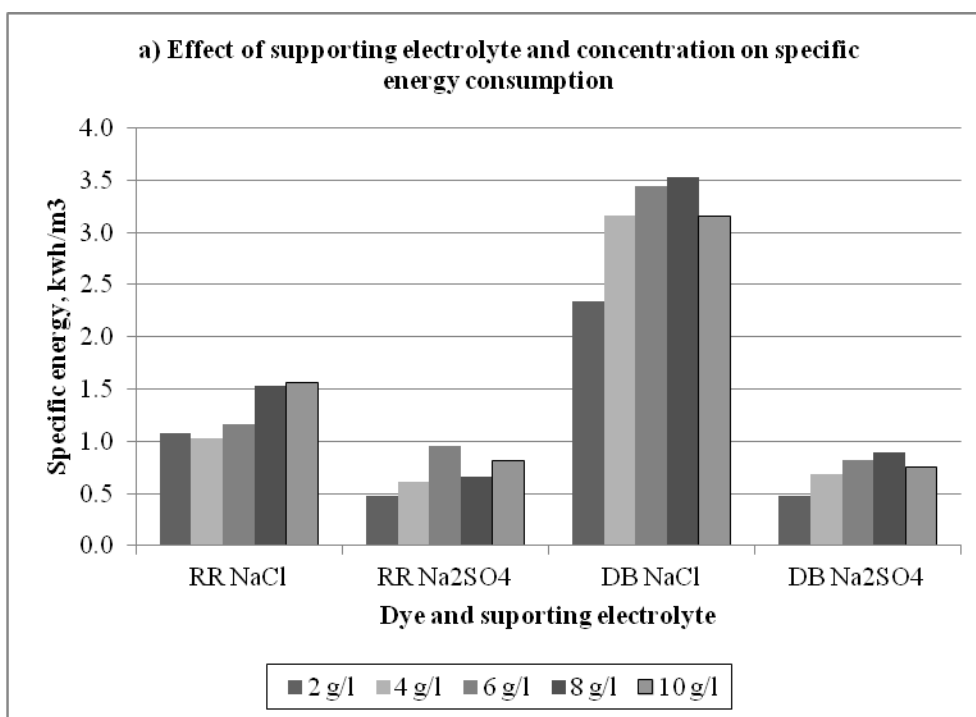
There was a slight reduction in specific energy consumption as the electrode gap was increased from 5 mm to 12 mm after which became stable up to 20 mm gap. This could be attributed to overpotential experienced at close distance. However, degradation time increased with increase in electrode gap distance (Fig.4.20b). DB had higher specific energy and took longer time to degrade than RR at all electrode gaps studied.

An electrode gap of 12 mm was found to be optimum because it had the lowest specific energy consumption. As the electrode gap increased from 5 mm to 20 mm, decolourization time also increased with RR recording an increase of 120 % and DB 94 % increase. Increasing the electrode gap above 12 mm had significant effect on

specific energy consumption ( $P < 0.05$ ) hence not economically viable. At narrow gaps of 5 and 10 mm, there was a high overpotential of up to 2 volts and this led to loss of current not usable in formation of radicals hence high specific energy consumption was recorded (Fig.4.20a).

#### 4.6.6 Effect of supporting electrolytes

Sodium chloride (NaCl) and sodium sulphate ( $\text{Na}_2\text{SO}_4$ ) solutions were used as supporting electrolytes. Their degradation efficiency was evaluated at 2, 4, 6, 8, 10, 20 and 30 g/L using 10 mg/L dye solutions of RR and DB dyes. Dye degradation times were compared and the results are presented in Figure 4.21.





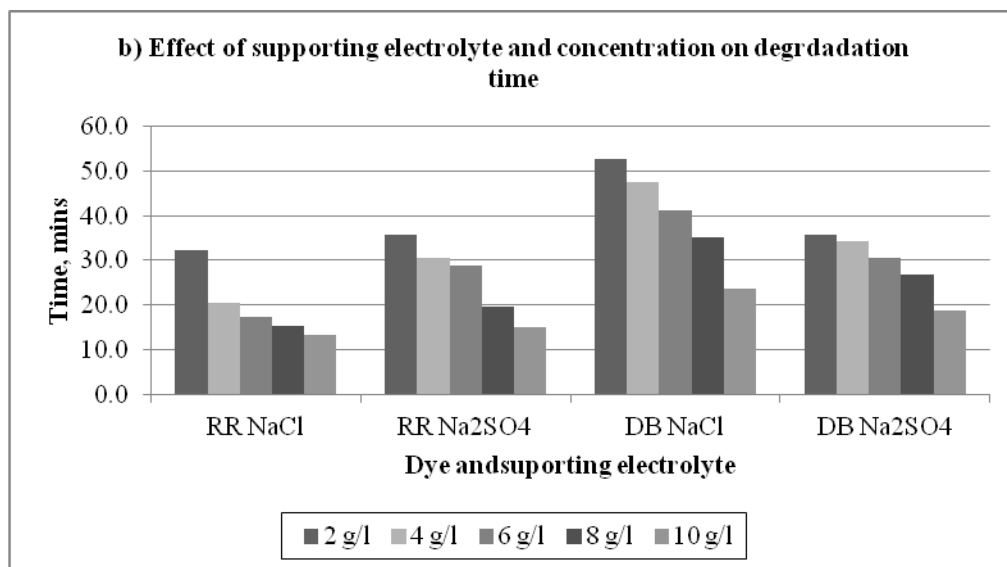


**Figure 4.21: Effect of supporting electrolytes and concentration on a) specific energy and b) degradation time of RR and DB at 10mg/L**

Degradation times were shorter when using NaCl as opposed to Na<sub>2</sub>SO<sub>4</sub> in RR and the opposite was seen in DB where sodium sulphate took shorter time. Sodium chloride recorded the highest specific energy consumption in both dyes and this could be attributed to its higher conductivity than Na<sub>2</sub>SO<sub>4</sub> as presented in Table 4.5. It took a shorter time to degrade RR with NaCl and Na<sub>2</sub>SO<sub>4</sub> than DB. The presence of NaCl in solution causes formation of hypochlorite ion at the anode that leads to increased dye removal through oxidation of dye molecules (Dalvand *et al.*, 2011). However, oxidation with OH<sup>•</sup> radicals is not the only oxidation mechanism occurring on conductive-diamond anodes. Panizza *et al.* (2001) found that some peroxodisulphates develop in solutions containing sulphates, during electrolysis with BDD electrodes (Eqn. 4.18).



This reagent has been known to be a very powerful oxidant and oxidizes organic matter leading to decreased COD and high colour removal rate (Panizza and Cerisola, 2008).

**Table 4.5: Conductivity of NaCl and Na<sub>2</sub>SO<sub>4</sub> as a function of concentration for RR and DB dyes (μS/cm)**

Conc., g/l	RR		DB	
	NaCl	Na <sub>2</sub> SO <sub>4</sub>	NaCl	Na <sub>2</sub> SO <sub>4</sub>
2	285	257	190	156
4	348	265	346	293
6	488	285	551	354
8	764	572	649	544
10	846	624	792	646

#### 4.7 UV-VIS studies for colour removal

Studies using UV-VIS spectrometry was carried out to determine the effect of colour removal from the dyes by BDD. The UV-VIS absorption spectra of raw samples of the dyes, samples with supporting electrolytes and treated samples were recorded with a UV-VIS spectrophotometer in the range 200 nm – 800 nm and the results are shown in Figure 4.22.

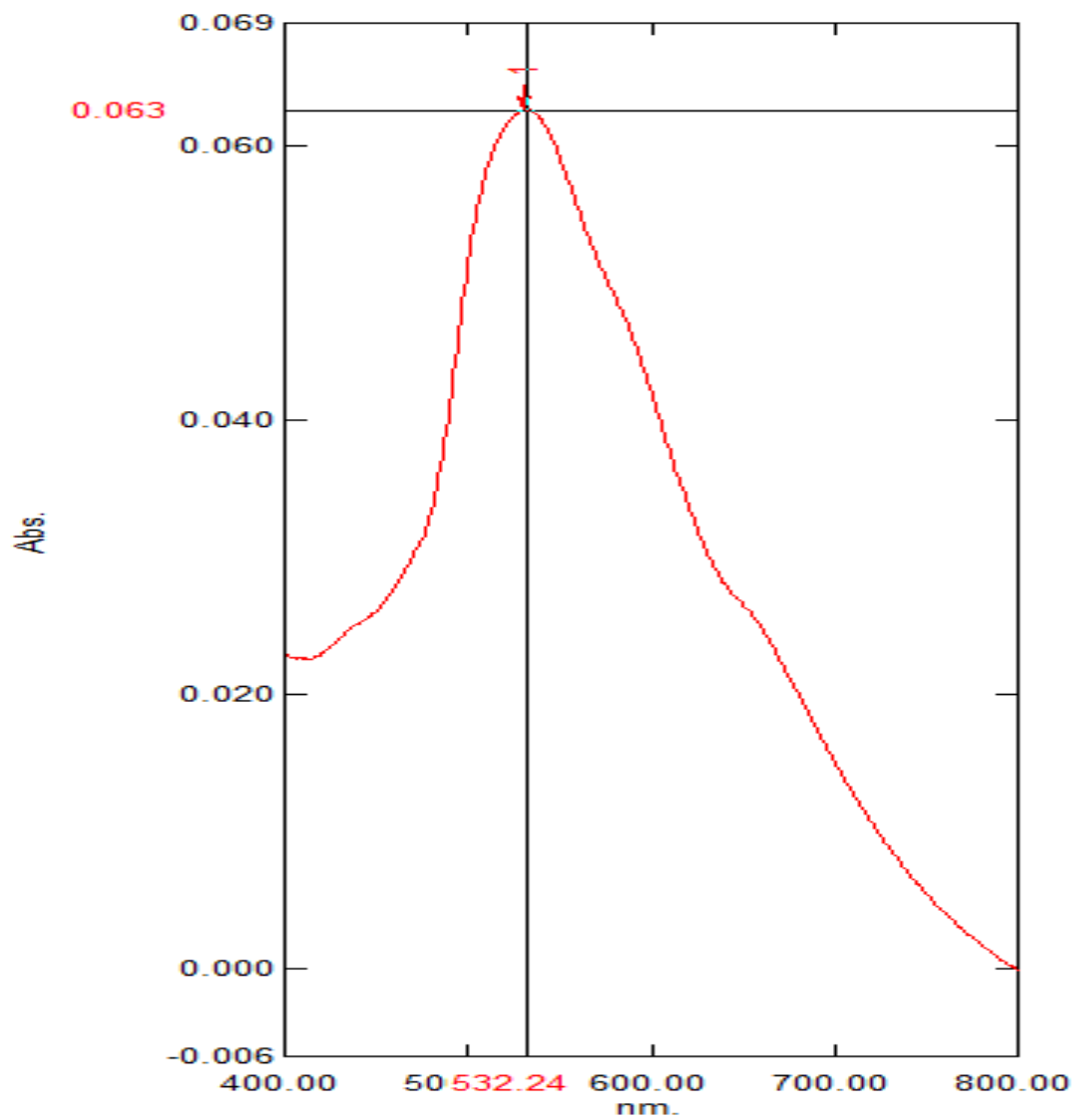


Figure 4.22a: UV-VIS absorption spectrum of DB

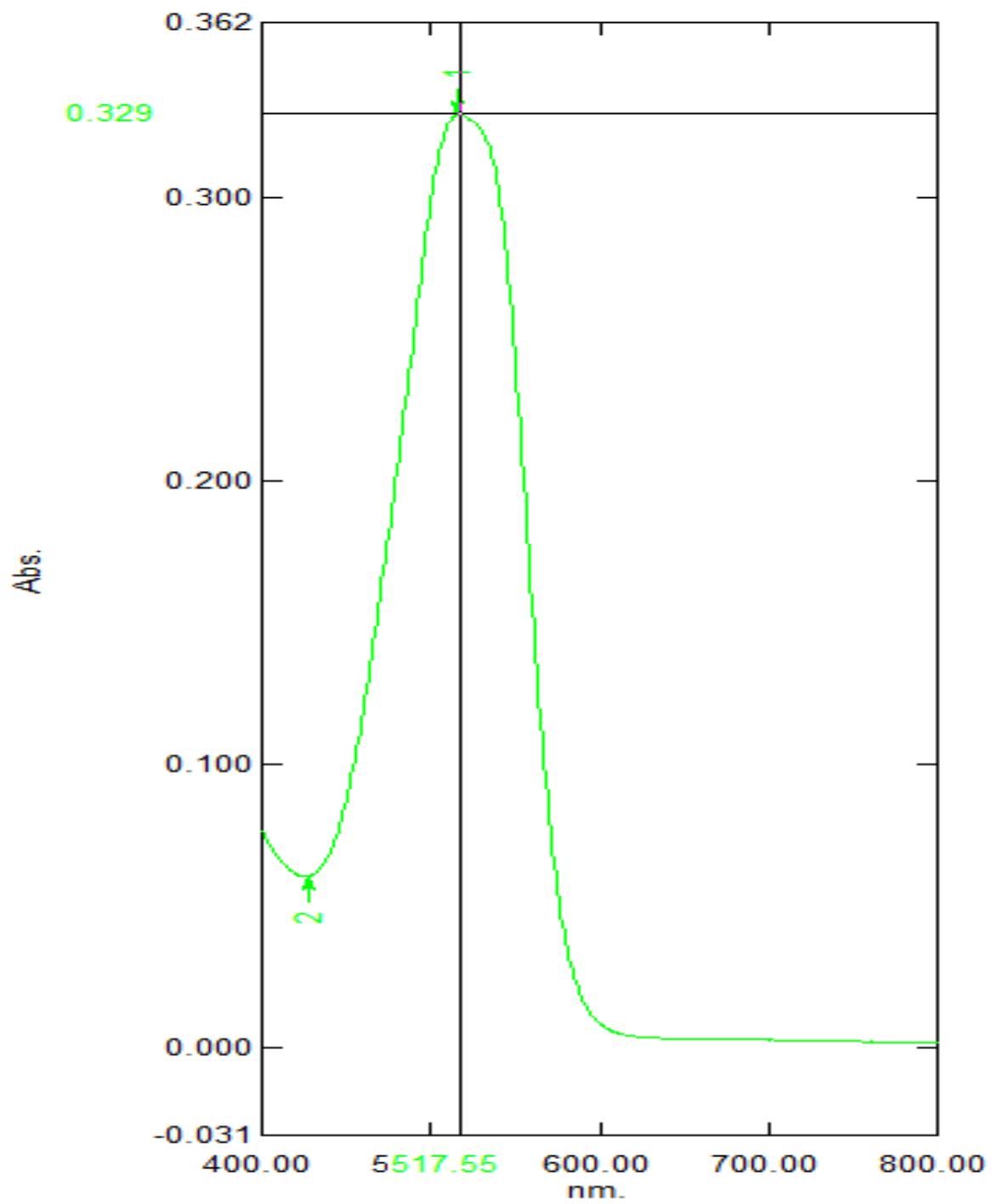
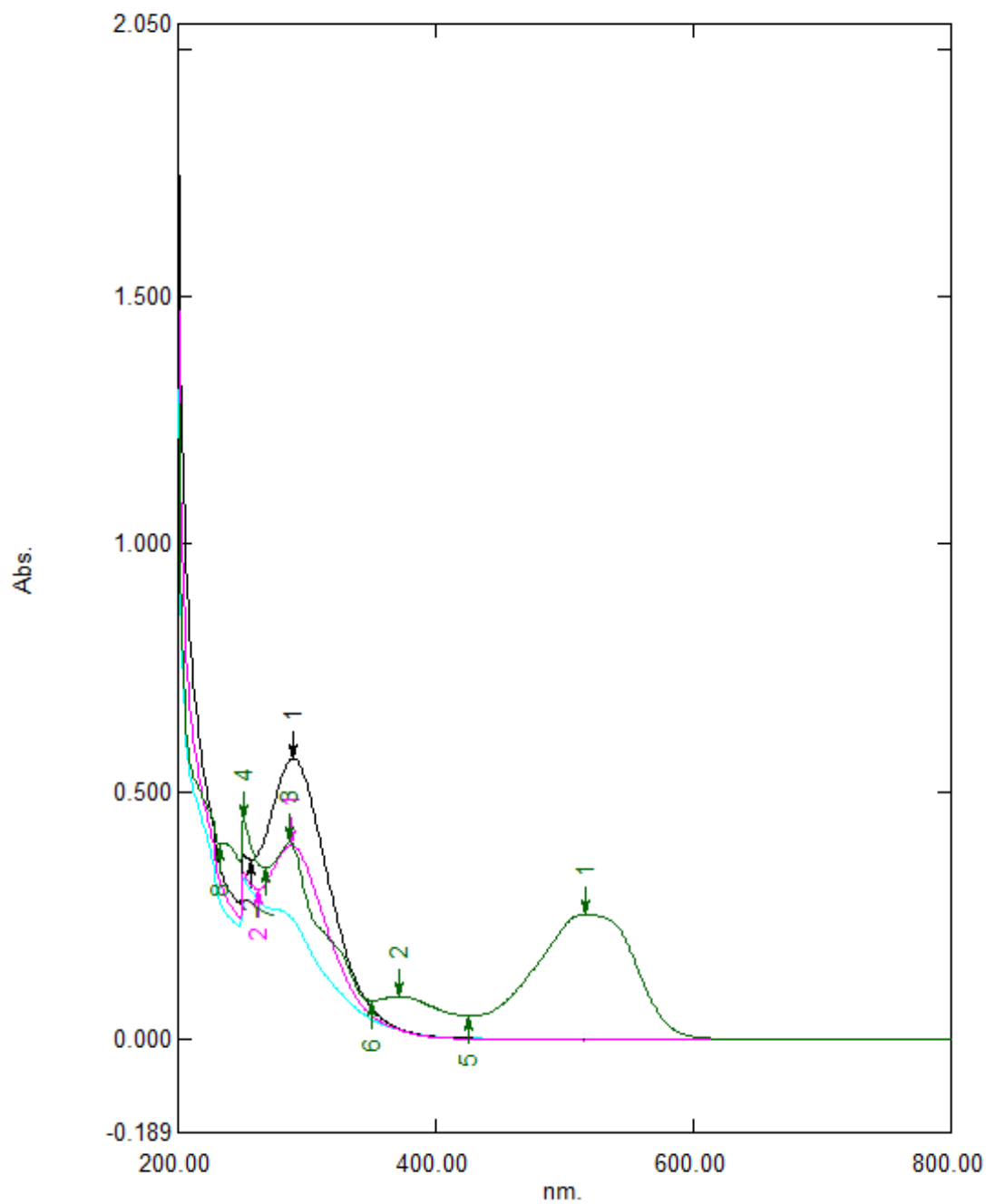
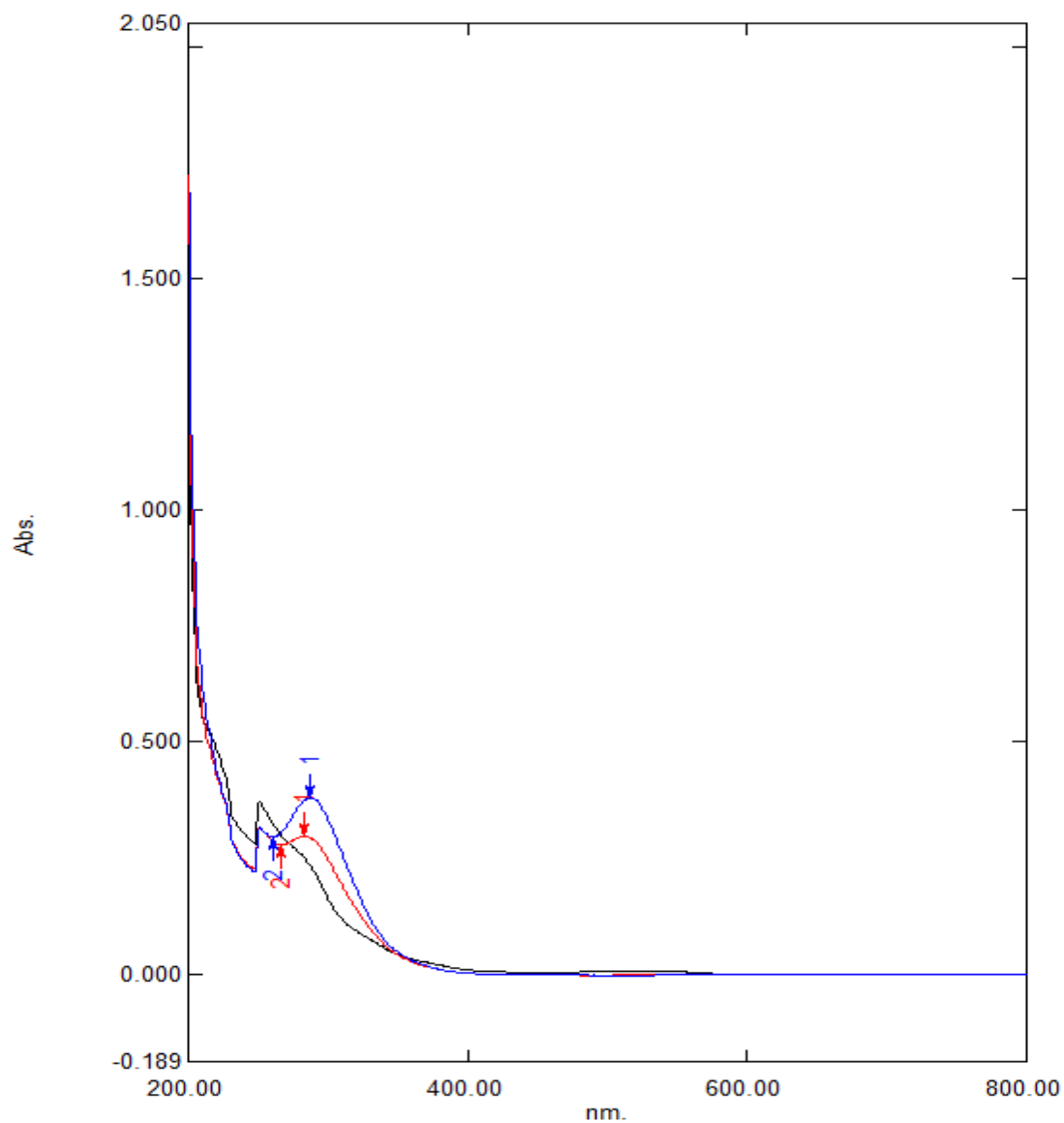


Figure 4.22b: UV-VIS absorption spectrum of RR



**Figure 4.22c: UV-VIS absorption spectrum of raw DB sample (green) with SE and clarified wastewater (blue and pink)**



**Figure 4.22d: UV-VIS absorption spectrum of Clarified water at DB 30 mg/L (blue), RR 30 mg/L (red) and DB 10 mg/L (black)**

The DB spectrum shows  $\lambda_{\max}$  at 532 nm (Figure 4.22a) while RR had  $\lambda_{\max}$  at 518 nm. Figure 4.22c indicates the disappearance of both peaks after mineralization with BDD confirming the colour chromophore had been removed from the dye wastewaters. There were two peaks in the UV region at 270 nm and 255 nm which are assigned to water and supporting electrolytes solutions, respectively. These peaks were present initially before the mineralization process and their intensities are directly proportional to the concentration of dyes as per the Beer-Lambert's Law.

#### **4.8 Effect of Stainless Steel electrocoagulation on chemical oxygen demand of synthetic dye wastewater**

Wastewater was electrochemically treated and after complete colour removal, the samples were analyzed for COD and the results in mg/L are given in Table 4.6.

**Table 4.6: Chemical oxygen demand using NaCl and Na<sub>2</sub>SO<sub>4</sub> supporting electrolytes, mg/L.**

<b>Sample</b>	<b>DB</b>	<b>RR</b>
10 mg/L dye concentration	180	150
NaCl	4	5
% Reduction	97.8	96.7
Na <sub>2</sub> SO <sub>4</sub>	17	15
% Reduction	90.6	90.0

Sodium chloride had a higher % reduction of COD than  $\text{Na}_2\text{SO}_4$  in both dyes; however, it was easier to degrade DB than RR.

#### 4.9 Electrochemical treatment of RIVATEX wastewater using Stainless Steel anode

RIVATEX wastewater was treated by electrocoagulation using stainless steel (SS) electrodes. The parameters studied were: - pH, electrode gap, surface area to volume ratio, supporting electrolytes and temperature.

##### 4.9.1 Effect of pH

The pH of the wastewater was varied between 4 – 9 and degradation studies carried out.

The results are presented in Figure 4.23.

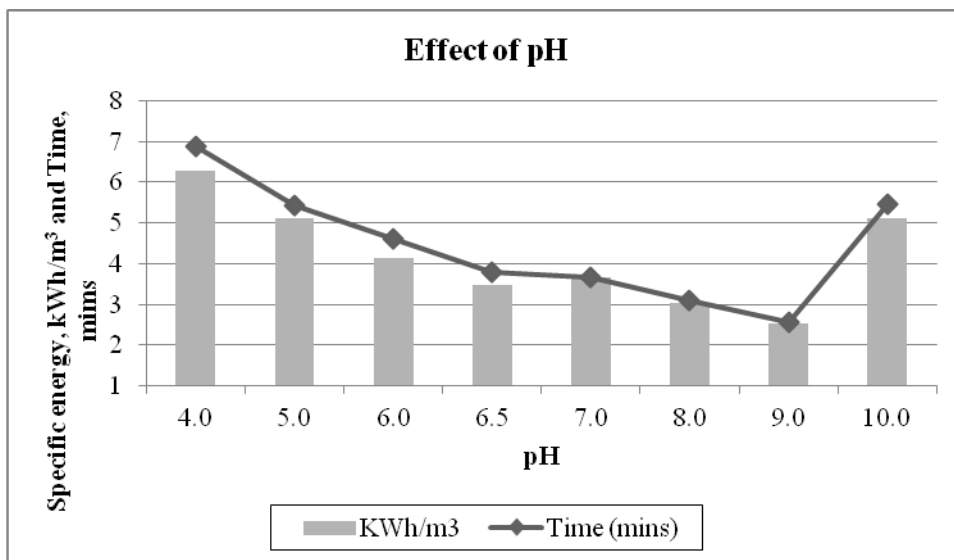


**Figure 4.23: Effect of pH on specific energy consumption ( $\text{kWh/m}^3$ ) and colour removal time.**

Specific energy consumption and treatment time reduced with increasing pH from 4 to 9



then increased at pH 10. Acidic media required high specific energy consumption than alkaline media and did not favour colour removal while basic media at pH 9 gave the best colour removal results. This phenomenon was observed in the model dyes where a high pH was favoured in colour removal. In electrocoagulation, pH plays an important role because it determines the stability of the metal hydroxide mainly the speciation of iron and also the dye characteristics. The raw effluent had a pH of 10.26 hence requires a slight adjustment to enable this process to be efficient.

#### 4.9.2 Effect of inter-electrode distance

Electrode gap was adjusted to give a spacing of 7, 10, 15, 20 and 30 mm and the results are shown in Figure 4.24.

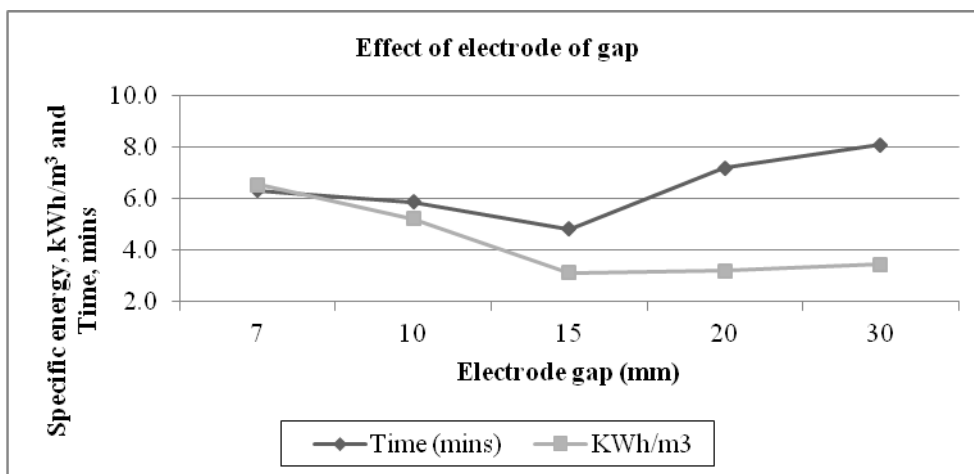


**Figure 4.24: Effect of electrode gap on specific energy consumption and colour removal time.**

Electrocoagulation time reduced with increasing electrode gap from 7 to 15 mm and increased as the gap increased beyond 15 mm. However, at an electrode gap of 15 mm specific energy consumption was the lowest. At 15 mm electrode gap, the time taken for complete colour removal was the shortest of the variations studied hence considered as

the optimum for the electrocoagulation process.

#### 4.9.3 Effect of surface area to volume ratio

Surface area to volume ratio (S/V) was varied to 13, 16, 19, 21, 24 and 27  $\text{m}^2/\text{m}^3$  and the results are shown in Figure 4.25. Specific energy consumption decreased as the S/V was increased from 13 to 19  $\text{m}^2/\text{m}^3$  then increased as the S/V increased to 27.

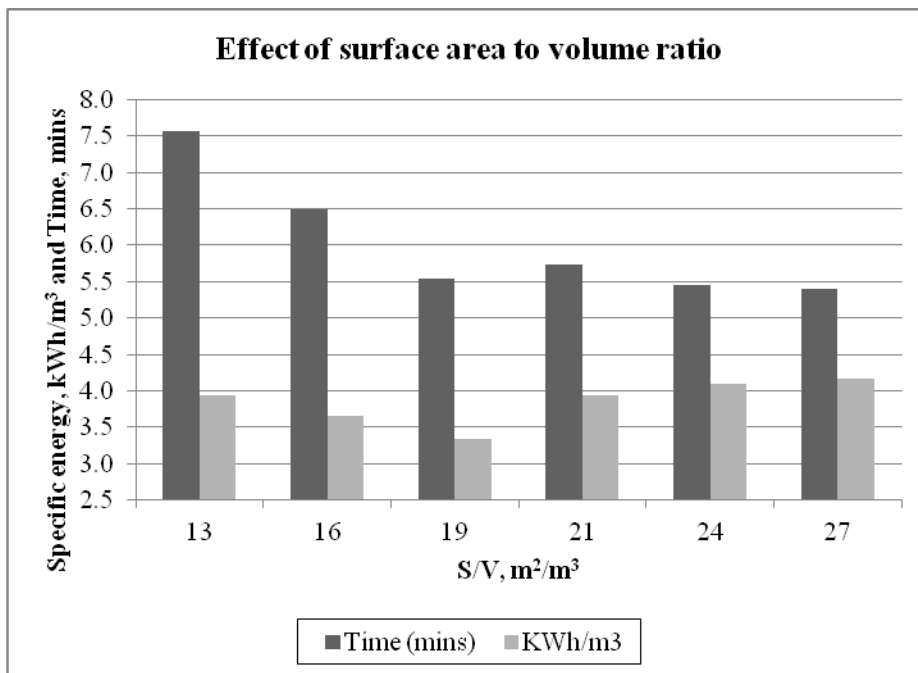


**Figure 4.25: Effect of surface area to volume ratio on specific energy consumption and colour removal time.**

However, the time was almost constant between S/V of 19 – 27  $\text{m}^2/\text{m}^3$ . The optimum value of 19  $\text{m}^2/\text{m}^3$  is comparable with studies using model dyes (Section 4.1-4.6) that gave an optimum of 16  $\text{m}^2/\text{m}^3$  for RR and 20  $\text{m}^2/\text{m}^3$  for DB dye

#### 4.9.4 Effect of supporting electrolyte

The effect of NaCl and  $\text{Na}_2\text{SO}_4$  electrolytes was investigated in the treatment of

RIVATEX wastewaters at 10 g/L concentrations and the results are shown in Figure 4.26. The time taken for decolourization and specific energy consumption was lower when NaCl electrolyte was used than when Na<sub>2</sub>SO<sub>4</sub> was used. This could be attributed to the higher oxidizing specific energy consumption of HOCl and OCl<sup>-</sup> produced by oxidation of NaCl at the anode compared to persulphates (Akrouit and Bousselmi, 2012).

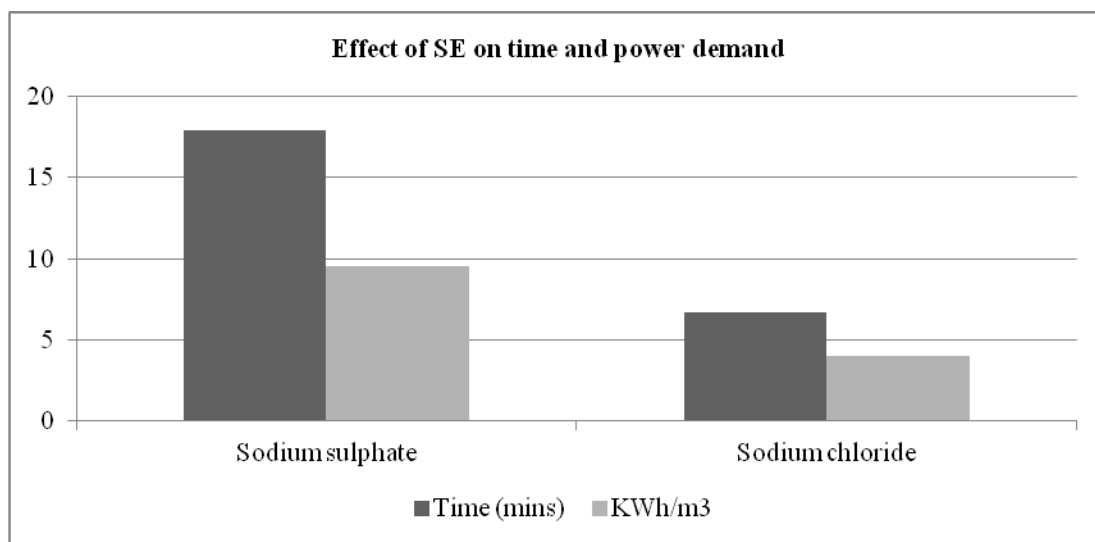


**Figure 4.26: Effect of supporting electrolytes on decolourization and specific energy of RIVATEX waste water.**

Many authors have reported that the use of NaCl as electrolyte has a positive effect due to active chlorine, HClO/CIO<sup>-</sup>, which depends on the pH of the medium (Panizza *et al.*, 2007). The active chlorine formation can occur in alkaline medium according to Equations 4.5- 4.7.

In neutral pH, HClO is the preponderant species. Results obtained differs what Martinez-Huitle and Brillias, (2009) which reported that no improvement was detected with the generation of active chloride when BDD is used but agree with Sakalis *et al.*, (2009) who reported that there was acceleration in dye degradation in the presence of chlorides. Use

of  $\text{Na}_2\text{SO}_4$  as a supporting electrolyte has also been found to accelerate dye degradation due to the generation of peroxosulphates ( $\text{S}_2\text{O}_8^{2-}$ ) which are very powerful oxidants (Akrouit and Bousselmi, 2012) as shown in Equation 4.10.

#### 4.9.5 Effect of temperature

The effect of temperature on specific energy consumption and coagulation time was investigated at 30, 40, 50 and 55 °C and the results are presented in Figure 4.27.

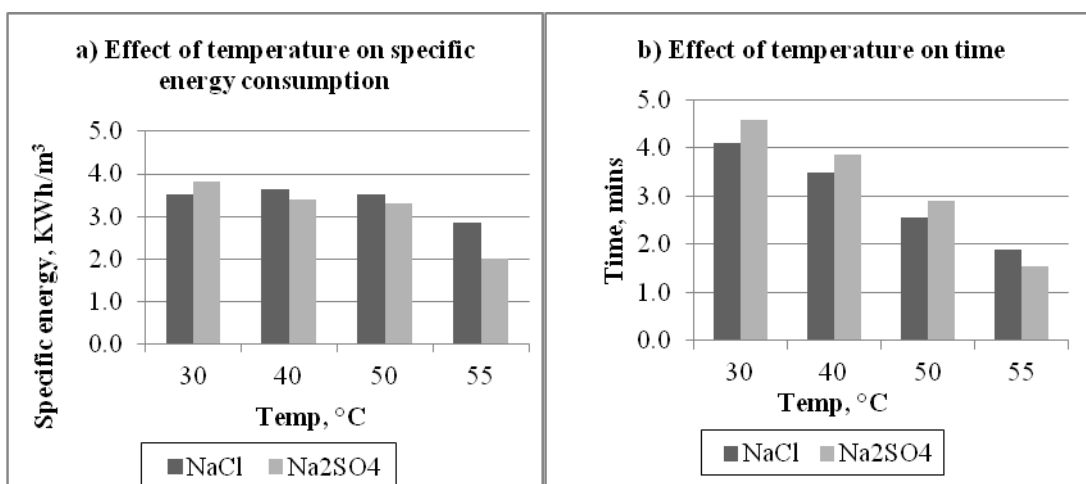


**Figure 4.27: Effect of temperature of on a) specific energy consumption and b) coagulation time of RIVATEX wastewater using NaCl and  $\text{Na}_2\text{SO}_4$**

As the temperature increased, the coagulation time reduced linearly hence an inverse proportionality was established between temperature and coagulation time. Above 40°C specific energy consumption using NaCl was higher than that of  $\text{Na}_2\text{SO}_4$ . This indicates that at temperatures above 40 °C,  $\text{S}_2\text{O}_8^{2-}$  species is less susceptible to decomposition than  $\text{HOCl}/\text{ClO}^-$  species; however, NaCl takes less time for coagulation (Fig. 4.27b).

Current density was found to increase with increasing temperature (Table 4.7) when both electrolytes were used, however NaCl led to higher current densities than  $\text{Na}_2\text{SO}_4$ . This

was as a result of increase in current flow that resulted in better conductivity of the solution as the temperature was increased. High temperatures favour electrocoagulation process (Springer *et al.*, 1995) and the results are similar to those obtained in electrocoagulation of RR and DB model dyes where an inverse relationship was established (Section 4.2.8).

**Table 4.7: Effect of temperature on current density and current using NaCl and Na<sub>2</sub>SO<sub>4</sub>**

Temp, °C	Current density, Am <sup>-2</sup>		Current, Amps	
	NaCl	Na <sub>2</sub> SO <sub>4</sub>	NaCl	Na <sub>2</sub> SO <sub>4</sub>
30	469	457	0.41	0.40
40	571	480	0.50	0.42
50	754	629	0.66	0.55
55	823	720	0.72	0.63

#### **4.9.6 Effect of Stainless Steel anode treatment on chemical oxygen demand**

Electrochemically treated RIVATEX samples by SS were analyzed for COD after colour removal and the results are shown in Table 4.8. The initial COD of raw wastewater was 251 mg/L. Sodium chloride supporting electrolyte led to a higher COD reduction than Na<sub>2</sub>SO<sub>4</sub>; however the levels were still higher than those recommended by NEMA. However, NaCl reduced COD by 11.1 % higher than Na<sub>2</sub>SO<sub>4</sub> and this is attributed to the high oxidation potential of the hypochloride (Table 4.9).

**Table 4.8: Effect of supporting electrolytes on Chemical Oxygen Demand levels**

Sample	COD, mg/L	% Reduction
Rivatex raw	251	
Raw sample + Na <sub>2</sub> SO <sub>4</sub>	120	52.2
Raw sample + NaCl	92	63.3

#### 4.10 Electrochemical mineralization of RIVATEX waste water using BDD anode

##### 4.10.1 Effect of pH on degradation

The effect of pH on RIVATEX wastewater degradation was investigated between pH 4 and 10 and the results are shown in Figure 4.28.

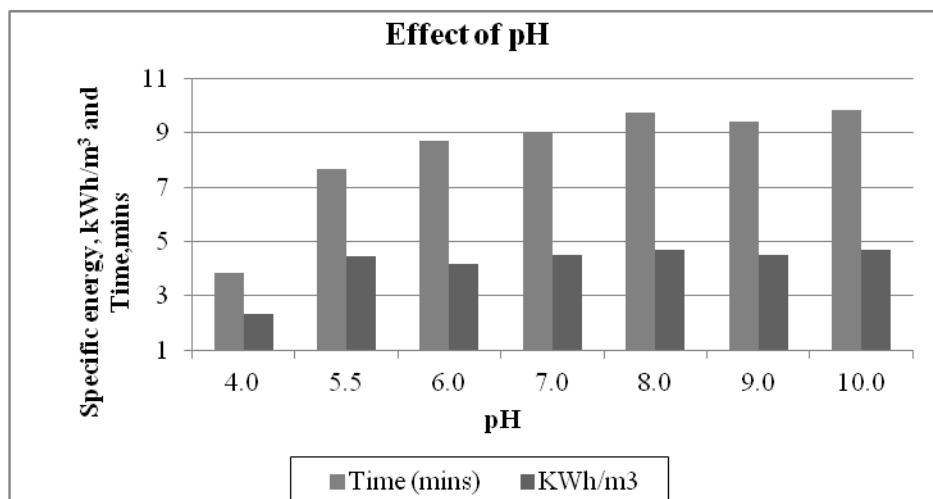


**Figure 4.28: Effect of pH on decolourization of RIVATEX wastewater using NaCl electrolyte.**

The lowest specific energy consumption was recorded at pH 4, as compared to the rest of acidic and alkaline pH. However, between pH 5 and 10, specific energy consumption was almost constant and not significantly different giving a wide electrochemical window for

BDD anodes.

The lowest specific energy consumption was at pH 4 and at this pH, decolourization time was the shortest compared to pH 5 – pH 7 above which it was almost constant. The low specific energy consumption at pH 4 could be attributed to the generation of HOCl species that is favoured in acidic conditions with NaCl electrolyte at low concentrations as reported by Cheng and Kelsall, (2007).

#### 4.10.2 Effect of Electrode gap

The effect of electrode gap was tested at 7, 10, 15, 20 and 30 mm and the results are shown in Figure 4.29.

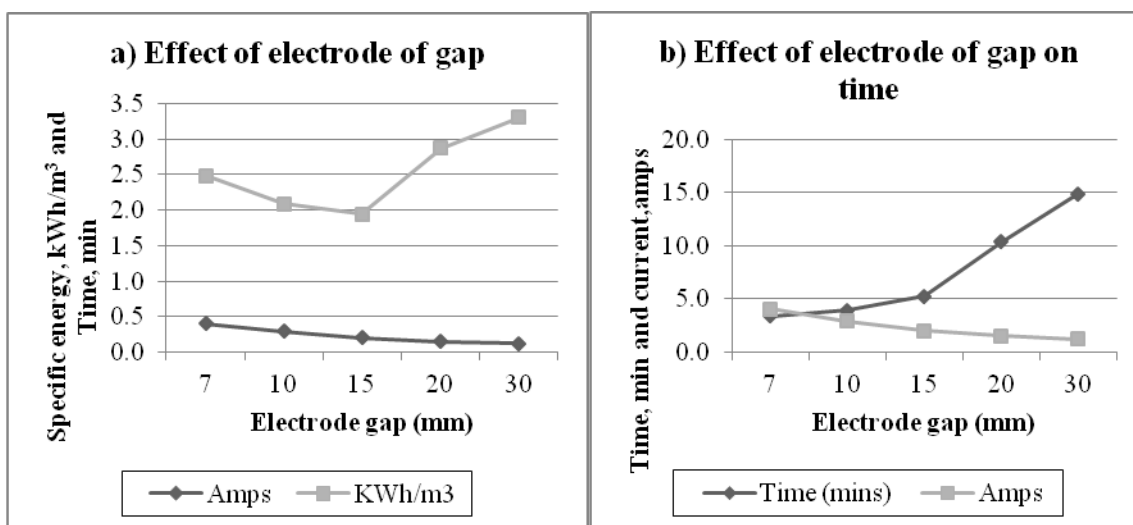


**Figure 4.29: Effect of electrode gap on decolourization of RIVATEX wastewater**

There was high current at the shortest gap of 7 mm which reduced linearly as the gap increased to 30mm. At 7 mm gap, specific energy consumption was 2.47 kWh/m<sup>3</sup> and reduced to a minimum of 1.95 kWh/m<sup>3</sup> at 15 mm electrode gap, then increased to

3.31kWh/m<sup>3</sup> at 30 mm (Fig 4.29a). At 7 mm there was very high overpotential (up to 2 volts) thus a lot of current was not utilized in oxidation reactions. Decolourization time increases with increasing electrode gap hence lowest at 7 mm and highest at 30 mm (Fig. 4.29b). The optimum gap obtained was found to be 15 mm for the RIVATEX effluent and is in agreement with results obtained by Springer *et al* (1995) which confirmed that each effluent requires to be optimized for electrode gap and S/V as these have direct effect on the efficiency of electrochemical decolourization process.

#### **4.10.3 Effect of supporting electrolytes**

Two supporting electrolytes were added to RIVATEX wastewater and their efficiencies in decolourization time and specific energy consumption are shown in Figure 4.30. Results indicate that NaCl was superior to Na<sub>2</sub>SO<sub>4</sub> in terms of specific energy consumption demand and treatment time. When Na<sub>2</sub>SO<sub>4</sub> was used as a supporting electrolyte, the time taken to degrade the wastewater was higher by 42 % compared to that of NaCl and this led to an increase in specific energy consumption by 42 %. This observation agrees well with what is reported in section 4.10.5, where SS electrodes are used. The better performance of NaCl is attributed to the oxidation specific energy of the intermediates HCO and ClO<sup>-</sup> formed (Equations 4.5-4.7) and that of Na<sub>2</sub>SO<sub>4</sub> arising from persulphates (Equation 4.10).



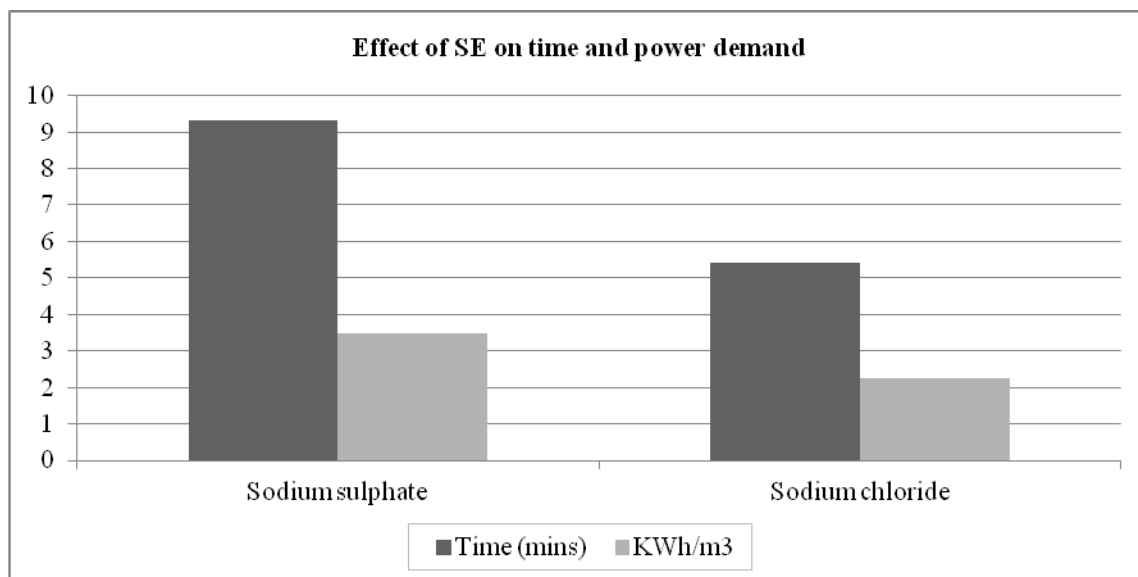


**Figure 4.30: Effect of supporting electrolytes on decolourization and specific energy consumption of RIVATEX wastewater**

The efficiency of NaCl as an electrolyte was found to be better than that of Na<sub>2</sub>SO<sub>4</sub> in the electrochemical treatment of RR and DB synthetic dye wastewaters (section 4.1 – 4.8). In the electrochemical treatment of RIVATEX wastewater, NaCl electrolyte was also found to be more efficient than Na<sub>2</sub>SO<sub>4</sub>.

#### 4.10.4 Effect of temperature

The effect of temperature on specific energy consumption and coagulation time was investigated at 30, 40, 50 and 55 °C and the results are presented in Figure 4.31. As the temperature increased, both the specific energy consumption and degradation time increased. This could be attributed to the decomposition of the indirect oxidation species generated by anodic oxidation of NaCl and Na<sub>2</sub>SO<sub>4</sub> electrolytes. Panizza and Cerisola, (2008) reported that temperature has little impact on electrochemical oxidation with OH• radicals and its influence must be interpreted in terms of the effect by mediated electro-

reagents. Therefore temperatures above room temperature have a negative effect on specific energy consumption demand and degradation times of RIVATEX wastewater using both NaCl and Na<sub>2</sub>SO<sub>4</sub> electrolytes.

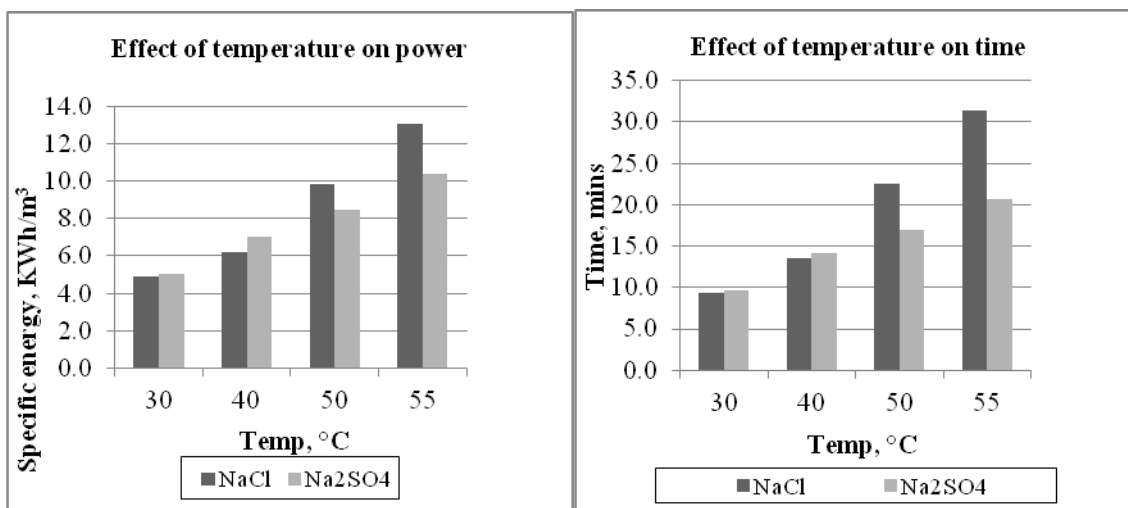


**Figure 4.31: Effect of temperature on a) specific energy consumption demand and b) degradation time of RIVATEX wastewaters**

#### 4.10.5 Effect of BDD treatment on Chemical oxygen demand

The effect of degradation time on the reduction of chemical oxygen demand (COD) was investigated by varying the time to 0, 30, 60, 90, 120, 150 and 180 min. The results are presented in Figure 4.32. The initial COD of the wastewater was 251 mg/L which was above the NEMA limit. COD reduction was rapid up to 80% reduction after 30 min then went on gradually. Increasing time from 30 – 180 min led to a reduction in COD by between 74-92 % with 3 g/l NaCl and 63-90 % with 3g/l Na<sub>2</sub>SO<sub>4</sub> electrolyte (Fig. 4.32b).

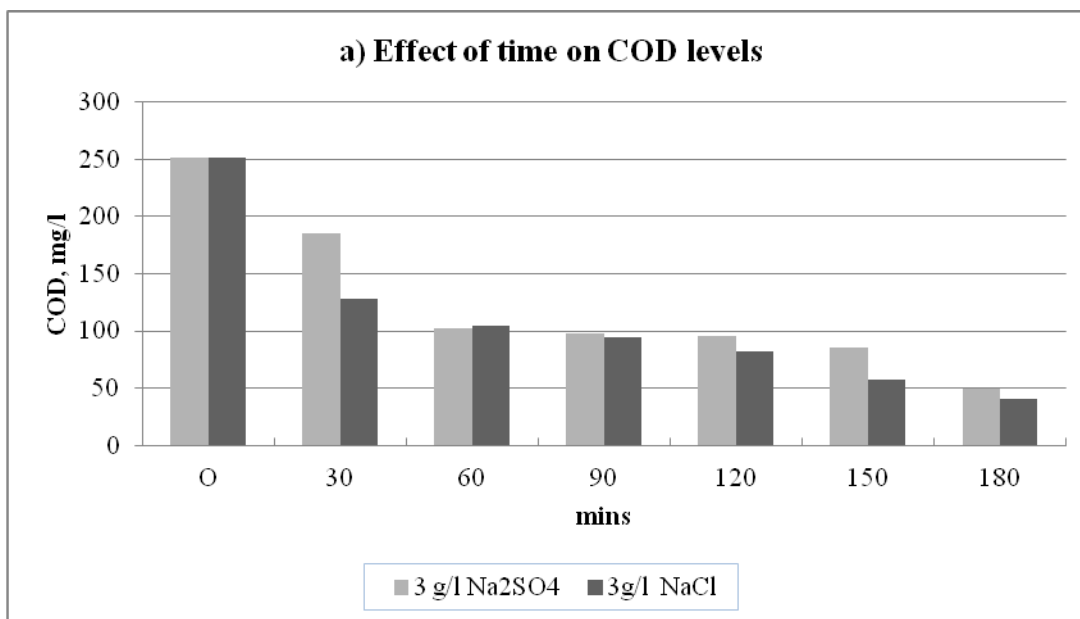


**Figure 4.32a: Effect of time on COD levels of RIVATEX wastewater using BDD.**

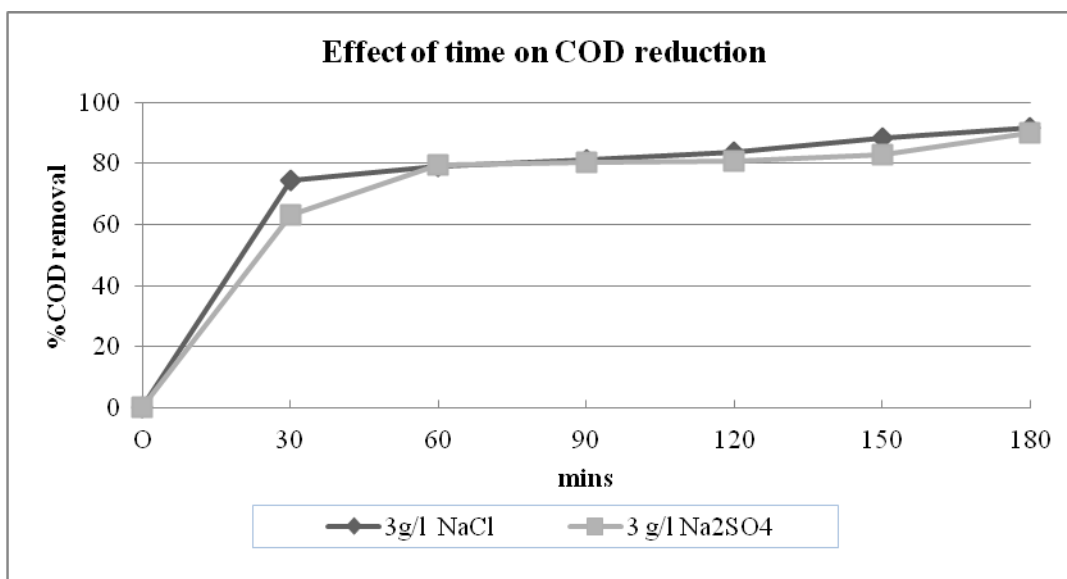


**Figure 4.32b: Effect of time on % COD reduction in RIVATEX wastewater using BDD**

Sodium chloride was a better electrolyte in both colour and COD reduction than sodium sulphate. This effect is attributed to the higher oxidation potential of the chlorine oxidized

species - the hypochlorite as shown in Table 4.9 (Zhou and Smith, 2002). Hydroxyl radical has a higher oxidizing potential than chlorine and hypochlorite hence is the main species in dye degradation. After 180 min, COD values of RIVATEX treated wastewater using both electrolytes were reduced to below the maximum contaminant level of 50 mg/L (Fig. 4.32a) set by NEMA (GOK, 1999).

**Table 4.9: Oxidizing potential for conventional oxidizing agents**

Oxidizing agent	Electrochemical oxidation potential (EOP),V	EOP relative to chlorine
Fluorine	3.06	2.25
Hydroxyl radical	2.80	2.05
Oxygen (atomic)	2.42	1.78
Ozone	2.08	1.52
Hydrogen peroxide	1.78	1.30
Hypochlorite	1.49	1.10
Chlorine	1.36	1.00
Chlorine dioxide	1.27	0.93
Oxygen (molecular)	1.23	0.90

**Source: Zhou and Smith (2002)**

#### 4.11 Specific energy consumption

Specific energy in kWh/m<sup>3</sup> after optimization of electrochemical treatment for both model dyes and RIVATEX wastewater is presented in Table 4.10. Sodium chloride electrolyte gave lower specific energy consumption than Na<sub>2</sub>SO<sub>4</sub> when model dyes and RIVATEX wastewater were electrochemically treated.

**Table 4.10: Specific energy consumption, kWh/m<sup>3</sup> for RIVATEX wastewater, RR and DB model dyes in presence of electrolyte using SS and BDD electrodes**

Electrode	Electrolyte	RR	DB	RIVATEX
SS	NaCl	0.79	1.11	9.36
	Na <sub>2</sub> SO <sub>4</sub>	0.99	1.54	9.62
BDD	NaCl	0.61	0.69	42.50
	Na <sub>2</sub> SO <sub>4</sub>	1.08	2.34	48.75

BDD electrodes required higher energy consumption than SS electrodes; however, the specific energy consumption for SS was obtained at decolourization while that of BDD was obtained after removal of COD to the acceptable NEMA limits of below 50 mg/L. It was noted that when electrocoagulation was conducted for longer periods above the decolourization time, the clarified wastewater oxidized to obtain a brownish solution of Fe (III) implying that there was excess of Fe (II) ions not utilized in colour removal. However, at low dye concentrations of 10 mg/L electrocoagulation can reduce COD to acceptable levels. Rivatex samples recorded a high specific energy consumption using SS electrodes as compared to the model dyes. However, electrocoagulation was effective only in colour removal but ineffective in COD removal while BDD was able to remove both colour and COD to acceptable levels. Specific energy consumption in BDD mineralization is quite high and a combination of the methods could reduce the cost.

## CHAPTER FIVE CONCLUSION AND RECOMMENDATIONS

### 5.1 Conclusion

This study investigated two electrochemical methods for the treatment of textile dye wastewater. The first method employed stainless steel (SS) electrode and the second used boron doped diamond electrode (BDD) as anode materials. Two model dyes; a reactive dye (C.I. Reactive Red 76, RR) and a disperse dye; (C.I. Disperse Blue 79, DB) were used in this study.

The results show that the optimum conditions for electrocoagulation using SS anode are; a potential difference of 10 V, S/V ratio of 16 m<sup>2</sup>/m<sup>3</sup> in RR and 20 m<sup>2</sup>/m<sup>3</sup> in DB, NaCl supporting electrolyte 4g/l and 6g/l in RR and DB respectively, inter-electrode distance of 12 mm and a pH of 6.5 for both RR and DB. Increasing current density led to a reduction in treatment time and an increase in COD reduction. Increasing temperature led to reduction in specific energy consumption as well as treatment time. Water pH increased by 1.74 % in DB and 1.24 % in RR as a result of removal of hydrogen ions at the cathode. DB had a lower specific energy consumption demand at optimized conditions than RR hence most suited for electrocoagulation. Removal of dye in wastewater by electrocoagulation was achieved by oxidation of Fe to Fe (III) forming Fe (III) hydroxide coagulant which was generated in “situ” by dissolution of SS electrode. The dye molecules formed flocs which were adsorbed on the surface of the coagulant.

SEM images for surface studies indicated that the iron electrode was highly corroded and the EDX spectrum indicated the active sites of iron on SS surface were later occupied by chlorine from the NaCl electrolyte. UV-VIS studies of SS raw and treated wastewater

indicated that the colour chromophore was removed. Electrochemically treated wastewater conformed to NEMA effluent discharge standards for pH, colour and COD (GOK, 1999).

Electrochemical mineralization studies using BDD anode indicated that degradation time reduced when NaCl and Na<sub>2</sub>SO<sub>4</sub> supporting electrolytes were added to the dye wastewater. It was found that NaCl was a better oxidant than Na<sub>2</sub>SO<sub>4</sub> in all the experiments performed. Raising current density enhanced degradation thus reducing treatment time by up to 50 %. However, high temperature was detrimental to degradation and a low temperature below 30 °C was required. Increasing dye concentration led to increased specific energy consumption as there was more demand for more hydroxyl radicals required for mineralization of the dye. The effect of pH on specific energy consumption was more pronounced in DB than in RR making RR to be treated easily over a wide pH window ranging from acidic to alkaline media. RR required lower specific energy consumption than DB hence took less time for complete mineralization.

UV-VIS studies of BDD raw and electrochemically treated wastewater indicated that the colour chromophore was removed. The BDD anodes in the wastewater generated reactive hydroxyl radicals on the BDD surface that degraded the colour chromophore in the organic molecule that led to a colourless solution and leaving the absorption spectrum to the UV region (200 – 400 nm).

Electrochemically treated wastewater (both synthetic and RIVATEX) by SS and BDD conformed to NEMA standards for pH, colour, and COD. Results revealed that SS electrode was able to reduce colour and COD at low dye concentrations of 10 mg/L. However at higher concentrations, SS could reduce colour effectively but unable to

reduce COD to meet NEMA standards. BDD electrode was able to reduce colour and COD to levels below 50 mg/L, although the time taken was much longer than that taken by SS to decolourize the wastewater. The COD levels of BDD- treated wastewater were lower than those of SS treated wastewater. Results showed that SS was useful in decolourization of textile dyes while BDD was useful for both decolourization and COD reduction hence BDD was found to be more superior.

It was concluded that the main parameters affecting electrochemical treatment were pH, current density, dye concentration and nature of supporting electrolytes. When treating dye wastewater for colour removal only, SS is the anode of choice and the wastewater must have high conductivity to give high current densities, pH of 6 -7 and presence of chloride ions at between 3- 10 g/l. However when reduction of both colour and COD is required, BDD is the anode of choice. The wastewater should be slightly acidic and the applied current density should be  $> 50 \text{ Am}^{-2}$  while chloride ions should be present at 3-10 g/l. It was observed that BDD was a more superior anode to SS in the treatment of textile dye wastewater since it was able to remove the colour completely and reduce the COD levels of wastewaters to less than 50 mg/L (MCL) hence RIVATEX can adopt the BDD electrochemical technology. However, to reduce on the cost of electrochemical treatment, the wastewater can be treated in two stages; first by electrocoagulation using SS anode for colour removal, then by BDD for COD reduction.



## 5.2 Recommendations

Based on the findings of this study, the following recommendations have been made:-

- i). These technologies can be adopted by Rivatex and other textile industries; however, wastewater can be treated by electrocoagulation then by mineralization.
- ii). There is need to carry out more research using different dye classes to ascertain interactions between the dye and supporting electrolyte.
- iii). There is need to study the effects of different cations and anions on BDD degradation efficiency including Fe (II).
- iv). There is need to carry out more studies to identify alternative conducting thin films that can be cheaper than BDD such as titanium- based dimensionally stable anodes (DSA).
- v). There is need to carry out more spectroscopic and electrochemical analysis to understand the interactions of dye and the metallic hydroxide and degraded products using Liquid Chromatography-Mass Spectroscopy (LC-MS), Fourier Transformed Infrared Spectroscopy (FTIR) and Zeta potentiometer.

## REFERENCES

- Akrou, H. and Bousselmi, L. (2012). Chloride ions as an agent promoting the oxidation of synthetic dyestuff on BDD electrode. *Desalination and Water treatment*, **46**:171 – 181.
- American Public Health Association (APHA), American Water Works Association (AWWA), and the Water Environmental Federation (WEF). 2002. *Standard Methods for Examinations of Water and Wastewater*, 21<sup>st</sup> ed. United Book Press, Inc. Baltimore, Maryland.
- Atkins, P. and Paula, J. Atkins' physical chemistry, 8<sup>th</sup> Edition, Oxford University Press 2006 pp 830 – 840.
- Augugliaro, V., Baiocchi, C., Prevot, A. B. (2002). Azo-dyes photocatalytic degradation in aqueous suspension of TiO<sub>2</sub> under solar irradiation. *Chemosphere*, **49** (10): 1223–1230.
- Ayten, N., Arslan-Alaton, I., Olmez-Hanci, T. (2011). Application of photo-fento-like oxidation for the degradation and detoxification of commercial naphthalene sulphonates: A case study with H-acid model pollutant. *Desalination Water Treatment Science Engineering* **26**:139–144.
- Azban, N., Yonar T. and Kestioglu, K. (2004). Comparison of advanced oxidation processes and chemical treatment methods for COD and colour removal from a polyester and acetate fiber dyeing effluent. *Chemosphere*, **55** (1) 35-43.
- Baklan, V.Y. and Kolesnikova, I.P. (1996). Influence of electrode material on the electrocoagulation. *Journal of Aerosol Science*, **27** (1): S209 – S210.

- Baiocchi, C., Brussino, M. C., Pramauro, E., Prevot, A. B., Palmisano, L., and Marc T, G. (2002) Characterization of methyl orange and its photocatalytic degradation products by HPLC/UV-VIS diode array and atmospheric pressure ionization quadrupole ion trap mass spectrometry". *International Journal of Mass Spectrometry*, **214** (2): 247–256.
- Baryamoglu, M., Eyvaz, E., Kobya, M. (2007), Treatment of textile wastewater by electrocoagulation: economic evaluation. *Journal of Chemical engineering*, **128**: 155 – 161.
- Benefield, D.L., Judkins, F.J. and Weand, L.B. (1982). Process chemistry for water and wastewater treatment. New Jersey: Prentice-Hall.
- Bobe, A., P. Meallier, J. F. Cooper, and C. M. Coste. (1998). Kinetics and mechanisms of abiotic degradation of fipronil (hydrolysis and photolysis). *Journal of Agriculture and Food Chemistry*. **46**: 2834-2839
- Boye, B., Brillas, E., Marselli, B., Michaud, P.-A., Comninellis, Ch. and Dieng, M.M. (2004). Electrochemical decontamination of waters by advanced oxidation processes (AOPS): Case of the mineralization of 2,4,5-T on BDD electrode. *Bulletin of the Chemical Society of Ethiopia*. **18**, 205–214.
- Boye, B., Brillas, E., Marselli, B., Michaud, P.-A., Comninellis, Ch., Farnia, G. and Sandon`a, G. (2006) Electrochemical incineration of chloromethylphenoxy herbicides in acid medium by anodic oxidation with boron-doped diamond electrodes. *Electrochimica Acta* **51**, 2872–2880.

- Brown, D. and Hamburger, B. (1987) The degradation of dyestuffs: Part III. Investigations of their ultimate degradability, *Chemosphere*, **16**, 1539-1553
- Burton, G. A., Jr., and R. E. Pitt. (2002). Storm Effects Handbook: A Toolbox for Watershed Managers, Scientists, and Engineers, Lewis Publishers, Boca Raton, FL.
- Canizares, P., Garcia-Gomez, J., Lobato, J., Rodrigo M.A. (2003). Electrochemical oxidation of aqueous carboxylic acid wastes using diamond thin-film electrodes. *Indiana Journal of Engineering in Chemical Research*. **42**: 956–962.
- Canizares, P., Garcia-Gomez, J., Saez, C., Rodrigo, M.A. (2004). Electrochemical oxidation of several chlorophenols on diamond electrodes. Part II. Influence of waste characteristics and operating conditions. *Journal of Applied Electrochemistry* **34**: 87–94.
- Cañizares, P., Martínez, L., Paz, R., Sáez, C., Lobato, J., & Rodrigo, M. A. (2006a). Treatment of Fenton-refractory olive oil mill wastes by electrochemical oxidation with boron-doped diamond anodes. *Journal of Chemical Technology and Biotechnology*, **81**: 1331–1337.
- Canizares, P., Martinez, P., Jimenez, C., Lobato, J., Rodrigo, M.A. (2006b). Coagulation and electrocoagulation of wastes polluted with dyes. *Journal of Environmental Science and Technology*, **40**, 6418–6424.
- Cerco , C. F. and Cole, T. (1994) . Three - dimensional Eutrophication Model of Chesapeake Bay. Volume 1: Main Report. Technical Report EL - 94 - 4. US Army Corps of Engineers
- Chen, X. and Chen, G. (2006). Anodic oxidation of Orange II on Ti/BDD electrode: Variable effects. *Separation and Purification Technology*, **48** (1): 45–49

- Chen, X., Gao, F. and Chen, G. (2005) Comparison of Ti/BDD and Ti/SnO<sub>2</sub>-Sb<sub>2</sub>O<sub>5</sub> electrodes for pollutants oxidation. *Journal of Applied Electrochemistry*, **35**, 185–191.
- Chen, X., Chen, G. and Yue P.L. (2003), Separation of pollutants from a restaurant wastewater by electrocoagulation. *Separation Purification Technology*, **19**: 65 – 76.
- Cheng, C. Y., & Kelsall, G. H. (2007). Models of hypochlorite production in electrochemical reactors with plate and porous anodes. *Journal of Applied Electrochemistry*, **37**:1203–1217.
- Cheng, G. H. (2004). Electrochemical technologies in wastewater treatment. *Separation and Purification* **49** (22-23): 3807-3820.
- Cominellis, C. and Chen, G. *Electrochemistry for the Environment* (2010). Springer, New York.
- Cominellis, C. and Pulgarin, C. (1991) Anodic oxidation of phenol for waste water treatment. *Journal of Applied. Electrochemistry*, **21**, 703–708.
- Dalvand, A., Gholami, M., Joneidi, A. and Mahmoodi, N. M. (2011), Dye Removal, Energy Consumption and Operating Cost of Electrocoagulation of Textile Wastewater as a Clean Process. *Clean Soil Air Water*, **39**: 665–672.
- De Pinho, M. M., Geraldes, V., Rosa, M. J., Afonso, D., Figueira, H., Taborda, F., Almeida, G., Ganho R., Creusen, R., Saijer, J., Gaeta, S., Amblard, P. Gavach, C and Gisard, C. (1996). Water recovery from bleached pulp effluents. *TAPPI Journal*, **79** (12): 117.
- DO, J. and Chen, L. (1994) Decolourization of dye containing solutions by electrocoagulation. *Journal of Applied Electrochemistry*, **24** (8): 785 – 790.

Etiégni, L., Oricho, O.D., Ofosu-Asiedu, K., Senelwa, K. A., Surtan, K. G. and Omutange, E. S. (2007), Removal of colour from Kraft pulp and paper mill effluent in Kenya using a combination of electrochemical method and phosphate rock. *Water Science and Technology*, **55**: 15 – 22.

Faraday's law of electromagnetic induction (1831-32) Physics. Dictionary of Theories; 2002, p196

Feng, J. W., Sun, Y. B., Zheng, Z., Zhang, J. B., Li, S., Tian, Y. C., (2007). Treatment of Tannery Wastewater by Electrocoagulation. *Journal of Environmental Sciences*, **19**: 1409 – 1415.

Feng, Y. J. and Li, X.Y. (2003) Electro-catalytic oxidation of phenol on several metal-oxide electrodes in aqueous solution. *Water Research*, **37**(10), 2399–2407.

Ghernaout, D., Naceur, M. W., & Aouabed, A. (2011). On the dependence of chlorine by-products generated species formation of the electrode material and applied charge during electrochemical water treatment. *Desalination*, **270**: 9–22.

GOK (1972). Water Act (Cap 372), sec 145-147 of the Laws of Kenya, Government Printers.

GOK (1986). Public Health Act (Cap 372), Part ix, sec 16 of the Laws of Kenya, Government Printers.

GOK (1999), Environmental Management and Coordination Act. Government Printers.

GOK. Standard Drainage, Sewerage and Trade Effluent By-Laws. Ministry of Local Government. Water and Sanitation Operations Units (WSOU). Nairobi, Kenya, 1993.

- Goldstein, J. Scanning electron microscopy and x-ray microanalysis. Kluwer Academic/Plenum Publishers, 2003, 689 p.
- Gunasekara, A. S., Truong T., Goh K. S., Spurlock F., and Tjeerdema R. S. (2007). Environmental fate and toxicology of fipronil. *Journal of Pesticide Science*, **32**(3): 189–199.
- Hameed, B. H., Ahmad, A. A. and Aziz, N. (2007). “Isotherms, kinetics and thermodynamics of acid dye adsorption on activated palm ash”, *Journal of Chemical Engineering* **3**: 251.
- Holt, P., Barton, G. and Mitchel, C. (2006). Electrocoagulation as a wastewater treatment. The third Annual Australian Environmental Engineering research Proceedings: 23 – 26.
- James, D., Wojciech, J. and Nigel, J.B. (1999). Electrochemical oxidation of chlorinated phenols. *Environmental Science and Technology*, **33**, 1453–1457.
- Kashefialasl, M., Khosravi, M., Marandi, R. and Seyyedi, K. (2006). Treatment of dye solution containing coloured index acid yellow 36 by electrocoagulation using iron electrodes. *International Journal of Environmental Science and Technology*, **2** (4): 365 – 371.
- Khataee, R. and Habibi, B. (2010). Photochemical oxidative decolouration of CI basic red 46 by UV/H<sub>2</sub>O<sub>2</sub> process: Optimization using response surface methodology and kinetic modeling. *Desalination Water Treatment Science Engineering*. **16**: 243–253.
- Koby, M., Bayramoglu, M., Eyvaz, M. (2007). Techno-economical evaluation of electrocoagulation for the textile wastewater using different electrode connections. *Journal of Hazardous Materials*. **148**, 311–318.

- Koby, M., Cifti C., Taner O., Baryamoglu, M . (2003), Treatment of Textile wastewaters by electrocoagulation using iron and aluminium electrodes. *Journal of Hazardous Materials*, **B100**: 163 – 178.
- Koby, M., Demirbaş, E., Dedeli, A., Şensoy, M.T. (2010). Treatment of Rinse Water From Zinc Phosphate Coating by Batch and Continuous Electrocoagulation Processes, *Journal of Hazardous Materials*, **173**: 326–334.
- Lai, C.L., Lind, S.H. (2003), Electrocoagulation of chemical and mechanical polishing (CMP) wastewater from semiconductor fabrication. *Journal of Chemical Engineering*, **95**: 205 – 211.
- Maghanga, J.K., (2008). Improvement of tea effluent Clarification By electrocoagulation: A Case Study of Chemomi Tea Factory, Nandi South District, Kenya. MPhl. Thesis, Moi University.
- Maghanga, J.K., Segor, F.K., Etiegni, L. and Lusweti, J.L. (2009a). Electrocoagulation method for colour removal in tea effluent: A case study of Chemomi tea factory in Rift valley. Kenya. *Bulletin of the Chemical Society of Ethiopia*, **23** (3):371-381.
- Maghanga J.K., Segor F.K., Etiégni L. and Kituyi J.L. (2009b). Electrochemical treatment of a Kenyan tea factory wastewater. *Journal of agriculture, pure and applied science and technology*, **2**: 68 – 75.
- Mameri, N. and Yeddou, A.R. (1998). Defluoridation of septentrional Sahara water of North Africa by electrocoagulation process using bipolar aluminium electrodes. *Water Research*, **32**, (5): 1604 – 1612.



- Manjunnath, D. and Mehrotra, I. (1981). Removal of Reactive Dyes using Alum: lignin Sludge. *Indian Journal of Environmental Health*, **23** (4): 309 – 315.
- Martinez- Huitle C.A., Brilllas, E.(2009). Decontamination of wastewaters containing synthetic organic dyes by electrochemical methods: A general review. *Applied Catalysis*, **87**:105–145.
- Modirshahla, N., Behnajady, M.S., Kooshaiian, S. (2007). Investigation of the effect of different electrode connections on the removal efficiency of tartrazine from aqueous solutions by electrocoagulation. *Journal of Dyes and Pigments*, **74**: 249–257.
- Mollah, M.Y.A., Schenah, R., Parga, J.P. and Coke, D.L. (2001). Electrocoagulation (EC) Science and application. *Journal of Harzadous Materials*, **B84**: 29 – 41.
- Muruganantham, M., Raju, G.B. Prabhakar, S. (2004), Separation of pollutants from tannery effluent by electro flotation. *Separation Purification Technology*, **40**: 69 – 75.
- Muruganathan, M. , Yoshihara, S., Rakuma, T., Uehara, N., Shirakashi, T. (2007). Electrochemical degradation of 17 $\beta$ -estradiol at Si/BDD thin film electrode, *Electrochimica Acta*, **52** ( 9): 3242–3249.
- Nasrullah, M., Singh, L. and. Wahid, Z. (2012). Treatment of Sewage by Electrocoagulation and the Effect of High Current Density. *Energy and Environmental Engineering Journal*, **1**(1): 2-12

- Nikolaev, N. V, Kozlovskii, A.S. and Utkin, I. I. (1982). Treating natural waters in small water systems by filtration with electrocoagulation. *Soviet Journal of Water Chemistry and Technology*, **4** (3): 244-247.
- Novikova, S.P. and Shkorbatova, T.T. (1982). Purification of effluents from the production of synthetic detergents by electrocoagulation. *Soviet Journal of Water Chemistry and Technology*, **4**, 335-357.
- Orori, B. O., Etiégni, L., Rajab, M. S., Situma, L. M., and Ofosu – Asiedu, K. (2005) Decolourization of pulp and paper mill effluent in Webuye Kenya by a combination of electrochemical and coagulation methods. *Pulp and Paper Canada* **106** (2005) 21-26.
- Panizza, M. and Cerisola, G. (2008). Removal of colour and COD from wastewater containing acid blue 22 by electrochemical oxidation. *Journal of Hazardous Materials* **153** : 83–88
- Panizza, M., Barbucci, A., Ricotti, R., Cerisola, G., (2007). Electrochemical degradation of methylene blue. *Separation and Purification. Technology*. **54**: 382–387.
- Panizza, M., Michaud, P.A., Cerisola, G., Cominellis, C. (2001). Anodic oxidation of 2-naphthol at boron-doped diamond electrodes. *Journal of Electroanalytical Chemistry*, **507**: 206.
- Park, K., Kuo , Shen Y. and Hamrick , J. (1995). A Three – dimensional Hydrodynamic - Eutrophication Model (HEM3D): Description of Water Quality and Sediment Processes Submodels. The College of William and Mary, Virginia Institute of Marine Science. Special Report 327, 113 pp.

- Paul, A. Proceedings of the 22nd WEDC Conference on Water Quality and Supply, New Delhi, India, 1996, p286.
- Pearce, C., Llyod J., and Guthrie, J. (2003). The removal of colour from textile wastewater using whole bacterial cells: a review. *Dyes and Pigments*, **58**:179-196.
- Pinho, M., Minhalma, M., Rosa, M. and Taborda, F. (2000). Integration of Flotation/Ultrafiltration for Treatment of Bleached Pulp effluent, “Helps to remove colour and Suspended Solids” *Journal of Pulp and Paper Canada*, **101** (4): 50 – 54.
- Pinheiro, M., Touraud, E., & Thomas, O. (2004). Aromatic amines from azo dye reduction: status review with emphasis on direct UV spectrophotometric detection in textile industry wastewaters. *Dyes and Pigments*, **61**:121–139.
- Ponnusamy, S., Neduvelanna, U., Rangasamy, G. (2010). Dye removal from aqueous solution by Electrocoagulation process using stainless Steel electrodes *Environmental Engineering and Management Journal*, **8**(9) 1031-1037.
- Polcaro, A., Palmas, S., Renoldi, F. and Mascia, M. (1999) On the Performance of Ti/SnO<sub>2</sub> and Ti/PbO<sub>2</sub> Anodes in Electrochemical Degradation of 2-Chlorophenol for Wastewater Treatment. *Journal of Applied Electrochemistry*, **29** (2) 147–151.
- Prasad, R., Kumar, R. and Srivastava, S. (2008). Design of optimum response surface experiments for electrocoagulation of distillery spent wash. *Water, Air, and Soil Pollution*, **191**: 5–13.

- Qaiser, S., Saleemi, A., and Umar, M. (2009). Biosorption of lead (II) and chromium (VI) on groundnut hull: Equilibrium, kinetics and thermodynamics study. *Electronic Journal of Biotechnology*, **12**, (4): DOI: 10.2225/vol12-issue4-fulltext-6.
- Reid, R. and Green, G. (1996). "A sound business decision (Part 1)". *Journal of Society of Dyers*, **13**: 8-9
- Sakalis, K., Fytianos, K., Nickel, U., Voulgaropoulos, A. (2006). A comparative study of platinised titanium and Nb/Sn. *Chemical Engineering Journal*, **119**: 127–133.
- Santos, V., Morão, A., José Pacheco, M., Ciríaco, L. and Lopes, A. (2008). Electrochemical Degradation Of Azo Dyes On Bdd: Effect Of Chemical Structure And Operating Conditions On The Combustion Efficiency. *Journal of Environmental Engineering and Management*, **18**(3), 193 – 204
- Schachtman, D., Reid R., and Ailing S. (1998). Phosphorus uptake by plants: from soil to cell. *Journal of Plant Physiology*, **116**:447-453.
- Schulz, C.R and Okun, D.A (1992). Surface water treatment for communities in developing countries. John Wiley and Sons, UK.
- Scialdone, O., Randazzo, S., Galia, A., Silvestri, G. (2009). Electrochemical oxidation of organics in water: Role of operative parameters in the absence and in the presence of NaCl. *Water Research*, **43**(8): 2260–2272.
- Sengal, I. and Oscar, M. (2006). Treatment of dairy wastewater by electrocoagulation using mild steel electrodes. *Journal of Hazardous Materials*, **137**: 1197 – 1205.

Skoog, A., West, M., and Holler, F. (1997). *Fundamentals of analytical chemistry*, 7th Edition. Orlando: Harcourt.

Singer, P. and Reckhow, D. (1999), Chemical oxidation, chapter 12, In: *R. D. letterman (editor), Water quality and treatment: A handbook of community*.

Song, Z., Williams, C. and Edyvean, R. (2004). Treatment of tannery wastewater by chemical coagulation. *Desalination*, **164**: 249–259.

Springer, A., Hand, V. and Jarvis, T. (1995). Electrochemical removal of colour and toxicity from bleached Kraft effluents. *TAPPI Journal*, **78** (12): 86-92.

Srinivasan, A. and Viraraghavan, T., Decolourization of dye wastewaters by biosorbents: a review (2010). *Journal of Environmental Management*, **91**(10): 1915–1929.

Stucki, S., Kötzt, R., Carcer, B. and Suter, W. J. (1991) Electrochemical waste-water treatment using high overvoltage anodes. 2. Anode performance and applications. *Journal of Applied Electrochemistry*, **21**, 99–104.

Tertian, R. and Claisse, F., *Principles of Quantitative X-Ray Fluorescence Analysis*, Heyden, London, 1982.

Vik, E.A, Carlson, D.A., Eijun, A.S. and Gjessing, E.T. (1984). Electrocoagulation of potable water. *Water Research*, **18** (11): 1355 – 1360.

Xueming, C. and Chen, G. (2006). Anodic oxidation of Orange II on Ti/BDD electrode: Variable effects. *Separation and Purification Technology*, **48** (1): 45–49

- Yangming, L, Zhemin, S., Xuejun, C., Jinpin, J. and Wenhua, W. (2006). Preparation and application of nano-TiO<sub>2</sub> catalyst in dye electrochemical treatment. *Water SA*, **32** (2): 205-209.
- Yavuz, Y. (2007), EC and EF processes for the treatment of alcohol distillery wastewater. *Separation Purification Technology*, **53**:135-140.
- Yildiz, Y.S., Koparal, A.S., Irdemez, S., Keskinler, B. (2007). Electrocoagulation of synthetically prepared waters containing high concentration of NOM using iron cast electrodes. *Journal of Hazardous Materials*. **B139**: 373–380.
- Zawani, Z, Luqman, A, Choong, T. (2009). Equilibrium, Kinetics and Thermodynamic Studies: Adsorption of Remazol Black 5 on the Palm Kernel Shell Activated Carbon (PKS-AC). *European Journal of Scientific Research* **37** (1) :67-76
- Zhen-Gang J., Hydrodynamics and Water Quality, John Wiley & Sons, Inc., Hoboken, New Jersey (2008) pp 322- 336.
- Zhou, H. and Smith, D. (2002), Advanced technologies in water and wastewater treatment. *Journal of Environmental Engineering Science*, **1**: 247-264.

## APPENDICES

**Appendix I: Electrochemical data using steel anode**

## 1.1 Effect of voltage on specific energy consumption in RR

Conc.(mg/L)	Voltage (Volts)	Rep	Current (Amps)	Time (min)	Time (hrs)	Specific energy (KWh/m <sup>3</sup> )	
10	10.0	1	0.21	4.75	0.079	0.665	
		2	0.22	4.80	0.080	0.704	
		3	0.21	4.87	0.081	0.681	
			0.21	4.81	0.080	0.683	
	12.0	1	0.23	4.37	0.073	0.803	
		2	0.21	4.63	0.077	0.778	
		3	0.21	4.77	0.079	0.801	
			0.22	4.59	0.076	0.794	
	20	10.0	1	0.20	4.20	0.070	0.560
			2	0.21	4.10	0.068	0.574
			3	0.21	4.03	0.067	0.565
				0.21	4.11	0.069	0.566
12.0		1	0.25	3.93	0.066	0.787	
		2	0.26	3.75	0.063	0.780	
		3	0.25	3.80	0.063	0.760	
			0.25	3.83	0.064	0.776	
30		10.0	1	0.20	4.10	0.068	0.547
			2	0.21	3.97	0.066	0.555
			3	0.21	4.03	0.067	0.565
				0.21	4.03	0.067	0.556
	12.0	1	0.25	3.37	0.056	0.673	
		2	0.26	3.25	0.054	0.676	
		3	0.25	3.17	0.053	0.633	
			0.25	3.26	0.054	0.661	
	40	10.0	1	0.20	4.07	0.068	0.542
			2	0.21	4.53	0.076	0.635
			3	0.21	4.40	0.073	0.616
				0.21	4.33	0.072	0.598
12.0		1	0.25	3.53	0.059	0.707	
		2	0.26	3.47	0.058	0.721	
		3	0.25	3.40	0.057	0.680	
			0.25	3.47	0.058	0.703	
50		10.0	1	0.19	4.97	0.083	0.629
			2	0.21	4.90	0.082	0.686
			3	0.21	4.87	0.081	0.681
				0.20	4.91	0.082	0.665
	12.0	1	0.25	3.23	0.054	0.647	
		2	0.26	3.17	0.053	0.659	
		3	0.26	3.20	0.053	0.666	
			0.26	3.20	0.053	0.657	

## 1.2 Effect of voltage on specific energy consumption in DB

Conc.mg/L	Voltage (Volts)	Rep	Current (Amps)	Time (min)	Time (hrs)	Specific energy (KWh/m <sup>3</sup> )
10	1	10	0.20	5.27	0.088	0.702
	2	10	0.18	5.33	0.089	0.640
	3	10	0.19	5.40	0.090	0.684
			0.19	5.33	0.089	0.675
	1	12	0.23	4.30	0.072	0.791
	2	12	0.22	4.25	0.071	0.748
	3	12	0.24	4.30	0.072	0.826
			0.23	4.28	0.071	0.788
	20	1	10	0.21	4.95	0.083
2		10	0.20	4.93	0.082	0.658
3		10	0.20	4.85	0.081	0.647
			0.20	4.91	0.082	0.666
1		12	0.24	3.82	0.064	0.733
2		12	0.25	3.60	0.060	0.720
3		12	0.23	3.78	0.063	0.696
			0.24	3.73	0.062	0.716
30		1	10	0.21	4.75	0.079
	2	10	0.20	4.70	0.078	0.627
	3	10	0.21	4.72	0.079	0.660
			0.21	4.72	0.079	0.651
	1	12	0.26	3.83	0.064	0.797
	2	12	0.25	3.92	0.065	0.783
	3	12	0.24	3.90	0.065	0.749
		12.00	0.25	3.88	0.065	0.776
	40	1	10	0.21	4.33	0.072
2		10	0.20	4.42	0.074	0.589
3		10	0.18	4.53	0.076	0.544
			0.20	4.43	0.074	0.580
1		12	0.22	3.75	0.063	0.660
2		12	0.23	3.83	0.064	0.705
3		12	0.23	3.93	0.066	0.724
			0.23	3.84	0.064	0.696
50		1	10	0.20	4.80	0.080
	2	10	0.20	4.87	0.081	0.649
	3	10	0.20	4.92	0.082	0.656
			0.20			0.648
	1	12	0.22	3.88	0.065	0.683
	2	12	0.23	3.90	0.065	0.718
	3	12	0.22	3.93	0.066	0.692
			0.22	3.91	0.065	0.698



## 1.3 Effect of surface area to volume ratio (S/V) on specific energy consumption in RR

S/V (m <sup>2</sup> /m <sup>3</sup> )	Voltage (Volts)	Rep	Current (Amps)	Time (min)	Time (Hrs)	Specific energy (KWh/m <sup>3</sup> )
28.0	10	1	0.11	10.37	0.173	0.760
28.0	10	2	0.11	9.90	0.165	0.726
28.0	10	3	0.11	9.70	0.162	0.711
			0.11	9.99	0.166	0.733
24.0	10	1	0.11	8.45	0.141	0.620
24.0	10	2	0.11	8.40	0.140	0.616
24.0	10	3	0.11	8.53	0.142	0.626
			0.11	8.46	0.141	0.620
20.0	10	1	0.11	7.88	0.131	0.578
20.0	10	2	0.12	7.77	0.129	0.621
20.0	10	3	0.11	7.83	0.131	0.574
			0.11	7.83	0.130	0.591
16.0	10	1	0.10	7.47	0.124	0.498
16.0	10	2	0.10	7.50	0.125	0.500
16.0	10	3	0.10	7.30	0.122	0.487
			0.10	7.42	0.124	0.495
12.0	10	1	0.08	12.23	0.204	0.652
12.0	10	2	0.08	11.97	0.199	0.638
12.0	10	3	0.08	11.92	0.199	0.636
			0.08	12.04	0.201	0.642
8.0	10	1	0.07	15.23	0.254	0.711
8.0	10	2	0.07	15.37	0.256	0.717
8.0	10	3	0.07	15.17	0.253	0.708
			0.07	15.26	0.254	0.712

## 1.4 Effect of surface area to volume ratio (S/V) on specific energy consumption in DB

S/V (m <sup>2</sup> /m <sup>3</sup> )	Voltage (Volts)	Rep	Current (Amps)	Time (min)	Time (Hrs)	Specific energy (KWh/m <sup>3</sup> )
28.0	10	1	0.11	7.05	0.118	0.517
28.0	10	2	0.11	7.13	0.119	0.523
28.0	10	3	0.11	7.10	0.118	0.521
			0.11	7.09	0.118	0.520
26.0	10	4	0.10	6.83	0.114	0.456
26.0	10	5	0.10	6.92	0.115	0.461
26.0	10	6	0.10	6.95	0.116	0.463
			0.10	6.90	0.115	0.460
24.0	10	1	0.10	6.80	0.113	0.453
24.0	10	2	0.10	6.77	0.113	0.451
24.0	10	3	0.10	6.75	0.113	0.450
			0.10	6.77	0.113	0.451
20.0	10	1	0.10	7.50	0.125	0.500
20.0	10	2	0.10	7.70	0.128	0.513
20.0	10	3	0.10	7.63	0.127	0.509
			0.10	7.61	0.127	0.507
16.0	10	1	0.09	6.83	0.114	0.410
16.0	10	2	0.09	7.03	0.117	0.422
16.0	10	3	0.09	7.08	0.118	0.425
			0.09	6.98	0.116	0.419
12.0	10	1	0.10	7.87	0.131	0.524
12.0	10	2	0.10	7.95	0.133	0.530
12.0	10	3	0.10	8.07	0.134	0.538
			0.10	7.96	0.133	0.531
8.0	10	1	0.08	8.95	0.149	0.477
8.0	10	2	0.08	9.05	0.151	0.483
8.0	10	3	0.08	9.10	0.152	0.485
			0.08	9.03	0.151	0.482

## 1.5 Effect of supporting electrolyte concentration on specific energy consumption in RR

SE NaCl (g/L)	Rep	Current (Amps)	Time (min)	Time (Hrs)	Specific energy (KWh/m <sup>3</sup> )
1	1	0.12	7.73	0.129	0.619
1	2	0.11	7.87	0.131	0.577
1	3	0.10	7.90	0.132	0.527
		0.11	7.83	0.131	0.574
2	1	0.06	10.62	0.177	0.425
2	2	0.06	12.78	0.213	0.511
2	3	0.06	10.70	0.178	0.428
		0.06	11.37	0.189	0.455
4	1	0.08	7.87	0.131	0.420
4	2	0.08	7.75	0.129	0.413
4	3	0.08	7.93	0.132	0.416
		0.08	7.85	0.131	0.416
6	1	0.13	7.03	0.117	0.610
6	2	0.13	6.97	0.116	0.604
6	3	0.13	6.98	0.116	0.605
		0.13	6.99	0.117	0.606
8	1	0.18	6.42	0.107	0.770
8	2	0.18	6.25	0.104	0.750
8	3	0.18	6.32	0.105	0.758
		0.18	6.33	0.105	0.759
10	1	0.21	5.97	0.099	0.835
10	2	0.21	5.88	0.098	0.824
10	3	0.21	5.93	0.099	0.831
		0.21	5.93	0.099	0.830

## 1.6 Effect of supporting electrolyte concentration on specific energy consumption in DB

SE NaCl (g/L)	Rep	Current (Amps)	Time (min)	Time (Hrs)	Specific energy (KWh/m <sup>3</sup> )
1	1	0.08	10.67	0.178	0.569
1	2	0.08	10.77	0.179	0.574
1	3	0.08	10.80	0.180	0.576
		0.08	10.74	0.179	0.573
2	1	0.09	9.07	0.151	0.544
2	2	0.09	9.30	0.155	0.558
2	3	0.09	9.22	0.154	0.553
		0.09	9.19	0.153	0.552
4	1	0.12	6.77	0.113	0.541
4	2	0.12	6.67	0.111	0.533
4	3	0.12	6.63	0.111	0.537
		0.12	6.69	0.111	0.537
6	1	0.13	6.13	0.102	0.532
6	2	0.13	6.07	0.101	0.526
6	3	0.13	5.97	0.099	0.517
		0.13	6.06	0.101	0.525
8	1	0.16	5.22	0.087	0.556
8	2	0.16	5.20	0.087	0.555
8	3	0.16	5.27	0.088	0.562
		0.16	5.23	0.087	0.558
10	1	0.24	4.70	0.078	0.752
10	2	0.23	4.73	0.079	0.726
10	3	0.22	4.78	0.080	0.702
		0.23	4.74	0.079	0.726

## 1.7 Effect of pH on specific energy consumption in RR

pH	Voltage (Volts)	Rep	Current (Amps)	Time (Min)	Time (Hrs)	Specific energy (KWh/m <sup>3</sup> )
4.0	10.0	1	0.09	9.117	0.152	0.547
4.0	10.0	2	0.09	9.167	0.153	0.550
4.0	10.0	3	0.09	9.183	0.153	0.551
			0.09	9.156	0.153	0.549
5.0	10.0	1	0.09	8.533	0.142	0.512
5.0	10.0	2	0.09	8.417	0.140	0.505
5.0	10.0	3	0.09	8.600	0.143	0.516
			0.09	8.517	0.142	0.511
6.0	10.0	1	0.08	7.633	0.127	0.407
6.0	10.0	2	0.08	7.800	0.130	0.416
6.0	10.0	3	0.08	7.867	0.131	0.420
	10.0		0.08	7.767	0.129	0.414
6.5	10.0	1	0.07	7.583	0.126	0.354
6.5	10.0	2	0.07	7.667	0.128	0.358
6.5	10.0	3	0.07	7.633	0.127	0.356
			0.07	7.628	0.127	0.356
7.0	10.0	1	0.08	8.600	0.143	0.459
7.0	10.0	2	0.08	8.700	0.145	0.464
7.0	10.0	3	0.08	8.750	0.146	0.467
			0.08	8.683	0.145	0.463
8.0	10.0	1	0.08	8.133	0.136	0.434
8.0	10.0	2	0.08	8.100	0.135	0.432
8.0	10.0	3	0.08	8.167	0.136	0.436
			0.08	8.133	0.136	0.434
8.5	10.0	1	0.07	8.067	0.134	0.376
8.5	10.0	2	0.07	8.033	0.134	0.375
8.5	10.0	3	0.07	8.000	0.133	0.373
			0.07	8.033	0.134	0.375
9.0	10.0	1	0.07	7.933	0.132	0.370
9.0	10.0	2	0.07	7.800	0.130	0.364
9.0	10.0	3	0.07	7.917	0.132	0.369
			0.07	7.883	0.131	0.368
10.0	10.0	1	0.09	6.933	0.116	0.416
10.0	10.0	2	0.08	6.967	0.116	0.372
10.0	10.0	3	0.08	7.050	0.118	0.376
			0.08	6.983	0.116	0.388

## 1.8 Effect of pH on specific energy consumption in DB

pH	Voltage (Volts)	Rep	Current (Amps)	Time (Min)	Time (Hrs)	Specific energy (KWh/m <sup>3</sup> )
4.0	10.0	1	0.08	7.93	0.132	0.423
4.0	10.0	2	0.08	7.95	0.133	0.424
4.0	10.0	3	0.08	8.03	0.134	0.428
			0.08	7.97	0.133	0.425
5.0	10.0	1	0.08	7.53	0.126	0.402
5.0	10.0	2	0.08	7.47	0.124	0.398
5.0	10.0	3	0.08	7.52	0.125	0.401
			0.08	7.51	0.125	0.400
6.0	10.0	1	0.08	7.13	0.119	0.380
6.0	10.0	2	0.08	7.03	0.117	0.375
6.0	10.0	3	0.08	6.98	0.116	0.372
	10.0		0.08	7.05	0.118	0.376
7.0	10.0	1	0.09	6.67	0.111	0.400
7.0	10.0	2	0.09	6.63	0.111	0.398
7.0	10.0	3	0.09	6.65	0.111	0.399
			0.09	6.65	0.111	0.399
8.0	10.0	1	0.11	5.92	0.099	0.434
8.0	10.0	2	0.11	5.97	0.099	0.438
8.0	10.0	3	0.11	5.93	0.099	0.435
			0.11	5.94	0.099	0.436
9.0	10.0	1	0.12	5.50	0.092	0.440
9.0	10.0	2	0.12	5.47	0.091	0.437
9.0	10.0	3	0.12	5.42	0.090	0.433
			0.12	5.46	0.091	0.437
10.0	10.0	1	0.14	4.95	0.083	0.462
10.0	10.0	2	0.14	5.00	0.083	0.467
10.0	10.0	3	0.14	4.98	0.083	0.465
			0.14	4.98	0.083	0.465

## 1.9 Effect of Electrode distance on specific energy consumption in RR

Distance (mm)	Voltage (Volts)	Rep	Current (Amps)	Time (Min)	Time (Hrs)	Specific energy (KWh/m <sup>3</sup> )
5	10	1	0.13	7.10	0.118	0.615
5	10	2	0.13	6.97	0.116	0.604
5	10	3	0.13	7.03	0.117	0.610
			0.13	7.03	0.117	0.610
7	10	1	0.09	10.22	0.170	0.613
7	10	2	0.09	10.33	0.172	0.620
7	10	3	0.09	10.18	0.170	0.611
			0.09	10.24	0.171	0.615
9	10	1	0.08	10.87	0.181	0.580
9	10	2	0.08	11.03	0.184	0.588
9	10	3	0.08	11.15	0.186	0.595
			0.09	10.24	0.171	0.615
10	10	1	0.08	11.57	0.193	0.617
10	10	2	0.08	11.50	0.192	0.613
10	10	3	0.08	11.60	0.193	0.619
			0.08	11.02	0.184	0.588
12	10	1	0.05	12.12	0.202	0.404
12	10	2	0.05	12.25	0.204	0.408
12	10	3	0.05	12.40	0.207	0.413
			0.05	12.26	0.204	0.409
14	10	1	0.05	12.87	0.214	0.429
14	10	2	0.05	12.93	0.216	0.431
14	10	3	0.05	13.07	0.218	0.436
			0.05	12.96	0.216	0.432
16	10	1	0.05	13.63	0.227	0.454
16	10	2	0.05	13.73	0.229	0.458
16	10	3	0.05	13.60	0.227	0.453
			0.05	13.66	0.228	0.455

## 1.10 Effect of Electrode distance on specific energy consumption in DB

Distance (mm)	Voltage (Volts)	Rep	Current (Amps)	Time (Min)	Time (Hrs)	Specific energy (KWh/m <sup>3</sup> )
5	10	1	0.12	5.67	0.094	0.453
5	10	2	0.12	5.90	0.098	0.472
5	10	3	0.12	6.00	0.100	0.480
			0.12	5.86	0.098	0.468
7	10	1	0.09	6.63	0.111	0.398
7	10	2	0.09	6.75	0.113	0.405
7	10	3	0.09	6.93	0.116	0.416
			0.09	6.77	0.113	0.406
9	10	1	0.08	7.57	0.126	0.404
9	10	2	0.08	7.63	0.127	0.407
9	10	3	0.08	7.53	0.126	0.402
			0.09	6.77	0.113	0.406
10	10	1	0.08	6.92	0.115	0.369
10	10	2	0.08	7.08	0.118	0.378
10	10	3	0.08	7.03	0.117	0.375
			0.08	7.58	0.126	0.404
12	10	1	0.04	8.83	0.147	0.236
12	10	2	0.04	8.92	0.149	0.238
12	10	3	0.04	8.97	0.149	0.239
			0.04	8.91	0.148	0.237
14	10	1	0.04	9.77	0.163	0.260
14	10	2	0.04	9.83	0.164	0.262
14	10	3	0.04	9.92	0.165	0.264
			0.04	9.84	0.164	0.262
16	10	1	0.04	12.37	0.206	0.330
16	10	2	0.04	12.42	0.207	0.331
16	10	3	0.04	12.33	0.206	0.329
			0.04	12.37	0.206	0.330
20	10	1	0.04	13.00	0.217	0.347
20	10	2	0.04	12.95	0.216	0.345
20	10	3	0.04	13.07	0.218	0.348
			0.04	13.01	0.217	0.347



## 1.11 Effect of current density on specific energy consumption in RR

Current density, (A/m <sup>2</sup> )	Target Current (Amps)	Volume of NaCl (mL)	Voltage (Volts)	Rep	Time (Min)	Time (Hrs)	Specific energy (KWh/m <sup>3</sup> )
10.0	0.04	3.1	10	1	15.07	0.251	0.402
10.0	0.04	3.1	10	2	15.17	0.253	0.404
10.0	0.04	3.1	10	3	15.13	0.252	0.404
					15.12	0.252	0.403
20.0	0.08	4.8	10	1	11.50	0.192	0.613
20.0	0.08	4.8	10	2	11.58	0.193	0.618
20.0	0.08	4.8	10	3	11.60	0.193	0.619
					11.56	0.193	0.617
30.0	0.12	8.8	10	1	10.30	0.172	0.824
30.0	0.12	8.8	10	2	10.33	0.172	0.827
30.0	0.12	8.8	10	3	10.05	0.168	0.804
					10.23	0.170	0.818
40.0	0.16	12.7	10	1	7.28	0.121	0.777
40.0	0.16	12.7	10	2	7.25	0.121	0.773
40.0	0.16	12.7	10	3	7.22	0.120	0.770
					7.25	0.121	0.773
50.0	0.20	16.8	10	1	5.88	0.098	0.784
50.0	0.20	16.8	10	2	5.93	0.099	0.791
50.0	0.20	16.8	10	3	5.92	0.099	0.789
					5.91	0.099	0.788

## 1.12 Effect of current density on specific energy consumption in DB

Current density (A/m <sup>2</sup> )	Target current (Amps)	Volume of NaCl (mL)	Voltage (Volts)	Rep	Time (min)	Time (Hrs)	Specific energy (KWh/m <sup>3</sup> )
10.0	0.04	3.0	10	1	7.78	0.130	0.208
10.0	0.04	3.0	10	2	10.05	0.168	0.268
10.0	0.04	3.0	10	3	8.05	0.134	0.215
					8.63	0.144	0.230
20.0	0.08	4.9	10	1	7.42	0.124	0.396
20.0	0.08	4.9	10	2	7.37	0.123	0.393
20.0	0.08	4.9	10	3	7.35	0.123	0.392
					7.38	0.123	0.393
30.0	0.12	9.4	10	1	6.72	0.112	0.537
30.0	0.12	9.4	10	2	6.68	0.111	0.535
30.0	0.12	9.4	10	3	6.72	0.112	0.537
					6.71	0.112	0.536
40.0	0.16	13.6	10	1	5.83	0.097	0.622
40.0	0.16	13.6	10	2	5.78	0.096	0.617
40.0	0.16	13.6	10	3	5.72	0.095	0.610
					5.78	0.096	0.616
50.0	0.20	18.6	10	1	4.87	0.081	0.649
50.0	0.20	18.6	10	2	4.90	0.082	0.653
50.0	0.20	18.6	10	3	4.92	0.082	0.656
					4.89	0.082	0.653
60.0	0.24	25.5	10	4	3.95	0.066	0.632
60.0	0.24	25.5	10	5	3.98	0.066	0.637
60.0	0.24	25.5	10	6	4.05	0.068	0.648
					3.99	0.067	0.639

## 1.13 Effect of temperature on specific energy consumption in RR

Temp ( <sup>o</sup> C)	Voltage (Volts)	Rep	Current (Amps)	Time (min)	Time (Hrs)	Specific energy (KWh/m <sup>3</sup> )
30	10	1	0.08	12.93	0.216	0.690
30	10	2	0.08	12.97	0.216	0.692
30	10	3	0.08	12.87	0.214	0.686
			0.08	12.92	0.215	0.689
40	10	1	0.10	9.33	0.156	0.622
40	10	2	0.10	9.37	0.156	0.624
40	10	3	0.10	9.40	0.157	0.627
			0.10	9.37	0.156	0.624
45	10	1	0.11	8.38	0.140	0.615
45	10	2	0.11	8.33	0.139	0.611
45	10	3	0.11	8.30	0.138	0.609
			0.10	8.34	0.156	0.612
50	10	1	0.12	7.47	0.124	0.597
50	10	2	0.12	7.43	0.124	0.595
50	10	3	0.12	7.42	0.124	0.593
			0.11	7.44	0.139	0.595

## 1.14 Effect of temperature on specific energy consumption in DB

Temp (°C)	Voltage (Volts)	Rep	Current (Amps)	Time (min)	Time (Hrs)	Specific energy (KWh/m <sup>3</sup> )
30	10	1	0.08	11.43	0.19	0.61
30	10	2	0.08	11.47	0.19	0.61
30	10	3	0.08	11.45	0.19	0.61
			0.08	11.45	0.19	0.61
40	10	1	0.09	9.50	0.16	0.57
40	10	2	0.09	9.60	0.16	0.58
40	10	3	0.09	9.57	0.16	0.57
			0.09	9.56	0.16	0.57
45	10	1	0.09	8.83	0.15	0.53
45	10	2	0.09	8.77	0.15	0.53
45	10	3	0.09	8.78	0.15	0.53
			0.09	8.79	0.16	0.53
50	10	1	0.11	6.98	0.12	0.51
50	10	2	0.11	7.17	0.12	0.53
50	10	3	0.11	7.20	0.12	0.53
			0.09	7.12	0.15	0.52

## APPENDIX II: Electrochemical mineralization using Boron Doped Diamond anode

### 2.1 Effect of current density in RR mineralization

Current density (A/m <sup>2</sup> )	Target Current (Amps)	Rep	Time(min)	Time (hrs)	Specific energy(KWh/m <sup>3</sup> )
150	0.13	1	5.23	0.087	1.145
150	0.13	2	5.27	0.088	1.152
150	0.13	3	5.28	0.088	1.156
			<b>5.26</b>	<b>0.088</b>	<b>1.151</b>
200	0.18	1	4.35	0.073	1.269
200	0.18	2	4.40	0.073	1.283
200	0.18	3	4.37	0.073	1.274
			<b>4.37</b>	<b>0.073</b>	<b>1.275</b>
250	0.22	1	4.13	0.069	1.507
250	0.22	2	4.17	0.069	1.519
250	0.22	3	4.18	0.070	1.525
			<b>4.16</b>	<b>0.069</b>	<b>1.517</b>
300	0.26	1	2.60	0.043	1.138
300	0.26	2	2.70	0.045	1.181
300	0.26	3	2.77	0.046	1.210
			<b>2.69</b>	<b>0.045</b>	<b>1.176</b>
350	0.31	1	2.52	0.042	1.285
350	0.31	2	2.53	0.042	1.293
350	0.31	3	2.53	0.042	1.293
			<b>2.53</b>	<b>0.042</b>	<b>1.290</b>
100	0.09	1	6.73	0.112	0.982
100	0.09	2	6.70	0.112	0.977
100	0.09	3	6.72	0.112	0.980
			<b>6.72</b>	<b>0.112</b>	<b>0.980</b>
50	0.04	1	8.75	0.146	0.638
50	0.04	2	8.73	0.146	0.637
50	0.04	3	8.77	0.146	0.639
			<b>8.75</b>	<b>0.146</b>	<b>0.638</b>

## 2.2 Effect of current density in DB mineralization

Current density (A/m <sup>2</sup> )	Target Current (Amps)	Rep	Time(min)	Time (hrs)	Specific energy (KWh/m <sup>3</sup> )
150	0.13	1	21.7	0.362	4.747
150	0.13	2	21.6	0.360	4.721
150	0.13	3	21.6	0.360	4.721
			<b>21.6</b>	<b>0.360</b>	<b>4.730</b>
200	0.18	1	15.5	0.259	4.526
200	0.18	2	15.5	0.259	4.531
200	0.18	3	15.6	0.259	4.535
			<b>15.5</b>	<b>0.259</b>	<b>4.531</b>
250	0.22	1	12.6	0.211	4.606
250	0.22	2	12.7	0.212	4.630
250	0.22	3	12.8	0.213	4.648
			<b>12.7</b>	<b>0.212</b>	<b>4.628</b>
300	0.26	1	11.6	0.194	5.082
300	0.26	2	11.6	0.194	5.090
300	0.26	3	11.6	0.194	5.082
			<b>11.6</b>	<b>0.194</b>	<b>5.085</b>
350	0.31	1	10.6	0.177	5.419
350	0.31	2	10.6	0.177	5.419
350	0.31	3	10.6	0.177	5.419
			<b>10.6</b>	<b>0.177</b>	<b>5.419</b>

## 2.3 Effect of pH in RR mineralization

pH	Current (Amps)	Time(min)	Time (hrs)	Specific energy
4.0	0.05	8.70	0.145	0.725
4.0	0.05	8.72	0.145	0.726
4.0	0.05	8.72	0.145	0.726
		<b>8.71</b>	<b>0.15</b>	<b>0.73</b>
5.0	0.06	7.65	0.128	0.765
5.0	0.06	7.63	0.127	0.763
5.0	0.06	7.65	0.128	0.765
		<b>7.64</b>	<b>0.13</b>	<b>0.76</b>
6.0	0.07	6.90	0.115	0.805
6.0	0.07	6.88	0.115	0.803
6.0	0.07	6.92	0.115	0.807
		<b>6.90</b>	<b>0.12</b>	<b>0.81</b>
6.5	0.10	6.07	0.101	1.011
6.5	0.10	6.03	0.101	1.006
6.5	0.10	6.00	0.100	1.000
		<b>6.03</b>	<b>0.10</b>	<b>1.01</b>
7.0	0.10	5.53	0.09	0.922
7.0	0.10	5.52	0.092	0.919
7.0	0.10	5.53	0.092	0.922
		<b>5.53</b>	<b>0.09</b>	<b>0.92</b>
8.0	0.07	5.00	0.083	0.583
8.0	0.07	4.98	0.083	0.581
8.0	0.07	5.03	0.084	0.587
		<b>5.01</b>	<b>0.08</b>	<b>0.58</b>
9.0	0.08	4.47	0.074	0.596
9.0	0.08	4.45	0.074	0.593
9.0	0.08	4.50	0.075	0.600
		<b>4.47</b>	<b>0.07</b>	<b>0.60</b>

## 2.4 Effect of pH in DB mineralization

pH	Current (Amps)	Time(min)	Time (hrs)	Specific energy (KWh/m <sup>3</sup> )
4.0	0.07	28.37	0.473	3.309
4.0	0.07	28.42	0.474	3.315
4.0	0.07	28.45	0.474	3.319
		<b>28.41</b>	<b>0.47</b>	<b>3.31</b>
5.0	0.08	26.83	0.447	3.578
5.0	0.08	26.90	0.448	3.587
5.0	0.08	26.87	0.448	3.582
		<b>26.87</b>	<b>0.45</b>	<b>3.58</b>
6.0	0.11	24.75	0.413	4.538
6.0	0.11	24.80	0.413	4.547
6.0	0.11	24.77	0.413	4.541
		<b>24.77</b>	<b>0.41</b>	<b>4.54</b>
6.5	0.12	22.40	0.373	4.480
6.5	0.12	22.42	0.374	4.483
6.5	0.12	22.43	0.374	4.487
		<b>22.42</b>	<b>0.37</b>	<b>4.48</b>
7.0	0.14	21.63	0.361	5.048
7.0	0.14	21.67	0.361	5.056
7.0	0.14	21.70	0.362	5.063
		<b>21.67</b>	<b>0.36</b>	<b>5.06</b>
8.0	0.16	20.47	0.341	5.458
8.0	0.16	20.43	0.341	5.449
8.0	0.16	20.45	0.341	5.453
		<b>20.45</b>	<b>0.34</b>	<b>5.45</b>
9.0	0.09	19.83	0.331	2.975
9.0	0.09	19.87	0.331	2.980
9.0	0.09	19.88	0.331	2.983
		<b>19.86</b>	<b>0.33</b>	<b>2.98</b>



## 2.5 Effect of temperature in RR mineralization

Temp, °C	Current (Amps)	Time(min)	Time (hrs)	Specific energy (KWh/m <sup>3</sup> )
30	0.09	6.63	0.111	0.995
30	0.09	6.67	0.111	1.000
30	0.09	6.65	0.111	0.998
		<b>6.65</b>	<b>0.11</b>	<b>1.00</b>
40	0.12	6.08	0.101	1.217
40	0.12	6.05	0.101	1.210
40	0.12	5.98	0.100	1.197
		<b>6.04</b>	<b>0.10</b>	<b>1.21</b>
45	0.13	5.17	0.086	1.119
45	0.13	5.15	0.086	1.116
45	0.13	5.13	0.086	1.112
		<b>5.15</b>	<b>0.09</b>	<b>1.12</b>
50	0.15	4.37	0.073	1.092
50	0.15	4.35	0.073	1.088
50	0.15	4.33	0.072	1.083
		<b>4.35</b>	<b>0.07</b>	<b>1.09</b>
55	0.15	3.50	0.058	0.875
55	0.15	3.47	0.058	0.867
55	0.15	3.48	0.058	0.871
		<b>3.48</b>	<b>0.06</b>	<b>0.87</b>

## 2.6 Effect of temperature in DB mineralization

Temp (°C)	Current (Amps)	Time(min)	Time (hrs)	Specific energy (KWh/m <sup>3</sup> )
30	0.06	28.60	0.477	2.860
30	0.06	28.58	0.476	2.858
30	0.06	28.53	0.476	2.853
		<b>28.57</b>	<b>0.48</b>	<b>2.86</b>
40	0.08	27.50	0.458	3.667
40	0.08	27.48	0.458	3.664
40	0.08	27.53	0.459	3.671
		<b>27.51</b>	<b>0.46</b>	<b>3.67</b>
45	0.11	25.33	0.422	4.644
45	0.11	25.28	0.421	4.635
45	0.11	25.37	0.423	4.651
		<b>25.33</b>	<b>0.42</b>	<b>4.64</b>
50	0.12	20.25	0.338	4.050
50	0.12	20.23	0.337	4.047
50	0.12	20.27	0.338	4.053
		<b>20.25</b>	<b>0.34</b>	<b>4.05</b>
55	0.14	18.25	0.304	4.258
55	0.14	18.23	0.304	4.254
55	0.14	18.27	0.304	4.262
		<b>18.25</b>	<b>0.30</b>	<b>4.26</b>

## 2.7 Effect of concentration in RR mineralization

Conc.(mg/L)	Current (Amps)	Time(min)	Time (hrs)	Specific energy (KWh/m <sup>3</sup> )
10	0.13	5.33	0.089	1.156
10	0.13	5.37	0.089	1.163
10	0.13	5.40	0.090	1.170
		<b>5.37</b>	<b>0.09</b>	<b>1.16</b>
20	0.12	5.65	0.094	1.130
20	0.12	5.60	0.093	1.120
20	0.12	5.53	0.092	1.107
		<b>5.59</b>	<b>0.09</b>	<b>1.12</b>
30	0.13	5.77	0.096	1.249
30	0.13	5.75	0.096	1.246
30	0.13	5.78	0.096	1.253
		<b>5.77</b>	<b>0.10</b>	<b>1.25</b>
40	0.13	6.10	0.102	1.322
40	0.13	6.07	0.101	1.314
40	0.13	6.07	0.101	1.314
		<b>6.08</b>	<b>0.10</b>	<b>1.32</b>
50	0.13	6.87	0.114	1.488
50	0.13	6.97	0.116	1.509
50	0.13	7.00	0.117	1.517
		<b>6.94</b>	<b>0.12</b>	<b>1.50</b>

## 2.8 Effect of concentration in DB mineralization

Conc.(mg/L)	Current (Amps)	Time(min)	Time (hrs)	Specific energy (KWh/m <sup>3</sup> )
10	0.13	29.75	0.496	6.446
10	0.13	29.73	0.496	6.442
10	0.13	29.70	0.495	6.435
		<b>29.73</b>	<b>0.50</b>	<b>6.44</b>
20	0.13	30.25	0.504	6.554
20	0.13	30.23	0.504	6.551
20	0.13	30.22	0.504	6.547
		<b>30.23</b>	<b>0.50</b>	<b>6.55</b>
30	0.13	31.75	0.529	6.879
30	0.13	31.77	0.529	6.883
30	0.13	31.78	0.530	6.886
		<b>31.77</b>	<b>0.53</b>	<b>6.88</b>
40	0.13	32.52	0.542	7.045
40	0.13	32.53	0.542	7.049
40	0.13	32.57	0.543	7.056
		<b>32.54</b>	<b>0.54</b>	<b>7.05</b>
50	0.13	34.07	0.568	7.381
50	0.13	34.10	0.568	7.388
50	0.13	34.08	0.568	7.385
		<b>34.08</b>	<b>0.57</b>	<b>7.38</b>

## 2.9 Effect of electrode gap on RR mineralization

Electrode gap (mm)	Current (Amps)	Time(min)	Time (hrs)	Specific energy (KWh/m <sup>3</sup> )
5	0.25	5.57	0.093	2.319
5	0.25	5.58	0.093	2.326
5	0.25	5.60	0.093	2.333
		<b>5.58</b>	<b>0.09</b>	<b>2.33</b>
10	0.23	6.78	0.113	2.600
10	0.23	7.90	0.132	3.028
10	0.23	7.93	0.132	3.041
		<b>7.54</b>	<b>0.13</b>	<b>2.89</b>
12	0.17	8.17	0.136	2.314
12	0.17	8.20	0.137	2.323
12	0.17	8.23	0.137	2.333
		<b>8.20</b>	<b>0.14</b>	<b>2.32</b>
14	0.16	8.83	0.147	2.356
14	0.16	8.87	0.148	2.364
14	0.16	8.90	0.148	2.373
		<b>8.87</b>	<b>0.15</b>	<b>2.36</b>
20	0.13	10.87	0.181	2.354
20	0.13	10.90	0.182	2.362
20	0.13	10.93	0.182	2.369
		<b>10.90</b>	<b>0.18</b>	<b>2.36</b>

## 2.10 Effect of electrode gap on DB mineralization

Electrode gap (mm)	Current (Amps)	Time(min)	Time (hrs)	Specific energy (KWh/m <sup>3</sup> )
5	0.23	12.87	0.214	4.932
5	0.23	12.90	0.215	4.945
5	0.23	12.88	0.215	4.939
		<b>12.88</b>	<b>0.21</b>	<b>4.94</b>
10	0.24	13.47	0.224	5.387
10	0.24	13.50	0.225	5.400
10	0.24	13.53	0.226	5.413
		<b>13.50</b>	<b>0.23</b>	<b>5.40</b>
12	0.16	14.15	0.236	3.773
12	0.16	14.12	0.235	3.764
12	0.16	14.17	0.236	3.778
		<b>14.14</b>	<b>0.24</b>	<b>3.77</b>
14	0.16	14.87	0.248	3.964
14	0.16	14.90	0.248	3.973
14	0.16	14.88	0.248	3.969
		<b>14.88</b>	<b>0.25</b>	<b>3.97</b>
20	0.09	22.47	0.374	3.370
20	0.09	22.50	0.375	3.375
20	0.09	22.53	0.376	3.380
		<b>22.50</b>	<b>0.38</b>	<b>3.38</b>